COMPLETED

NUREG/CR-4822

ORIGINAL

Broad Band Seismic Data Analysis

September 1984 - September 1986

Prepared by J. A. Carter, N. Barstow, G. H. Sutton, P. W. Pomeroy

Rondout Associates, Incorporated

Prepared for
U.S. Nuclear Regulatory
Commission

BEST COPY AVAILABLE

NOTICE

This report was prepared as an account of work sponsored by an agency of the United States Government. Neither the United States Government nor any agency thereof, or any of their employees, makes any warranty, expressed or implied, or assumes any legal liability of responsibility for any third party's use, or the results of such use, of any information, apparatus, product or process disclosed in this report, or represents that its use by such third party would not infringe privately owned rights.

NOTICE

Availability of NRC Publications

NRC publications sold by GPO, NRC publications will be available from one of the following sources:

1. The NRC Public Document Room, 1717 H Street, N.W.
Washington, DC 20555

2. The Superintendent of Documents, U.S. Government Printing Office, Post Office Box 37082
Washington, DC 20013-7082

3. The National Technical Information Service, Springfield, VA 22161

Although the listing that follows represents the majority of documents cited in NRC publications, it is not intended to be exhaustive.

Referenced documents available for inspection and copying for a fee from the NRC Public Document Room include NRC correspondence and internal NRC memoranda; NRC Office of Inspection and Enforcement bulletins, circulars, information notices, inspection and investigation notices; Licensee Event Reports; vendor reports and correspondence; Commission papers; and applicant and licensee documents and correspondence.

The following documents in the NUREG series are available for purchase from the GPO Sales Program: formal NRC staff and contractor reports, NRC-sponsored conference proceedings, and NRC booklets and brochures. Also available are Regulatory Guides, NRC regulations in the *Code of Federal Regulations*, and *Nuclear Regulatory Commission Issuances*.

Documents available from the National Technical Information Service include NUREG-series reports and technical reports prepared by other federal agencies and reports prepared by the Atomic Energy Commission, forerunner agency to the Nuclear Regulatory Commission.

Documents available from public and special technical libraries include all open literature items, such as books, journal and periodical articles, and transactions. *Federal Register* notices, federal and state legislation, and congressional reports can usually be obtained from these libraries.

Documents such as theses, dissertations, foreign reports and translations, and non-NRC conference proceedings are available for purchase from the organization sponsoring the publication cited.

Single copies of NRC draft reports are available free, to the extent of supply, upon written request to the Division of Technical Information and Document Control, U.S. Nuclear Regulatory Commission, Washington, DC 20555.

Copies of industry codes and standards used in a substantive manner in the NRC regulatory process are maintained at the NRC Library, 7920 Norfolk Avenue, Bethesda, Maryland, and are available there for reference use by the public. Codes and standards are usually copyrighted and may be purchased from the originating organization or, if they are American National Standards, from the American National Standards Institute, 1430 Broadway, New York, NY 10018.

BEST COPY AVAILABLE

NUREG/CR-4822
RA

Broad Band Seismic Data Analysis

September 1984 - September 1986

Manuscript Completed: December 1986
Date Published: April 1987

Prepared by
J. A. Carter, N. Barstow, G. H. Sutton, P. W. Pomeroy

Rondout Associates, Incorporated
P. O. Box 224
Stone Ridge, NY 12484

Prepared for
Division of Engineering Safety
Office of Nuclear Regulatory Research
U.S. Nuclear Regulatory Commission
Washington, DC 20555
NRC FIN D1196
Under Contract No. NRC-04-84-136

BEST COPY AVAILABLE

EXECUTIVE SUMMARY

This report describes the three component broad band digital seismic station SRNY located in Stone Ridge, New York and documents the stations reliability; the seismic noise levels recorded there; its detection, location and depth determination capabilities as a single station; and addresses the relative merits of three component stations and networks of single component stations. The salient points and conclusions of this report are listed below.

1. Broad band Wielandt seismometers are used as the sensors at station SRNY. They have performed quite well but may be hampered by system noise above 6 Hz. Data are digitized at 60 samples/sec for each of the three channels and recorded on 1/4" magnetic tape cartridges. Each tape holds 38 hours of data. A personal computer performs the task of data recording.

2. In the first six months of 1986, the station recorded data 97.2% of the time. The primary causes of data loss were computer and tape drive malfunctions followed by power losses due to severe weather conditions. Future system designs should include a faster and more reliable computer system. A random access storage medium would simplify the task of data retrieval.

3. Absolute noise levels at SRNY are comparable to those reported for the New York station (RSNY) of the Regional Seismic Test Network. At frequencies between approximately 2 and 6 Hz, however, only the quietest SRNY noise spectra match the levels reported at RSNY. For quiet samples above 6 Hz, the SRNY spectra may exhibit system noise.

4. A summary of the detection and location capabilities of a single three component broad band station is given in Table 2 and Figure 11. Magnitude 4 events can be detected at SRNY at distances up to 7.5 degrees and located (although not with as much accuracy as with a network) using azimuth and range up to 5 degrees. Better location estimates can be made if more than one three component station can locate the event.

5. Depth is determined from a single three component station by isolating and identifying the depth phases *pP* and/or *sP* and comparing the results to synthetic seismograms. Ten events were analyzed of which 4 were assigned depths in agreement with network depth determinations, 3 had no network depth assigned and only 2 were in disagreement with the network depths.

6. Three component seismic stations are a valuable seismological tool. A network of stations, however, provides better detection levels, locations, and depth determinations than a single three component station. To monitor a specific area with a fixed number of seismic data channels we would

BEST COPY AVAILABLE

recommend a network of vertical component, three component, and three component strong motion stations. The benefits of each type of station could then be utilized; dense areal coverage using vertical component stations, complete particle motion from the three component stations, and strong motion records in three dimensions from the strong motion stations. The volume of data recorded can be reduced by using event triggering for high-data-rate stations and continuous recording at a low data rate over a sparse subset of the network.

BEST COPY AVAILABLE

TABLE OF CONTENTS

SECTION		PAGE
	EXECUTIVE SUMMARY	i
	LIST OF FIGURES	v
	LIST OF TABLES	viii
SECTION I.	INTRODUCTION	1
SECTION II.	SRNY STATION DESCRIPTION	2
	Physical Description	2
	System Response	3
	Station Performance	5
SECTION III.	ANALYSIS TECHNIQUES	6
	Polarization Analysis	6
	Synthetic Seismograms	11
	Spectral Analysis and Filtering	12
SECTION IV.	NOISE, DETECTION, AND LOCATION	13
	Noise Characteristics	13
	Detection and Location Capability	14
	Depth Determination	18
SECTION V.	SUMMARY	23
	REFERENCES	25

BEST COPY AVAILABLE

FIGURES 27

APPENDIX A 61

APPENDIX B 67

BEST COPY AVAILABLE

LIST OF FIGURES

FIGURE		PAGE
Figure 1.	A- SRNY seismic vault exterior. B- Seismic vault interior. C- Recording station.	28
Figure 2.	Digital seismic recording system.	29
Figure 3.	Velocity response of SRNY vertical seismograph (dB re one du/nm/sec and phase angle in radians): left and right, with and without anti alias filter, respectively. Horizontal response are the same except for slight difference in amplification constant, A.	30
Figure 4.	Vertical (sz), north-south horizontal (sn), and east-west horizontal (se) components of a signal rotating in azimuth but with constant angle of incidence.	31
Figure 5.	Output of the track program for a signal rotating in azimuth but with a constant angle of incidence. sz=vertical; sr=adapted radial; st=adapted transverse; rz=radial times vertical; az=azimuth with error bars; ai=angle of incidence with error bars.	32
Figure 6.	Results of trying to track two different sets of random noise traveling in different directions. One set is traveling to the northeast; the other is traveling due north and is more than twice the amplitude of the first.	33
Figure 7.	Vertical component synthetic seismograms for the Ardsley, NY aftershock and data at station SRNY, Δ = 100 km.	34
Figure 8.	Instrument-corrected power spectra of displacement for four noise samples in dB (re 1 nanometer^2 /Hz). One sample is in the summer, three are in the fall; two are at night, two in	

BEST COPY AVAILABLE

the morning.
8A shows the broad-band noise characteristics and 8B focuses on the higher frequencies - from 1.0 to 20.00 Hz 35

Figure 9. Power spectra for two times taken Saturday, July 26, 1986. The higher amplitudes between 1 to 15 Hz are from the noise sample beginning at 10:00 AM, local time. Note that the spike at about 15 Hz occurs on both day (10:00) and "night" (03:00) samples. Excepting the 15 Hz spike, the 03:00 spectrum is nearly flat above 6 Hz. 36

Figure 10. Noise spectrum at SRNY (heavy line) compared to noise at RSNY. The microseisms (.1-.3 Hz) are quieter at SRNY for the particular sample chosen. At the high frequencies, though, SRNY flattens out, whereas the RSNY samples continued to fall-off to about 15 Hz (figure adapted from Rodgers *et al.*, 1986). 37

Figure 11. Earthquake magnitudes versus distance from station SRNY. 'L' indicates locatable earthquakes, 'D' detected earthquakes and 'N' not detected earthquakes. Stars denote earthquakes not examined in this study. Most earthquakes are from the NEUSSN published bulletins for the period 7/84 through 3/85. Dashed lines are sketched to separate magnitude/distance regions of locatable, detectable and not detectable earthquakes. 38

Figure 12. Adaptive polarization analysis of band pass filtered SRNY recording (1-4 Hz) of the Adirondack earthquake on 10/23/84. Labeled traces are: Z=vertical, R=adaptive radial, T=adaptive transverse, RZ=radial vertical product, AZ=back azimuth, receiver-to-source angle, AA=apparent angle of incidence. 39

Figure 13. SRNY single station earthquake locations (triangles) compared to network locations (circles). Events and location differences are listed in Table 3. 40

Figure 14. RSNY single station earthquake locations (triangles)

BEST COPY AVAILABLE

compared to network locations (circles). Events and location differences are listed in Table 4. 41

Figure 15. Locations of the 10/23/84 Adirondack earthquake. The Lamont-Doherty network location is plotted as a closed circle. Locations from RSNY and SRNY are plotted as triangles. Error boxes are ± one standard deviation in range and azimuth based on data in Tables 3 and 4. 42

Figure 16. Location of events and stations used in this study. Events are indicated by circles and a date. The two stations, RSNY and SRNY are indicated by triangles. 43

Figure 17A.- 17I.
Seismograms recorded at RSNY of the January 19, 1982 New Hampshire earthquake. The top three traces are the vertical, north-south, and east-west components, unfiltered. The bottom three traces are the three components after state-filtering for rectilinear particle motion. The rest of the events shown in Figure 16 are similarly depicted in Figures 17B through 17I. 44-52

Figure 18A.- 18H.
Synthetic seismograms calculated for a suite of depths. Source = January 19, 1982 Earthquake. Strike = 280, Dip = 75, Rake = − 11. Receiver response = RSNY short period (sp). Azimuth = 295. In Figures 18A through 18H several primary and depth phases are identified. All but Figure 18G are vertical components. *PiP* is reflected within the crust and *PmP* is reflected at the Moho. 53-60

BEST COPY AVAILABLE

LIST OF TABLES

TABLE		PAGE
Table 1	Poles and zeros of the SRNY Wielandt Seismometers	4
Table 2	Detection and location capabilities of station SRNY for selected events to a distance of 7.5 °	15
Table 3	SRNY locations vs. network locations for 8 events	17
Table 4	RSNY locations vs. network locations for 7 events	18
Table 5	List of events and event parameters	19
Table 6	Velocity/Q models of the Northeastern U.S.	20
Table 7	Source depths of Northeast U.S. earthquakes	22

BEST COPY AVAILABLE

I. INTRODUCTION

This report contains a detailed description of the SRNY station including its response function, description of the techniques and software used to analyze the data, and evaluations of both the station and the processing methods. The station was evaluated through noise studies under both quiet and noisy conditions; its detection and location thresholds; and the frequency, duration, and causes of data loss. The report has been divided into three main sections.

The first section gives a description of the broad band digital seismic station SRNY installed near the Rondout Associates, Incorporated (RAI) offices in Stone Ridge, New York. Included in the discussion are the system response functions and an analysis of the causes of data loss.

The second section gives details of the data analysis methods used in studying broad band and array data. Although several methods have been studied, much of this section is devoted to the adaptive polarization method which has shown promise as a single station location tool.

The final section examines the noise characteristics at SRNY during both quiet and noisy conditions and compares these levels to the Regional Seismic Test Network station RSNY in the Adirondack Mountain region of northern New York. The detection and location capabilities of SRNY are also described and single-station locations at SRNY, as well as RSNY are compared to network locations.

Appendices A and B document the software that has been implemented on the Columbia PC for data collection and monitoring (Appendix A) and on the RAI SUN microcomputer for tape certification, data playback and data analysis (Appendix B). These latter programs have been designed for ease of use and make extensive use of the graphics capabilities of the SUN computer. The data retrieval software puts the data into the Center for Seismic Studies (CSS) format version 2.6.

BEST COPY AVAILABLE

II. SRNY STATION DESCRIPTION

Physical Description

SRNY is located at the southeastern corner of the Catskill range in Stone Ridge, New York, at 41.849 ° N, 74.151 ° W at an elevation of 106 meters and is operated by RAI for the Nuclear Regulatory Commission. The sensors sit on a concrete pier that was poured on Paleozoic limestone bedrock two meters below the surface and is covered by a 1.8m by 2.7m concrete box (Figure 1a). Power and signal cables extend underground approximately 400 meters from the vault site to the RAI office building where the recording electronics are housed.

Inside the vault (Figure 1b) along with the three seismometers are amplifiers, anti-alias filters, the digitizer, a multiplexer, and a line driver all purchased from Refraction Technology. The sensors are Wielandt wide-band feedback seismometers (manufactured by Streckheisen) which are flat to velocity from .2 to 20 seconds period and have a 140 dB dynamic range. (Wielandt and Streckeisen, 1982). Output from the seismometers is amplified, digitized at approximately 60 samples per second per channel, multiplexed and transmitted by cable to the recording station (Figure 1c). A 16 bit digitizing scheme is used with a 14 bit mantissa and a 2 bit exponent. Each gain step is 12 dB making the dynamic range of the digitized signal 120 dB.

At the recording station, the digital signals are sent to a Columbia Personal Computer (an IBM-PC look-alike) that controls the digital recording of the signals. The signal is also sent to a digital-to-analog converter from which any one of the three channels may be input to a Helicorder (Figure 2). Paper records from the Helicorder offer a quick look at the seismic activity and are very useful in identifying problems with the seismometers. Time is provided to both the digital and analog recording devices by a Kinemetrics satellite clock. The Columbia formats the data and time information for recording and then writes that data to one of two tape recorders (3-M 1/4" cartridge tape drives with controllers, assembled by Secondary Computer Storage). The 1/4" magnetic tape cartridges each have a capacity of 67 megabytes and can store 38 hours of data. Using two transports, a total of 76 hours of data can be recorded unattended. Control of the tape drives and recording by the Columbia is provided through two programs, *scs* and *rai*. Descriptions of these programs and the data format used to record on the 1/4" cartridges can be found in Appendix A.

As part of the station operation, each new tape cartridge must be certified and a table of bad blocks generated and stored on the tape. The bad block information allows the tape drive to skip those blocks when recording. Because the Columbia is not a multitasking machine, a second computer must be used for certification

BEST COPY AVAILABLE

and playback. At RAI, a SUN Microsystems workstation is used for these tasks as well as for data analysis. Descriptions of the certification and playback routines may be found in Appendix B.

System Response

The broad-band seismometer displacement response function of the Streckeisen instruments is given by:

$$T(\omega) = \frac{-i\omega^3 A}{-\omega^2 + 2i\omega\omega_0 h_0 + \omega_0^2} \quad \frac{\omega_1^2}{-\omega^2 + 2i\omega\omega_1 h_1 + \omega_1^2} \tag{1}$$

where

$\omega_0 = 2\pi/20\text{sec}$

$h_0 = 1/\sqrt{2}$

$\omega_1 = 2\pi/0.2\text{sec}$

$h_1 = 0.6235$

$A \approx 12000\text{Vsec/m}$

This equation describes a broad band seismometer that is flat to velocity from .05 to 5 Hz, rises at 12 dB/octave (for constant input velocity) from DC to .05 Hz, and falls at 12 dB/octave at frequencies above 5 Hz. To improve the high frequency response, one of the low-pass filters (corner frequency of 5 Hz) was removed so that the modified displacement response for station SRNY is given by:

$$T_{SRNY}(\omega) = T(\omega)\frac{i\omega + \omega_1}{\omega_1} \tag{2}$$

Substituting $s = i\omega$

$$T_{SRNY}(\omega) = \frac{s^3 A\omega_1 (s + \omega_1)}{(s + a)(s + b)(s + c)(s + d)} \tag{3}$$

BEST COPY AVAILABLE

where

$$a = h_0\omega_0 + \omega_0(h_0^2-1)^{1/2}$$
$$b = h_0\omega_0 - \omega_0(h_0^2-1)^{1/2}$$
$$c = h_1\omega_1 + \omega_1(h_1^2-1)^{1/2}$$
$$d = h_1\omega_1 - \omega_1(h_1^2-1)^{1/2}$$

Equation (3) has three zeros at s=0 and one at $s=-\omega_1$. There are poles at s=−a, −b, −c and −d. The amplitude factor, A, is given on calibration sheets for each individual instrument. For the vertical component A=11,920 V sec/m so that

$$A\omega_1 = 3.745 \times 10^5 \text{ V/m}$$

The digitizer supplied by Refraction Technology at the 12 dB gain setting gives 4.77×10^{-6} V/du so that

$$A_d\omega_1 = 78.506 \text{ du/nm}$$

where A_d is the amplitude factor in du sec/nm.

TABLE 1

Poles and zeros of the SRNY Wielandt Seismometers

poles	zeros
−.22214 ± *i* .22214	−31.4159
−19.5878 ± *i* 24.5617	0
	0
	0
Poles of the anti-alias filter	
−14.165 ± *i* 143.82	
−41.950 ± *i* 138.29	
−68.123 ± *i* 127.45	
−91.678 ± *i* 111.71	
−111.71 ± *i* 91.678	
−127.45 ± *i* 68.123	
−138.29 ± *i* 41.950	
−143.82 ± *i* 14.165	

Data are digitized at 60 samples/sec and a 16 pole Butterworth anti-alias filter

BEST COPY AVAILABLE

with a 23 Hz corner frequency is applied to the data before digitization. The poles and zeros of the seismometers and of the anti-alias filter are given in Table 1. Figure 3 shows the theoretical velocity response at SRNY both with and without the anti-alias filter.

Station Performance

In general the station performance of SRNY has been excellent. For the first 6 months of 1986 the station was down for an average of about 40 minutes per day, or 2.8% of the time. On several occasions the station has run for 17 days or more without loss of data. The causes of data loss can usually be placed in one of three categories: 1) computer/tape drive malfunction, 2) power loss or 3) maintenance. On one occasion a lightning strike near the seismic vault damaged the electronics in the vault. During repairs, protection was added to the cards to prevent this from happening again.

By far the most persistent problem has been with the Columbia PC and the 1/4" tape drives and controllers. In the first year of operation the tape drives were extremely sensitive - just removing a tape and inserting a new one in the inactive drive was enough to cause the active tape drive to crash. At that point we discovered that one of the tape drives was bad and replaced it. The performance of the station improved markedly.

With only two tape drives, one had to be free for new tape certification and data playback and thus two tape controllers were necessary. On occasion, while both controllers were in operation, the system would crash. This problem was remedied by purchasing a third tape drive and placing both data-recording tape drivers on a single controller. After these modifications were made to the hardware, the amount of data loss due to computer and tape drive errors decreased significantly. Computer and tape drive crashes, though, are still the major source of data loss for SRNY.

Power loss becomes a problem primarily in the late summer months when thunderstorms are frequent in southern New York and in the winter during heavy snow and ice storms. Over the 30 months of the stations' operation (May, 1984 to November 1986), data was lost because of power failures 23 times. A backup power supply could remedy this problem but would be very expensive.

BEST COPY AVAILABLE

III. ANALYSIS TECHNIQUES

A number of analysis techniques were used to complete the work presented in this report but the vast majority of the processing was devoted to event location and depth determination. Adaptive Polarization Analysis (*apa*) was the most useful for single station event location, and polarization state filters combined with *apa* and synthetic seismogram depth sections proved to be valuable for depth determination.

Polarization Analysis

Polarization analysis of a three-component wavefield is very useful for determining the vector particle motion characteristics such as the degree of polarization, direction of propagation and ellipticity. This information can be used to design filters that emphasize or eliminate waves having specific polarization properties. In seismology, this method has been applied to analyze and filter waves coming from certain directions, or having rectilinear or elliptical particle motion, and to discriminate against isotropic noise (Sutton and Pomeroy, 1963; White, 1964; Archambeau *et al.*, 1965) .

Polarized arrivals can be enhanced, their wave type identified, and their direction of propagation, as well as their phase velocity for body waves and ellipticity for Rayleigh waves, determined. This information can then be used for phase identification, epicentral location, source depth determination, earth structure studies, ...etc. Data filtered for polarized signal are more amenable to comparison with synthetic seismograms, providing a better determination of relevant parameters.

The polarization state method was proposed by Samson (1977) for the analysis and filtering of seismograms. It makes use of the spectral matrix, which is the frequency domain equivalent of the cross-correlation matrix of the data, smoothed over a frequency window. Various spectral estimators can be obtained from the spectral matrix, such as the degree of polarization, the degree of rectilinear polarization, a detector for signal in a specific "pure state" (i.e. completely polarized) or with specific polarization characteristics. Such estimators can then be used to filter the data in order to discriminate against unpolarized noise or to enhance signal in some specific polarization state (Samson and Olson, 1981). Since the polarization characteristics of seismograms continuously change with time, such filters have to be data-adaptive: a sliding time window of data is analyzed and a filter is specifically designed for that window. Polarization properties are determined and used not only as a function of time, but also as a function of frequency, since the processing is done in the frequency domain. This is an advantage that methods which operate purely in the time domain do not have.

BEST COPY AVAILABLE

In the Adapative Polarization Analysis method developed at RAI, the horizontal components are adaptively rotated to the time varying radial and transverse directions and the time variable azimuth and apparent angle of incidence are given. This process helps in the identification of phases. Below we present the theory behind this method assuming rectilinear motion at a constant azimuth and angle of incidence. Later in the discussion, we will consider simultaneous arrivals from different directions.

We seek to determine the azimuth and angle of incidence over a small time window; one that is at least as long as one or two cycles of the predominant frequency. The azimuth is determined by examining the zero lag cross covariance between the two horizontal components as a function of azimuth angle. One of the angles at which this function is zero is the azimuth of the predominant particle motion. The horizontal components of motion as functions of the north (N) and east (E) horizontals and the azimuth (θ) are written:

$$\begin{aligned} H_1(t) &= N(t)\cos\theta + E(t)\sin\theta \\ H_2(t) &= E(t)\cos\theta - N(t)\sin\theta \end{aligned} \tag{4}$$

and, the cross-covariance between H_1 and H_2 at zero lag is:

$$ccv_o = \frac{1}{n}\sum_{i=0}^{n}\bar{H}_1(t+i\Delta t)\bar{H}_2(t+i\Delta t)$$

where $\bar{H}(t) = H(t) - \mu_H$, μ_H is the mean value of H(t) over the interval, and Δt is the sampling interval. In terms of $\bar{N}$ and $\bar{E}$:

$$ccv_0(\theta) = a\cos 2\theta + b\sin 2\theta \tag{5}$$

where

$$a = \frac{1}{n}\sum_{i=0}^{n}\bar{N}(t + i\Delta t)\bar{E}(t + i\Delta t)$$

$$b = \frac{1}{n}\sum_{i=0}^{n}[\bar{E}^2(t + i\Delta t) - \bar{N}^2(t + i\Delta t)]/2$$

BEST COPY AVAILABLE

Solving for θ at $ccv_0\theta = 0$:

$$\theta = \tan^{-1}(-a/b)/2 \qquad (6)$$

The azimuth θ obtained from (6) will be between -45° and 45° and could represent any one of four directions; the direction of particle motion, its supplement, its transverse, or the transverse supplement. Without using the vertical component, the direction obtained from (6) can be determined with a 180° ambiguity by examining the behavior of (5). The zero lag cross-covariance as a function of azimuth given by (5) is a sinusoid. Suppose that the θ determined from (6) aligns the H_2 component with the direction of maximum particle motion. Increasing this θ in (5) will place the direction of particle motion between the H_1 and H_2 components and the value of ccv_0 will increase. Conversely, if H_1 is aligned with the direction of particle motion by (6) then increasing θ in (5) will decrease ccv_0. Thus, when the slope of the sinusoid given by (5) at the azimuth determined in (6) is positive, then θ is transverse to the direction of particle motion (or its supplement) and when the slope of the sinusoid given by (5) at the azimuth determined in (6) is negative, then θ is the direction of particle motion (or its supplement). Rather than computing the slope from the derivative of (5) with respect to θ, we can find its sign by examining (5) at $\theta = 0$ where $ccv_0(0) = a$, If the signs of a and the θ found from (6) are similar (i.e. both have the same sign), then the slope is negative and θ is the direction of particle motion or its supplement. If the signs are dissimilar, then the slope is positive and the direction of particle motion is at either $\theta + 90°$ or $\theta - 90°$. The direction of particle motion can be either longitudinal or transverse to the propagation direction depending on whether the particle motion is *P/SV* or *SH*. If the azimuth from the event to the station is known, then particle motion between ± 45° of that azimuth can be considered radial and between 45° and 135° or −45° and −135° can be considered transverse. The azimuth obtained from (6) together with the assumed azimuth to the event can be used to rotate the horizontal components to the radial and transverse directions at the center of the window. The window is then advanced one sample and the process repeated.

The apparent angle of incidence is calculated in much the same manner as the azimuth. For this measurement, the adapted radial and vertical components are used as the orthogonal components from which the angle of incidence is determined.

An estimate of the relative accuracy of the azimuth and angle of incidence measurements is obtained through the maximum value of the zero lag cross-correlation function. At its maximum value, where the predominant direction of motion bisects H_1 and H_2, the zero lag cross-correlation function ($ccf_0(\theta + 45°)$) will be between 0 and 1, inclusive. A large value is indicative of strong rectilinear motion

BEST COPY AVAILABLE

over the window and a small value indicates the lack thereof. Where there is little or no rectilinear motion, confidence in the results obtained is also small and we expect the error to be close to 90°. Conversely, a large value for $ccf_o(\theta + 45°)$ indicates strong rectilinear motion and should have an error close to 0°. This subjective error evaluation can be written:

$$\text{error} = 90° (1 - ccf_o(\theta + 45°)).$$

Error determined in this manner is not an absolute quantity but rather a relative measure of the accuracy of the value.

Because the method presented here relies on the determination of the predominant direction of motion, the question arises; "What angle would be determined if two uncorrelated signals arrived at the station at the same time from different directions?". Let the two uncorreiated signals be x(t) and y(t) where the standard deviations of x and y are equal and define the north and east components of motion as

$$\begin{aligned} N(t) &= jx(t) + ky(t) \\ E(t) &= rx(t) + sy(t) \end{aligned} \tag{7}$$

j, k, r, and s are scaling factors that can be set to simulate any combination of direction and amplitude for x and y. Substituting the values for N and E in (7) into equation (6)

$$\theta = \frac{1}{2}\tan^{-1}\left\{ \frac{\sum[(jx + ky)(rx + sy)]}{\sum[(r^2x^2 + s^2y^2 + 2rsxy - j^2x^2 - k^2y^2 - 2jkxy)]/2} \right\} \tag{8}$$

Because x and y are not correlated, the xy terms tend to zero as the length of the series gets large. Rewriting (8)

BEST COPY AVAILABLE

$$\theta = \frac{1}{2}\tan^{-1}\left\{ \frac{\sum 2(rjx^2 + ksy^2)}{\sum[(j^2 - r^2)x^2 + (k^2 - s^2)y^2]} \right\} \qquad (9)$$

Equation (9) may be used to predict θ for two time series passing a station at different azimuths. The worst case occurs when the two wavetrains are traveling at azimuths 45 ° apart, for when one of the signals is showing no correlation at its azimuth, the other will be at a maximum. If the two signals are orthogonal, then the proper azimuth would be chosen.

The above analysis is valid only in the case that the two signals are not coherent. When the two signals are perfectly coherent then the azimuth determined will be that of the vector sum of the two signals. Partial coherency would result in some combination of the completely non-coherent result and the perfectly coherent result.

In Figure 4, we show synthetic vertical and horizontal components to be used as the input to the polarization program. The modulated arrivals on the horizontal components represent a constant amplitude signal that rotates smoothly in azimuth. A constant amplitude vertical component maintains an unchanging angle of incidence. The results of processing this data with the polarization program are shown in Figure 5. There are six output traces; the vertical, adapted radial, and adapted transverse components of motion, the product of the radial and vertical traces, and the azimuth and apparent angle of incidence traces plotted with error bars. The radial trace exhibits a constant amplitude and the transverse component shows very little motion at all. Thus, the radial follows the predominant direction of motion. In the case of a short duration arrival, the rz trace would help to identify the first arrival and its direction but in this case, where the signal is continuous, rz has little use. The azimuth trace tracks the motion of the rotating arrival quite well and shows very little error. The same is true of the apparent angle of incidence trace where there is no change throughout the duration of the analysis.

For the second example, two independent samples of random noise were combined on the N, E and Z components of motion to simulate one set of arrivals traveling at 0 ° azimuth, 72 ° angle of incidence with an amplitude of 1000 and another set of arrivals traveling N45 °E, 55 ° angle of incidence and amplitude 547 (amplitudes are relative). In terms of the independent non-coherent time series x(t) and y(t):

BEST COPY AVAILABLE

$$N(t) = 3.0\,x(t) + y(t)$$
$$E(t) = y(t)$$
$$Z(t) = x(t) + y(t)$$

Using these numbers in equation (9), we obtain values of 6° for the azimuth and 67° for the angle of incidence (assuming an azimuth of 6° for the radial trace). The results of the polarization analysis are shown in Figure 6. The azimuth trace is centered about 6° over the length of the trace in excellent agreement with the theory. Error for the azimuth is large and is due to the fact that the two arrival sets are traveling at azimuths 45° apart; the worst possible case. For the apparent angle of incidence, the measured value of 67° is also in excellent agreement with theory and in this case the error is very small. The small error arises because the two arrival groups are traveling at a similar angle of incidence in the vertical plane at 6° azimuth.

The adaptive polarization analysis program is a useful tool for locating earthquakes when only a single three-component data set is available. The azimuth from the initial *P*-wave, where presumably the error will be smallest and no conflicting arrivals are present, combined with the distance obtained from the *S-P* time gives a fairly accurate location. An account of how well this procedure works on a set of data from both SRNY and the New York station of the Regional Seismic Test Network (RSNY) is given in the Detection and Location Capability section.

Synthetic Seismograms

Synthetic seismograms are an important part of the analysis procedure for determining the depth and orientation of an event as well as helping to verify velocity depth functions along the propagation path. Accurate depths for earthquakes can be determined employing phases such as *pP* and *sP* reflected from the surface near the source. At teleseismic distances, high frequencies are attenuated relative to the low frequencies and consequently the depth of shallow focus earthquakes is difficult to determine to better than 10 kilometers. The initial arrivals overlap the surface reflected phases and limit the ability to pick phases arriving within a second of each other. At local distances, however, there is still a substantial amount of high frequency energy in the coda and discrimination of these phases is easier.

Synthetic seismograms computed for a suite of depths show the sensitivity of the different seismic phases to depth of focus (Figure 7). Except for the direct arrival, the primary phases arrive earlier with increasing focal depth and the surface reflected phases arrive later. For this model, assuming that the arrivals could be picked to an accuracy of 0.1 seconds and that there are no other errors, the depth

BEST COPY AVAILABLE

could be determined to better than .5 km using a single station. Of course, the depth determination is extremely model dependent and misidentification of phases can lead to unreliable depths.

The locked mode seismogram synthesis program of Harvey (1981), was used for generation of the synthetics illustrated in this report.

Spectral Analysis and Filtering

The spectral analysis programs available allow standard power, Fourier, and signal-to-noise spectra as well as spectragrams. The spectragram plots power in dB as a grey scale with horizontal and vertical axes of time and frequency, respectively. Except for the spectragram, the dB and frequency limits, the amount of averaging between samples, and the frequency scale type (log or linear) are easily controlled by the user. In addition, the cursor may be used to obtain specific values for any point on the plot.

Filtering routines are also available but will not be described here as excellent descriptions can be found in most texts on digital filtering. All of these routines are described in detail in the Appendix B.

BEST COPY AVAILABLE

IV. NOISE, DETECTION, AND LOCATION

Noise Characteristics

Analyses of noise spectra at SRNY are shown in Figures 8 and 9 and a comparison to another system is shown Figure 10. All noise spectra shown are the instrument-corrected power spectra of displacement. Several vertical-component noise samples, each two minutes long, have been selected. Day versus night, different seasons and different weather conditions were examined.

Four noise spectra are plotted in Figure 8 and we discuss the general characteristics of these four samples which are representative of the range of observations. The highest noise levels are in the frequency band roughly between 0.08 and 0.4 Hz, the microseism band, and are attributed, principally, to ocean waves. Amplitude levels of the microseisms at SRNY (Figure 8A) vary by as much as 30 dB, and depend largely on the weather. Between about 0.4 and 1.8 Hz the noise power falls off sharply with a slope of -90 dB/decade or a rate of $f^{-4.5}$ in amplitude. At about 1.5 Hz this sharp negative slope suddenly changes and the power spectra rise slightly to a frequency of 3 Hz. The cause of this shelf-like feature is unknown. A similar flattening in noise spectral content has been observed at the noisier RSTN stations - RSSD in South Dakota, RSCP in Tennessee, and RSNY in New York (Rodgers *et al.*, 1986). Other studies show a change in the slope of spectral fall-off near 2 Hz, and it has been suggested that sources of noise above 2 Hz are different than those below 2 Hz.

Between 3 and 6 Hz the spectra appear to be falling off at about -50 dB/decade (Figure 8A). As can be seen in the blow up of higher frequencies (Figure 8B), the absolute levels vary considerably from one noise sample to the next. Above 6 Hz it is impossible to assign a characteristic slope. Amplitudes vary by as much as 15 dB. This suggests high levels of cultural noise, because in areas of low cultural noise the spectra are very stable in time for frequencies higher than 2 to 3 Hz (e.g. Bungum *et al.*, 1985). Several daytime samples at SRNY show a broad peak centered near 10 Hz. We do not yet know the source of this increased noise. It is probably cultural, but not necessarily confined to daytime noise sources because it is has been observed on a night-time noise sample as well. We also observe narrow peaks (up to 15dB in amplitude) at different frequencies (e.g. 3, 4, 7, 8, 9, 10, and 15 Hz) on different days and nights.

At quiet times, SRNY appears to be limited by system noise above about 6 Hz (Figures 9 and 10). The lower curve in Figure 9 is calculated from a 2 minute sample starting at 3:00 A.M. local time on July 26, 1986, whereas the upper curve - the same day - starts at 10:00 A.M. local time. Looking first at the quiet, night sample, a slope of approximately -50 dB/decade or $f^{-2.5}$ in amplitude fits the

BEST COPY AVAILABLE

data between about 3 and 6 Hz, but at frequencies greater than 6 Hz, the spectrum flattens out: this may be the level of system noise contamination. Between 20 Hz, the highest frequency shown in Figures 9 and 10, and the 30 Hz Nyquist frequency the spectrum follows the fall-off of the anti-alias filter. Thus, the source of the spectral flattening is in advance of the filter and not in the digital system or processing.

A comparison of the quiet SRNY noise power spectrum with five noise power spectra at the RSTN station in NY (RSNY) is shown in Figure 10. Noise studies at RSTN stations have been reported by Taylor (1981) and Rodgers *et al.*, (1986); Figure 10 is adapted from Rodgers *et al.*, (1986). Absolute noise levels at SRNY and RSNY are comparable. If, as is likely, the cause of spectral flattening above about 6 Hz at SRNY is system generated and could be eliminated, then at quiet times we might expect amplitude levels similar to RSNY above 6 Hz.

Detection and Location Capability

The detection and location capability of a single station is extremely important for studies of earthquake statistics and for the design of future seismic networks. We need to know how earthquake detection and location capabilities will be affected as a function of the density of seismic stations in operation. Changes in instrumentation as well as numbers of stations, will affect earthquake detectability. Since some sort of broad-band three-component instrument will probably be used in a national seismic network, we think it is important to know something of the detection and location ability of such instrumentation. In this section we evaluate the detection capability of SRNY as well as the location capabilities of SRNY and RSNY.

We used magnitudes and locations published in the Northeastern U.S. Seismic Network (NEUSSN) Bulletin for the period 7/84 through 3/85 plus selected, larger earthquakes published in the National Earthquake Information Service (NEIS) monthly bulletin from 4/85 through 10/86. On a plot of earthquake magnitude vs. distance from SRNY (Figure 11) we indicate which earthquakes are locatable (L), which were detected (D), and which were not detected (N). Table 2 is a list of the earthquakes analyzed in order of increasing distance from SRNY. Events we did not examine (from the NEUSSN Bulletins) are indicated by the small star symbol in Figure 11. The two dashed curves are sketched to suggest regions of locatable, detectable, and undetectable earthquakes from station SRNY with the instrumentation described in earlier sections.

Earthquakes that are merely detected and not located, exhibit lower signal-to-noise ratios than locatable earthquakes. For some, only the *S/Lg* portion of the wavetrain is visible above noise. For others, the *P*-wavetrain is barely visible

BEST COPY AVAILABLE

TABLE 2

Detection and Location Capability of SRNY

Distance degrees	Magnitude	Source	Date	detect Y/N	*S-P* Y/N	Azimuth Y/N
0.29	1.6	WCC	05/26/85	Y	Y	Y
0.40	2.2	WES	03/16/85	Y	Y	Y
0.71	2.3	WES	02/02/85	Y	Y(-)	N
0.77	2.1	WCC	11/27/86	Y	Y(-)	N
0.77	3.0	WCC	10/20/86	Y	Y	Y
0.89	2.2	LDO	01/26/85	Y	Y	Y
0.96	2.2		01/05/86	Y	Y	Y
1.02	2.4	LDO	08/12/84	Y	Y	Y
1.03	2.1	LDO	08/12/84	Y	Y	N
1.04	1.8(2.1)	LDO	12/15/84	Y	N	N
1.04	2.0	LDO	10/25/84	N	N	N
1.89	2.5	LDO	02/04/84	Y	Y(-)	N
2.07	3.0	WES	10/15/85	Y	Y	Y
2.10	2.5	LDO	12/08/84	Y	Y(-)	N
2.10	2.8	LDO	04/18/86	Y	Y	Y(-)
2.42	2.7	LDO	09/29/84	Y	Y	N
2.46	3.8	WES	10/25/86	Y	Y	Y
2.47	2.7	WES	10/25/86	Y	Y(-)	N
2.95	2.6	LDO	07/28/84	Y	N	N
3.12	2.3	WES	09/26/84	N	N	N
3.48	3.3	EPB	11/01/85	Y	Y	Y
3.77	2.4	LDO	08/02/84	Y	Y(-)	N
4.06	2.4	EPB	10/30/84	N	N	N
4.51	2.9	EPB	02/06/85	Y	N	N
4.85	2.4	EPB	01/18/85	N	N	N
5.11	4.2	NEI	08/17/84	Y	Y	Y
5.70	4.9	NEI	01/31/86	Y	Y	Y
6.09	4.2	EPB	09/19/86	Y	Y(-)	N
6.21	3.0	EPB	12/22/84	N	N	N
6.83	3.3	EPB	10/13/84	N	N	N
7.46	4.0	EPB	10/05/85	Y	N	N

BEST COPY AVAILABLE

above noise and a rough estimate of distance can be made, but the azimuth cannot be determined because the initial *P* is not well-recorded on the horizontals. For both cases, however, a general direction of the source (albeit with a 180° ambiguity) can be estimated from the relative amplitude of *S/Lg* recorded on two horizontal components since regional *S/Lg* is generally larger in the transverse direction.

The data in Figure 11 allow us to estimate the capabilities of station SRNY. For example, SRNY may detect magnitude 2 1/2 earthquakes up to a maximum distance of about four degrees. Magnitude 3.0 earthquakes are probably detectable up to distances of 5.5 degrees, magnitude 4.0's up to 7.5 degrees and perhaps farther.

To locate an earthquake we require a clear recording of *P* and *S* waves so that distance can be estimated using the relationship:

$$X = \frac{\Delta t \; V_P V_S}{V_P - V_S}$$

where X = distance, V_P and V_S are average crustal *P*- and *S*-wave velocities respectively, and Δt is the time between the *P*-wave and the *S*-wave arrivals. In addition, the *P*-wave must be clearly recorded on the two horizontal components to estimate azimuth using the adaptive polarization analysis program (*apa*) as illustrated in Figure 12. In Figure 13, eight single-station earthquake locations are plotted as triangles and, for comparison, network locations are plotted as circles (the differences between the two are presented in Table 3). Within a few degrees distance of SRNY, single-station locations are generally within 20 km of network locations. In addition, several locations of recorded blasts from eastern Pennsylvannia were found to be within about 20 km of the presumed quarries. Two locations, however, are 90 km from their network locations.

From Figure 13 we observe that most of the location errors result from a clockwise error in azimuth, with larger errors generally associated with greater ranges. Assuming that the mean error of 8.5° (from Table 3) results from an 8.5° misorientation of the horizontal sensors and recomputing the SRNY locations, a reduction in the average location error from 37 km (from Table 3) to less than 20 km is obtained. The maximum error is reduced to 54 km (earthquake of 10/15/85).

In summary, we estimate maximum distances for earthquake detectability from SRNY to be approximately 2 degrees for magnitude 2 earthquakes, 5.5 degrees for magnitude 3 earthquakes and about 8 degrees for magnitude 4 earthquakes. To clearly record and thus locate earthquakes, we estimate that a magnitude 2

BEST COPY AVAILABLE

earthquake can be located within 0.8 degrees of SRNY, a magnitude 3 earthquake within about 2.5 degrees, and a magnitude 4 up to 5 degrees away. Since magnitude 3 and greater earthquakes will often be recorded by several three-component stations, locations should improve with the additional data.

TABLE 3

SRNY Event List

Date	Network	SRNY Location	Δ Location	ΔΘ
10/23/84	43.59 ° N 73.94 ° W	43.45 ° N 73.72 ° W	23 km	−5 °
05/26/85	41.75 ° N 73.78 ° W	41.79 ° N 73.82 ° W	7 km	6 °
10/15/85	42.49 ° N 71.50 ° W	41.68 ° N 71.56 ° W	90 km	−21 °
10/19/85	40.99 ° N 73.83 ° W	40.89 ° N 74.13 ° W	27 km	−12 °
11/01/85	45.29 ° N 73.45 ° W	44.68 ° N 72.70 ° W	90 km	−11 °
10/20/86	42.62 ° N 74.12 ° W	42.57 ° N 73.96 ° W	15 km	−10 °
10/25/86	43.42 ° N 71.56 ° W	43.20 ° N 71.45 ° W	26 km	−4 °
11/23/86	40.96 ° N 74.82 ° W	41.08 ° N 75.00 ° W	21 km	−11 °

Using the same location technique, a set of seven earthquakes in the northeastern United States and the adjacent Canadian provinces were located with data recorded at station RSNY (44.548 ° N, 74.530 ° W). The seven events cover a wide range of azimuths around RSNY and are located between 69 and 440 km distant. All of the events have been independently located by the NEIS. The NEIS location, the RSNY single station location, and the differences in azimuth and location between the two locations are listed in Table 4 and shown in Figure 14.

When this location study was originally undertaken, it was found that all of the RSNY locations were rotated counterclockwise from the NEIS locations. These observations were presented to the RSTN network operators and a decision was made to pull the seismometers from the borehole and resurvey their orientation. This was done in the summer of 1986 and the orientation was found to be 17 ° off. Corrected values are shown in the Figure 14 and Table 4. The mean azimuth difference between the NEIS and RSNY locations is only −3 ° for these events and the single station locations are all within 45 km of the NEIS locations.

Improved estimates of event locations or location uncertainties can be made if more than one station is used. Station SRNY was in operaton during the 23 October, 1984 Adirondack earthquake and single station locations were obtained from both SRNY and RSNY. The two locations along with boxes delimiting areas less than one standard deviation in range and azimuth from the solutions,

BEST COPY AVAILABLE

are shown in Figure 15. The Lamont-Doherty Geological Observatory's multi-station location, which is based on approximately 25 stations with an azimuthal gap of only 43 degrees, falls within the small area of overlap of the error boxes.

TABLE 4

RSNY Event List

Date	NEIS Location	RSNY Location	Δ Location	Δ Θ
01/19/82	43.50 ° N 71.60 ° W	43.19 ° N 71.92 ° W	43 km	−10 °
08/31/82	43.21 ° N 74.20 ° W	43.20 ° N 74.07 ° W	11 km	4 °
05/29/83	44.50 ° N 70.41 ° W	44.45 ° N 70.56 ° W	12-8 km	−1 °
10/04/83	43.44 ° N 79.79 ° W	43.70 ° N 79.73 ° W	29 km	−3 °
10/07/83	43.94 ° N 74.26 ° W	43.97 ° N 74.27 ° W	3 km	0 °
10/11/83	45.21 ° N 75.77 ° W	45.28 ° N 75.58 ° W	17 km	−8 °
10/23/84	43.59 ° N 73.94 ° W	43.59 ° N 74.00 ° W	5 km	−2 °

Depth Determination

The depth determination capabilities of a single broad-band station were examined using eight local and regional earthquakes and one quarry blast. The events were chosen for their size, location, and availability of data. A list of these events is given in Table 5 along with location, depth, magnitude, strike, dip, and rake of the focal mechanism, the region (either New England or Grenville), and references for the focal parameters. The event and station locations are plotted in Figure 16, showing their spatial distribution. Many of the earthquakes in Table 5 have been studied by others and, for some, the focal depths and focal mechanisms are well determined and offer an excellent base of comparison.

In addition to reviewing the literature, we examined travel time data from local seismic networks originally used to invert for hypocentral location. In three cases the estimated error on focal depth was so large that to use the reported depth would be misleading. For these we indicate (Table 5) an unknown depth.

Figures 17A through 17I, all in essentially the same format, show the three-component seismograms for events in Figure 16. Most were recorded by the Regional Seismic Test Network (RSTN) station, RSNY, in northern New York and several of the recent events were recorded by SRNY. Just the *P*-wave portion of the seismograms is shown in these figures since depth phases are our primary interest. One of the keys to understanding the data and being able to compare them to synthetic seismograms is to extract discrete phase arrivals from the

BEST COPY AVAILABLE

TABLE 5

LIST OF EVENTS AND EVENT PARAMETERS

Date	Time	Lat	Lon	Depth	M	Strike	Dip	Rake	Reg	Refs
Jan 19, 1982	00:14:42.00	43.49	-71.59	3 - 11	4.5 M_b	280	75	-11	NE	1,2,3,4
Aug 31, 1982	10:16:58.10	43.21	-74.20	?	2.6 M_n	173	60	110*	G	1,5
May 29, 1983	05:45:49.80	44.50	-70.41	2	4.2 M_b	355	52	78	NE	1,6
Oct 07, 1983	10:18:46.10	43.94	-74.26	7-12	5.2 M_b	173	60	110	G	1,5,7,8,9
Oct 11, 1983	04:10:55.00	45.21	-75.77	12	4.1 M_{bLg}	071	75	98	G	1,10
Oct 23, 1984	06:26:21.71	43.59	-73.94	?	3.4 M_c	173	60	110*	G	1,5
Oct 02, 1985	21:10:07.00	42.90	-74.14	0	2.3 M_c	Chem	Ex		App(NE)	
Oct 19, 1985	10:07:40.30	40.98	-73.83	5	4.0 M_L	022	90	180	App(NE)	1,11
Oct 30, 1985	03:42:48.60	42.93	-74.11	?	2.7 M_{bLg}	018	60	156**	App(NE)	1,12

* Generic Adirondack Fault Plane Solution (from 7)
** Generic Mid-Hudson Fault Plane Solution (from 12)

References:

1. Preliminary Determination of Epicenters
2. Pulli et al., 1983
3. Brown and Ebel, 1985
4. Barstow et al., 1986
5. Regional Seismicity Bulletin of Lamont-Doherty Seismic Network
6. Ebel and McCaffrey, 1984
7. Suarez et al., 1984
8. Seeber et al., 1984a
9. Seeber et al., 1984b
10. Wahlstrom, 1983
11. Seeber et al., 1986
12. Houlday et al., 1984

BEST COPY AVAILABLE

P-coda waves. Along with the unfiltered or high-pass filtered data (the top three traces in Figures 17A through 17I), we present three-component state filtering of the data (the bottom three traces). These are filtered to pass rectilinear particle motion as a function of both frequency and time (as described above in the section on analysis methods). In all cases, polarization-state filtering serves to enhance some portions of the seismograms relative to other portions.

The synthetic seismograms were computed for frequencies from zero to 5 Hz. Regional geology in the Northeast required that two different velocity/attenuation models be used for the computation; a New England model for the events in New England and southern New York, and a Grenville model for events within the Grenville province (Figure 16, Table 6). The New England velocity model was derived by Taylor *et al.*, (1980) using regional travel times of *P*- and *S*- waves recorded across the Northeastern United States Seismic Network operated by several academic, governmental and private institutions in the northeast. The Grenville model was from unpublished refraction results. The frequency and depth dependent Q model for the New England model was adapted from work by Mitchell (1981) and a simple frequency dependent Q was used for the Grenville model. Although there are significant differences in the Q models, there is little effect on the synthetics, mainly because the ranges at which they are being computed are relatively small.

TABLE 6

New England Model (Taylor *et al.*, 1980)

Thickness	$V_P(km/s)$	V_S	$\rho(g/cm^3)$	Q_α	Q_β
2	6.0	3.5	2.5	$9Q_\beta/5$	$250f^{0.2}$
13	6.1	3.6	2.6		$500f^{0.2}$
25	7.0	4.1	2.9		$1000f^{0.2}$
	8.1	4.7	3.2		$3000f^{0.2}$
Grenville Model					
Thickness	V_P	V_S	ρ	Q_α	Q_β
4	6.1	3.5	2.5	$110+150f$	$5Q_\alpha/9$
31	6.6	3.7	2.7		
	8.1	4.6	3.2		

Synthetics were computed for each event at several depths with the reported focal mechanism listed in Table 5. The instrument response was convolved with the

BEST COPY AVAILABLE

synthetics for comparison to the data.

Station RSNY lies within the Grenville structure close to the boundary with the New England Structure. While the travel paths to RSNY from New England events must pass through both structures, the majority of the path is within the New England structure and so the New England structure may be a good approximation to the true path.

In Figures 18A through 18H we show the synthetic depth sections for the events in Table 5. Only the first 20 or so seconds are shown as we wish to emphasize the characteristics of the depth phases with focal mechanism, depth, range, and velocity model. Some of the phases are identified in the synthetic sections with labeled lines. Reflections off of the 13 km discontinuity in the New England model and the 4 km discontinuity in the Grenville model are indicated with an *i* (e.g. *PiP*). Mantle reflections are indicated by an *m*. The depth phases are characterized by progressively later arrivals with increased depth and the primary phases by either very little change in arrival time with depth for the direct arrivals or progressively earlier arrivals with increased depth. Notice that in some of the sections, the depth phases dominate, while in others, the primary phases dominate. This is a function of the theoretical radiation pattern predicted by the input focal mechanism. Because the input velocity structure will influence the take-off angle of each phase and hence its position on the focal sphere, both focal mechanism and velocity model are contributing to the relative amplitudes of primary and depth phases.

A comparison of the processed data shown in Figures 17A - 17H to the synthetic depth sections of Figures 18A - 18H gives the results shown in Table 7. The results in Table 7 are grouped into three categories from top to bottom:

1. results that agree well with the reported depths,
2. results for which depths are not well determined by network data, and
3. results which are in disagreement with the reported depths.

All but two of the events have depth estimates that are in agreement with the reported depths or had no reported depths. There are no significant differences between the magnitudes or ranges of the two events that would account for the discrepancy. The most probable explanation for the discrepancy between the depth estimates of the two events is that both the Maine and Ontario events were emergent (Figures 17C and 17E) making the depth phase identification and synthetic match difficult.

Although this implies that our depth estimates are in error rather than those of the reported depth, we cannot be certain which is the more accurate. The

BEST COPY AVAILABLE

reported depths of both Maine and Ontario mainshocks were deduced from aftershock depths, well-constrained by data collected from portable instruments close to the epicenters. If the mainshocks indeed occurred at the same depths as the aftershocks, then our one-station depth estimates for these two earthquakes are incorrect.

TABLE 7

Source Depths of Northeast U.S. Earthquakes

Date	Event	Magnitude	Reported Depth	This Study
Oct 07, 1983	Goodnow	5.2 m_b	7-12	7-10
Jan 19, 1982	New Hampshire	4.5 m_b	3-11	6
Oct 19, 1985	Ardsley	4.0 M_L	5	4.5-5
Oct 02, 1985	Quarry	2.3 M_C	0	0
Aug 31, 1982	Adirondack	2.6 M_N	?	4
Oct 23, 1985	Adirondack	3.4 M_C	?	13
Oct 30, 1985	Amsterdam	2.7 m_{bLg}	?	3
May 29, 1983	Maine	4.2 m_b	2	9
Oct 11, 1983	Ontario	4.1 m_{bLg}	12	5-6

BEST COPY AVAILABLE

V. SUMMARY

For 2 1/2 years, the broad-band, three-component digital station SRNY in Stone Ridge, New York has been collecting data for the NRC. RAI has analyzed that data and the station's performance for the purpose of evaluating the usefulness of broad-band three-component seismic stations in the United States. In general, our experience has been very good although we do have recommendations for future generations of broad-band stations.

The Wielandt sensors are excellent. We have had very little trouble with them and expect that they will continue to operate flawlessly. For local seismicity studies, however, the 5 Hz low-pass corner frequency is limiting, especially for low magnitude events. Above 6 Hz sensitivity is limted by system noise at quiet times. We recommend that an additional set of sensors be included covering the frequency band from 1 Hz to 100 Hz.

The 16 bit gain ranging format has allowed us to record with a 120 dB dynamic range and has been fairly reliable. With 24 bits digitizers on the horizon, new designs could increase the dynamic range of the recording system and eliminate the loss of resolution inherent in gain ranging systems at low gain.

The recording systems' (Columbia PC and 1/4" tape drives) performance has been under our expectations. We have had repeated trouble with the drives and PC crashing for no obvious reason. In addition, it would not be able to handle the increase in sample rate or number of sensors that we recommend for future systems. We also recommend that a better recording medium be found. Although the 1/4" tapes hold 67 megabytes of data, the data retrieval process is slow and a high speed random access medium would greatly improve the system.

The major advantage of the present system is its price. To make the improvements recommended here will certainly increase the cost of the recording systems although we feel that the additional cost is justified for improved data quality, system versatility, and data retrieval.

We have shown in this report that a single three component station is a valuable tool for earthquake location and depth determination. We also recognize that a single three-component station is a not a substitute for a network of seismometers. Consistently, more confidence is placed on network locations than on single station earthquake locations. A network can also provide valuable information about the focal mechanism that is difficult or impossible to obtain from a single three component station. A dense network of three component and strong motion instruments would be ideal. However, if the total number of data channels is fixed, then a network of three component stations must sacrifice station density

BEST COPY AVAILABLE

for the advantages of three component data. The solution is to design a network containing single component stations, three component stations, and strong motion three component stations.

Two of the factors that fix the total number of channels available are the data transmission costs for a satellite telemetered network and the volume of data being recorded. An easy way to reduce both problems is to use event triggering on the high data rate channels and record continuously at low data rates only on a subset of the network stations. The continuous recording would provide a record of general seismicity against which the triggered channels could be compared.

The event triggered continuous recording network of vertical component stataions, three component station and strong motion three component stations described above attempts to utilize the advantages of each station type and thus maximize the network usefulness.

BEST COPY AVAILABLE

REFERENCES

Archambeau, C. B., J. C. Bradford, P. W. Broome, W. C. Dean, E. A. Flinn, and R. L. Sax, "Data processing techniques for the detection and interpretation of teleseismic signals," *Proc. IEEE*, vol. 53, pp. 1860-1884, 1965.

Barstow, N. L., J. A. Carter, and A. Suteau-Henson, "Focal depths of shallow local earthquakes from comparison of polarization filtered data with synthetics," *abstr. Earthquake Notes*, vol. 57, No. 1, p. 18, 1986.

Brown, E. J. and J. E. Ebel, "An investigation of the January 1982 aftershock sequence near Laconia, New Hampshire," *submitted to Earthquake Notes*, 1985.

Bungum, H. S., S. Mykkeltveit, and T. Kvaerna, "Seismic noise in Fennoscandia with emphasis on high frequencies," *BSSA*, vol. 75, pp. 1489-1514, 1985.

Ebel, J. E. and J. P. McCaffrey, S. J., "Hypocentral parameters and focal mechanisms of the 1983 earthquake near Dixfield, Maine," *Earthquake Notes*, vol. 55, No. 2, pp. 21-24, 1984.

Harvey, D., "Seismogram synthetics using normal mode superpostion: the locked mode approximation method," *Geophys. J. Roy. Astr. Soc.*, vol. 66, pp. 37-69, 1981.

Houlday, M., R. Quittmeyer, K. Mrotek, and C. T. Statton, "Recent seismicity in north and east-central New York State," *Earthquake Notes*, vol. 55, No. 2, pp. 16-24, 1984.

Mitchell, B. J., "Regional variation and frequency dependence on Q_β in the crust of the United States," *BSSA*, vol. 71, No. 5, pp. 1531-1538, 1981.

Pulli, J. J., J. C. Nabelek, and J. M. Sauber, "Source parameters of the January 19, 1982 Gaza, New Hampshire earthquake," *abstr. Earthquake Notes*, vol. 54, No. 3, pp. 28-29, 1983.

Rodgers, P. W., S. R. Taylor, and V. K. Nakanishi, "System and site noise in the regional seismic test network," *Lawrence Livermore Laboratory USRL-94073 Preprint*, 1986.

Samson, J. C., "Matrix and stokes vector representations of detectors for polarized waveforms: theory with some applications to teleseismic waves," *Geophys. J. Roy. Astr. Soc.*, vol. 51, pp. 583-603, 1977.

Samson, J. C. and J. V. Olson, "Data-adaptive polarization filters for multichannel geophysical data," *Geophysics*, vol. 46 No. 10, pp. 1423-1431, 1981.

Seeber, L., E. Cranswick, N. Barstow, J. Armbruster, G. Suarez, K. Coles, and C. Aviles, *Grenville structure and the Central Adirondack seismic zone including the October 7, 1983 mainshock-aftershock sequence Canadian Geophysical Union Meeting*, Halifax, Nova Scotia, 1984a.

BEST COPY AVAILABLE

Seeber, L., E. Cranswick, J. Armbruster, and N. Barstow, "The October 1983 Goodnow, NY aftershock sequence; regional seismicity and structural features in the Adirondacks," *AGU abstr.*, vol. 65, No. 16, p. 239, 1984b.

Seeber, L., J. G. Armbruster, and D. Coyle, "A prolonged, but spatially concentrated earthquake sequence at the northern outskirts of New York City," *abstr. SSA, Earthquake Notes*, vol. 57, No. 1, p. 18, 1986.

Suarez, G., L. Seeber, C. Aviles, and E. Schlesinger, "The Goodnow, NY earthquake: results of a broad band teleseismic analysis," *AGU abstr.*, vol. 65, No. 16, p. 239, 1984.

Sutton, G. H. and P. W. Pomeroy, "Analoganalysis of seismograms recorded on magnetic tape," *J. Geophys. Res.*, vol. 68, pp. 2791-2815, 1963.

Taylor, S. R., M. N. Toksoz, and M. P. Chaplin, "Crustal structure of the Northeastern United States: Contrasts between Grenville and Appalachian Provinces," *Science*, vol. 208, pp. 595-597, 1980.

Taylor, S. R., "Properties of ambient seismic noise and summary of nosie spectrum in the vicinity of RSTN sites," *LLNL UCID-18928, Jan. 26*, 1981.

Wahlstrom, R., "The North Gower, Ontario, earthquake of 11 October, 1983; focal mechanism and aftershocks," *submitted to Earthquake Notes*, October 1985.

White, J. E., "Motion product sesismograms," *Geophys.*, vol. 29, pp. 288-298, 1964.

Wielandt, E. and G. Streckeisen, "The leaf-spring seismometer: design and performance," *BSSA*, vol. 72, pp. 2349-2367, 1982.

AVAILABLE

FIGURES

BEST COPY AVAILABLE

BEST COPY AVAILABLE

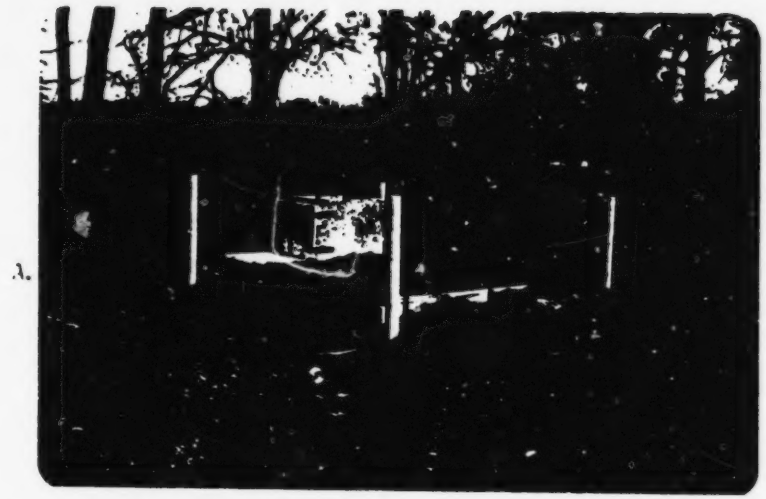

A.

B.

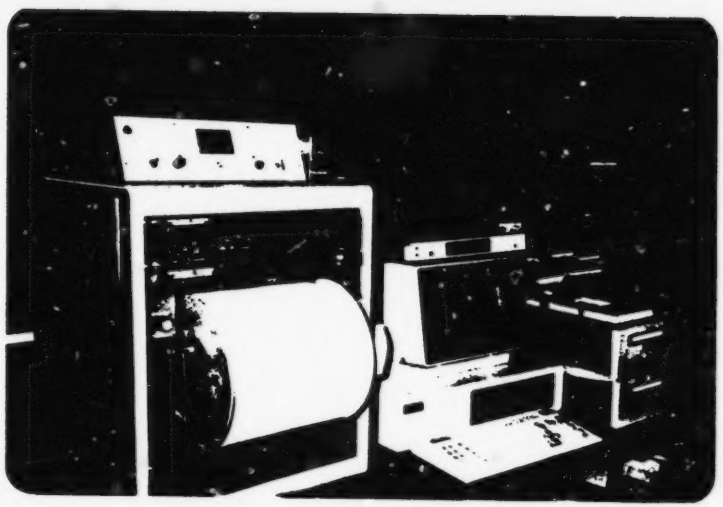

C.

Figure 1. **A- SRNY seismic vault exterior. B- Seismic vault interior. C- Recording station.**

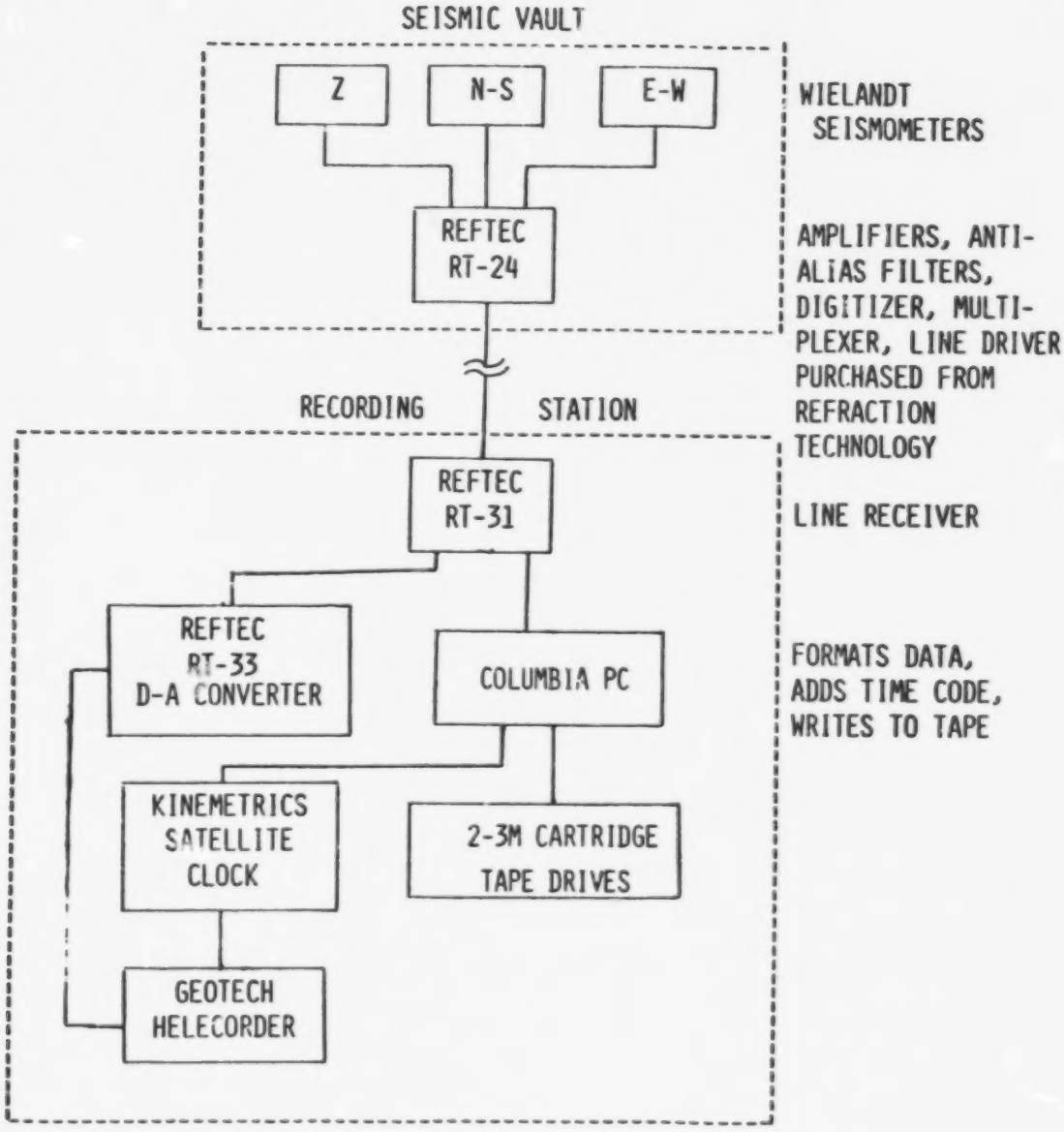

Figure 8. **Digital seismic recording system.**

BEST COPY AVAILABLE

BEST COPY AVAILABLE

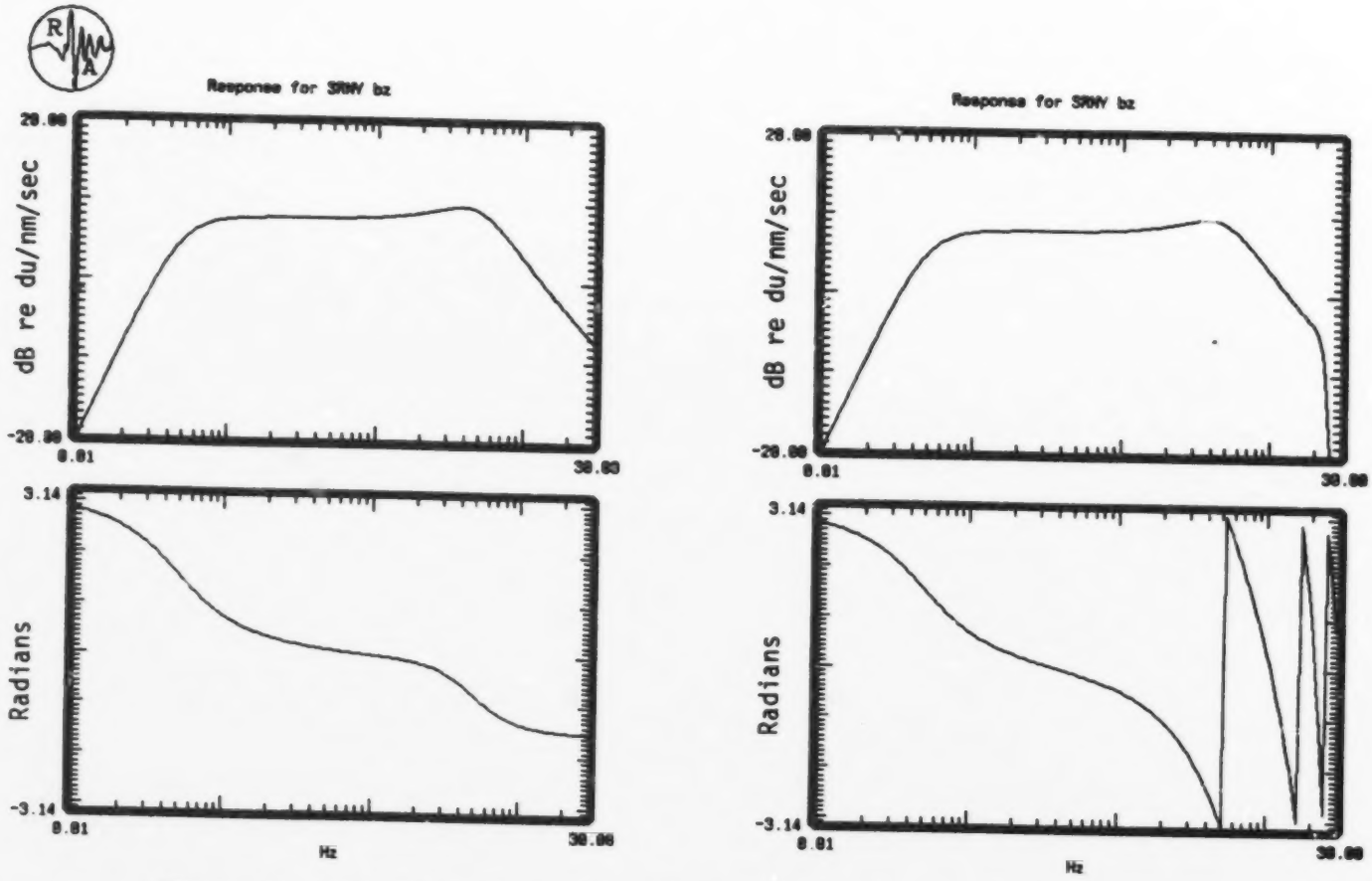

Figure 9. Velocity response of SRNY vertical seismograph (dB re one du/nm/sec and phase angle in radians): left and right, with and without anti alias filter, respectively. Horizontal response are the same except for slight difference in amplification constant, A.

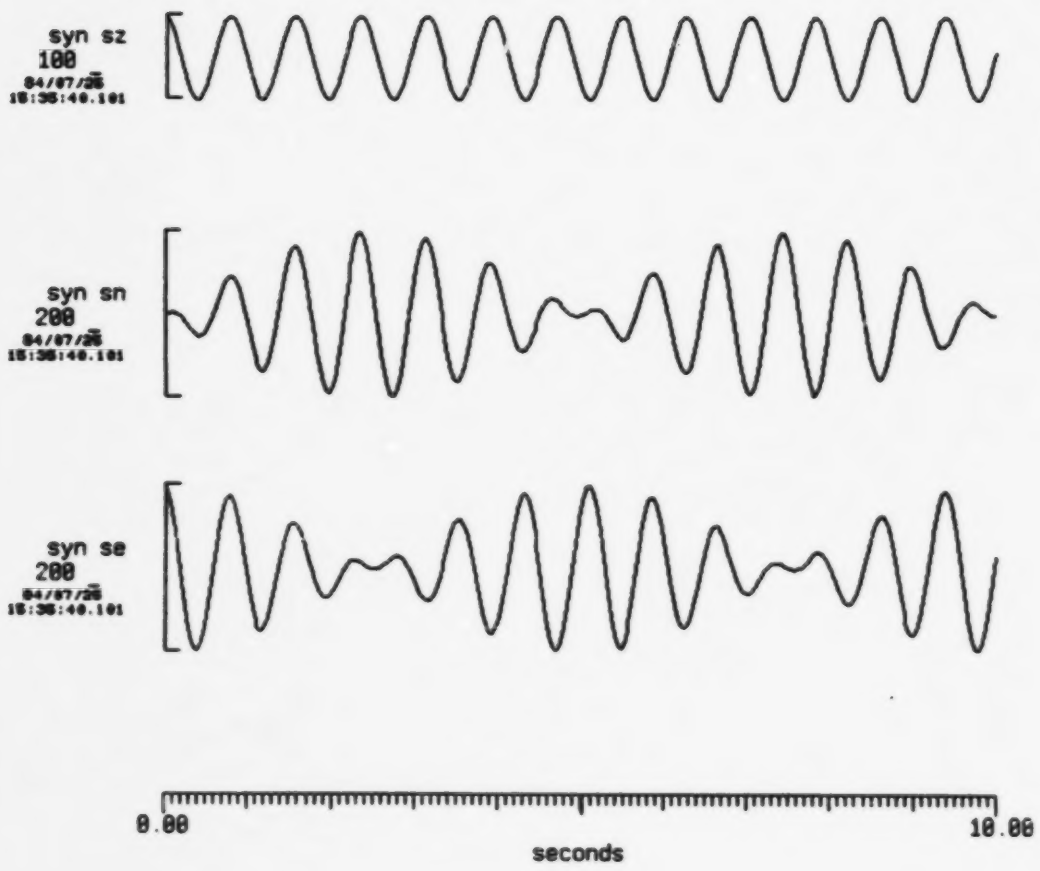

Figure 4. **Vertical (sz), north-south horizontal (sn), and east-west horizontal (se) components of a signal rotating in azimuth but with constant angle of incidence.**

BEST COPY AVAILABLE

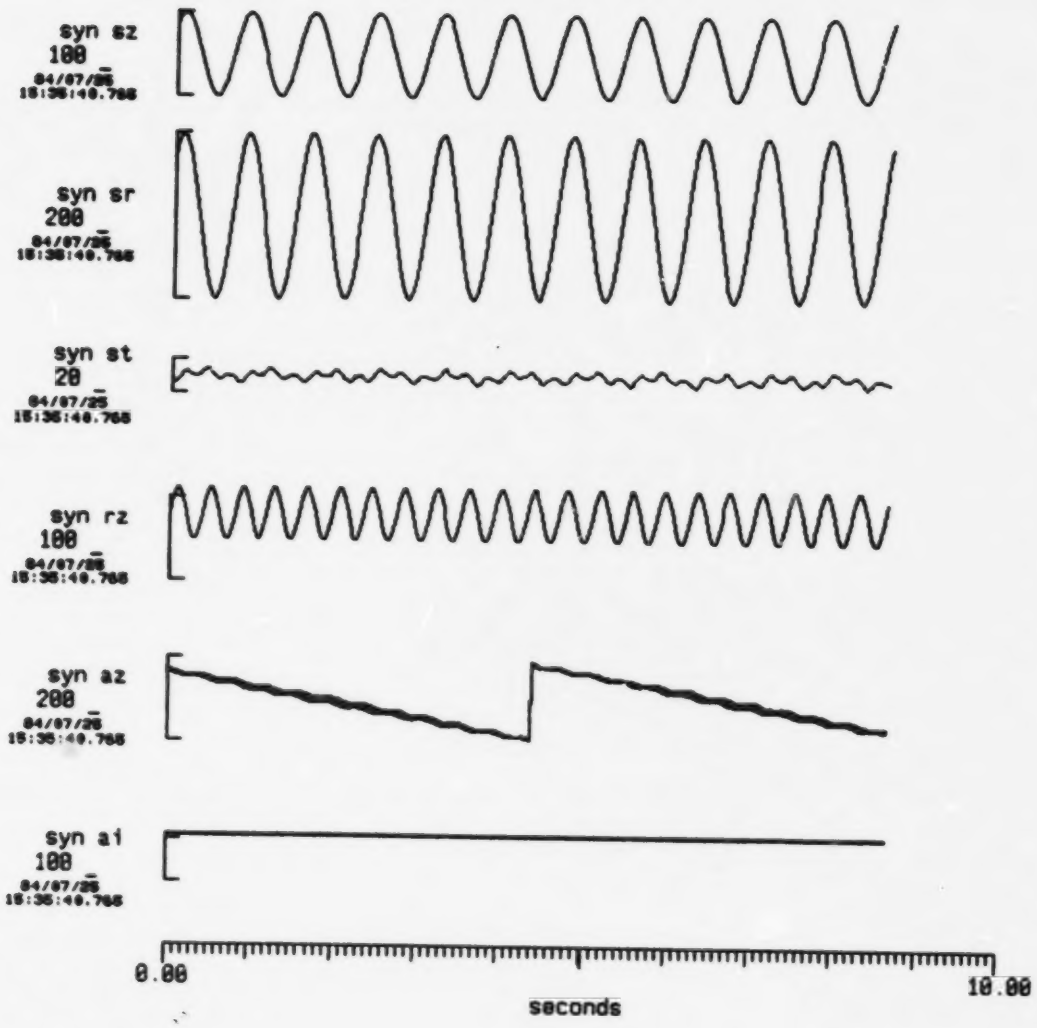

Figure 5. Output of the track program for a signal rotating in azimuth but with a constant angle of incidence. sz=vertical; sr=adapted radial; st=adapted transverse; rz=radial times vertical; az=azimuth with error bars; ai=angle of incidence with error bars.

BEST COPY AVAILABLE

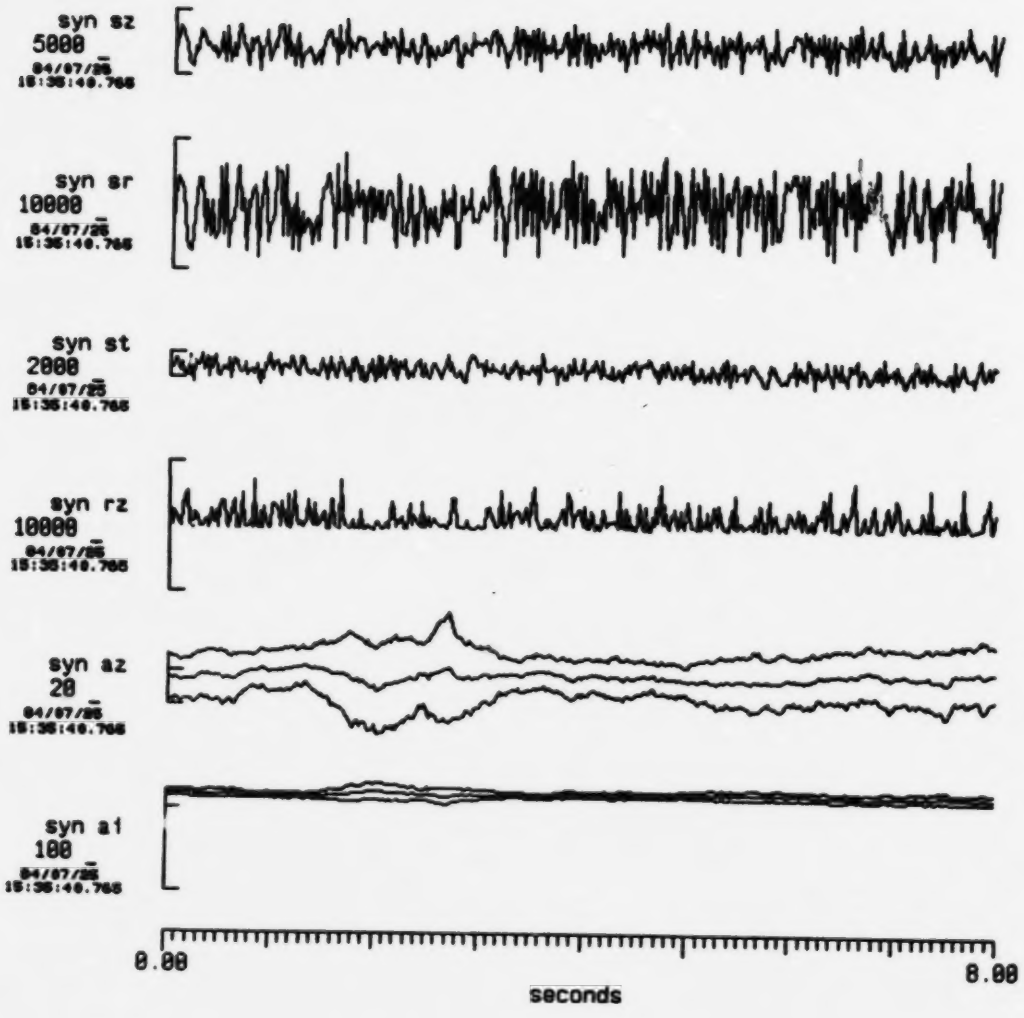

Figure 6. **Results of trying to track two different sets of random noise traveling in different directions. One set is traveling to the northeast; the other is traveling due north and is more than twice the amplitude of the first.**

BEST COPY AVAILABLE

BEST COPY AVAILABLE

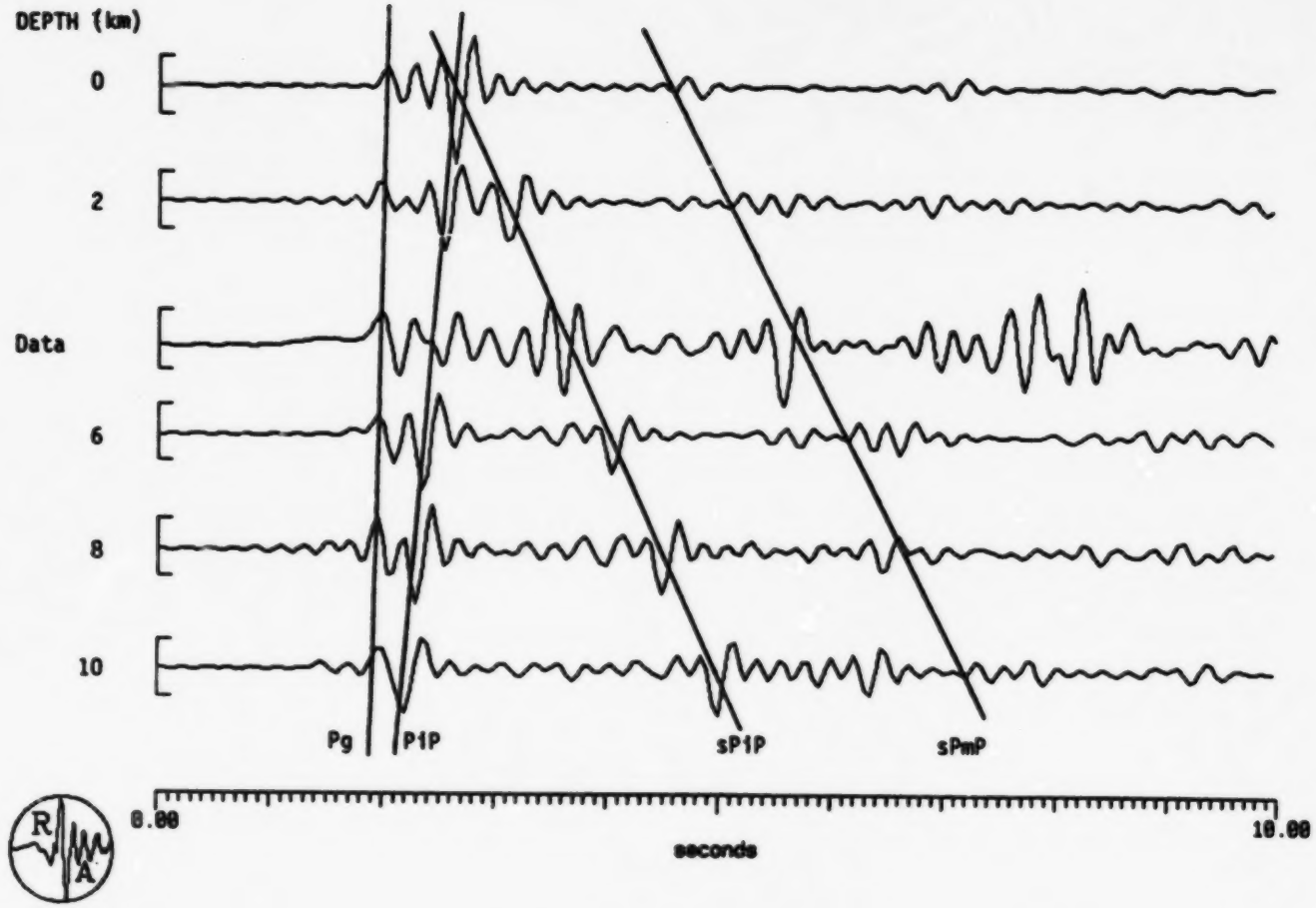

Figure 7. **Vertical component synthetic seismograms for the Ardsley, NY aftershock and data at station SRNY, Δ = 100 km.**

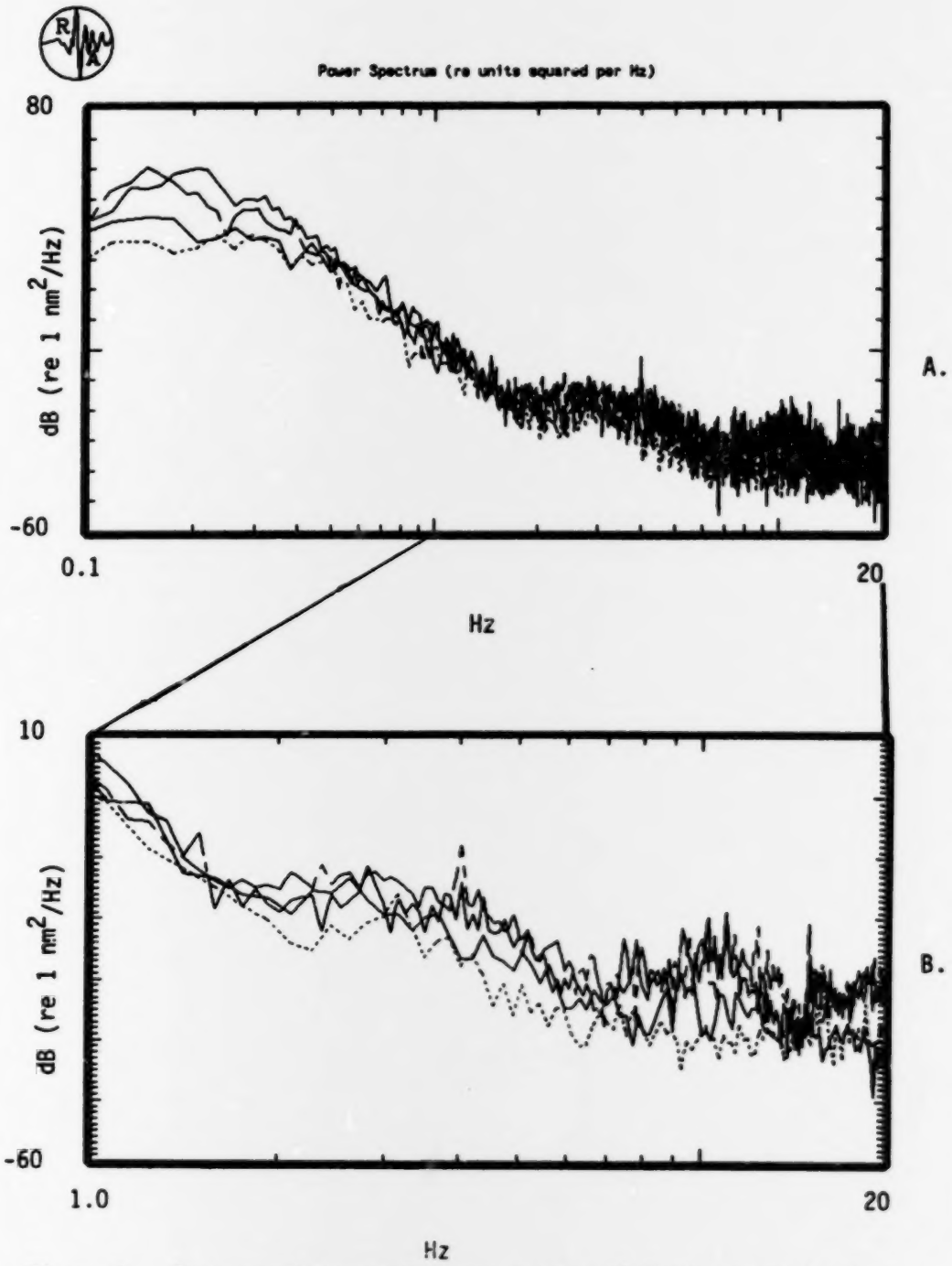

Figure 8. **Instrument-corrected power spectra of displacement for four noise samples in dB (re 1 nanometer^2/Hz). One sample is in the summer, three are in the fall; two are at night, two in the morning.**
8A shows the broad-band noise characteristics and 8B focuses on the higher frequencies - from 1.0 to 20.00 Hz

BEST COPY AVAILABLE

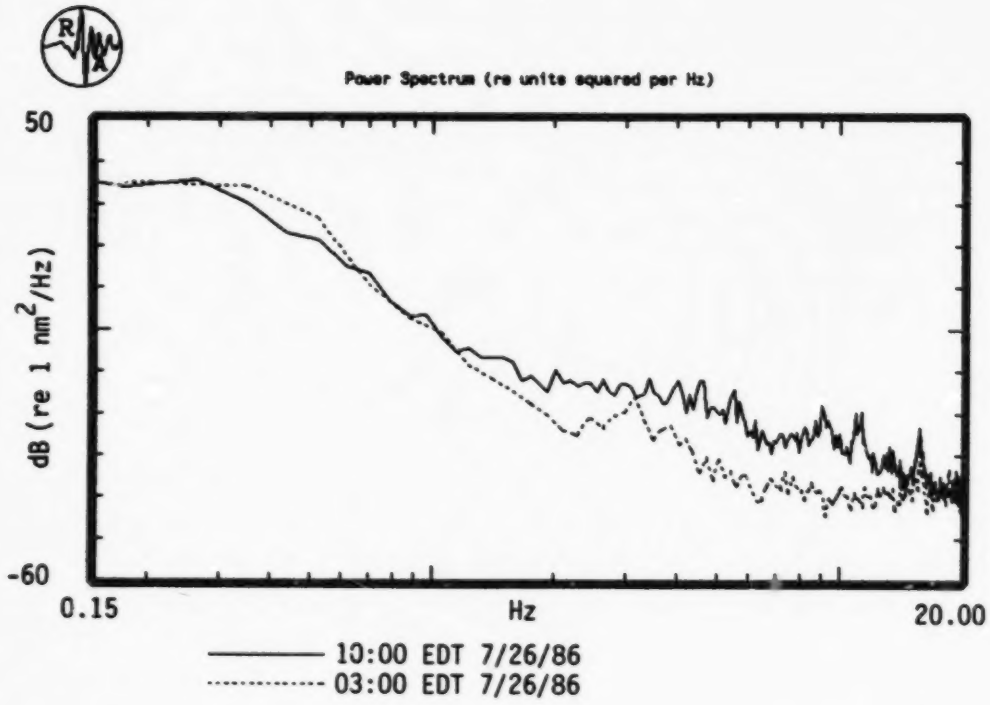

Figure 9. Power spectra for two times taken Saturday, July 26, 1986. The higher amplitudes between 1 to 15 Hz are from the noise sample beginning at 10:00 AM, local time. Note that the spike at about 15 Hz occurs on both day (10:00) and "night" (03:00) samples. Excepting the 15 Hz spike, the 03:00 spectrum is nearly flat above 6 Hz.

BEST COPY AVAILABLE

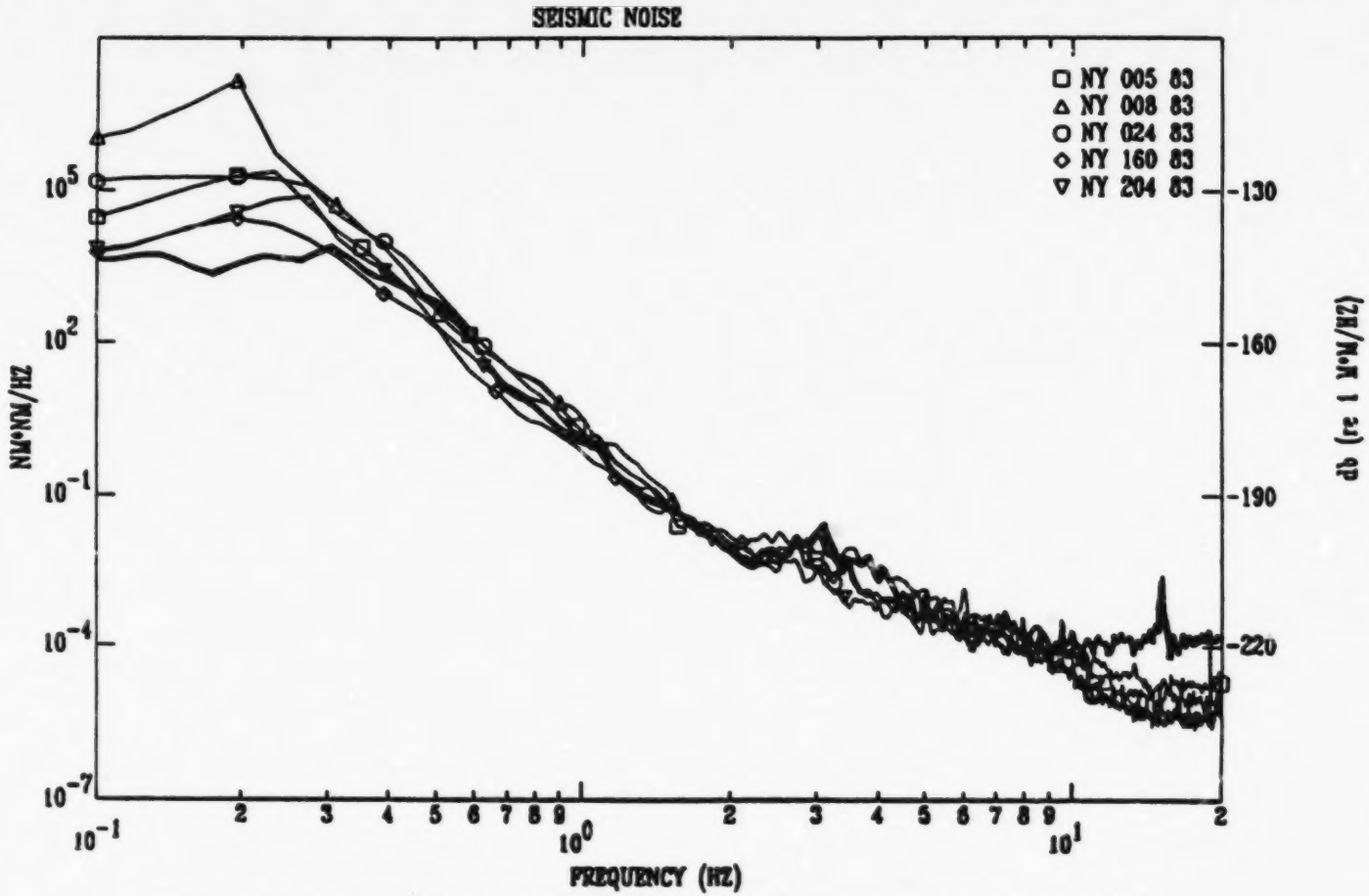

Figure 10. **Noise spectrum at SRNY (heavy line) compared to noise at RSNY. The microseisms (.1-.3 Hz) are quieter at SRNY for the particular sample chosen. At the high frequencies, though, SRNY flattens out, whereas the RSNY samples continued to fall-off to about 15 Hz (figure adapted from Rodgers *et al.*, 1986).**

BEST COPY AVAILABLE

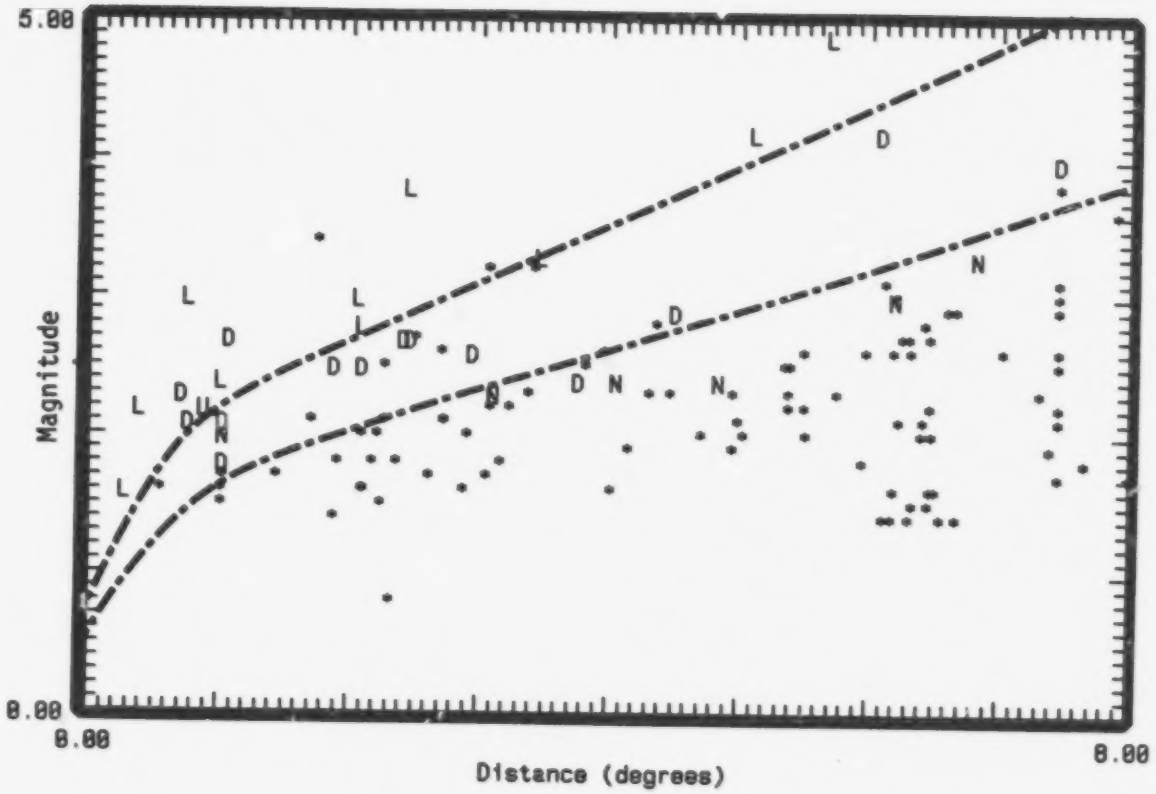

Figure 11. **Earthquake magnitudes versus distance from station SRNY. 'L' indicates locatable earthquakes, 'D' detected earthquakes and 'N' not detected earthquakes. Stars denote earthquakes not examined in this study. Most earthquakes are from the NEUSSN published bulletins for the period 7/84 through 3/85. Dashed lines are sketched to separate magnitude/distance regions of locatable, detectable and not detectable earthquakes.**

BEST COPY AVAILABLE

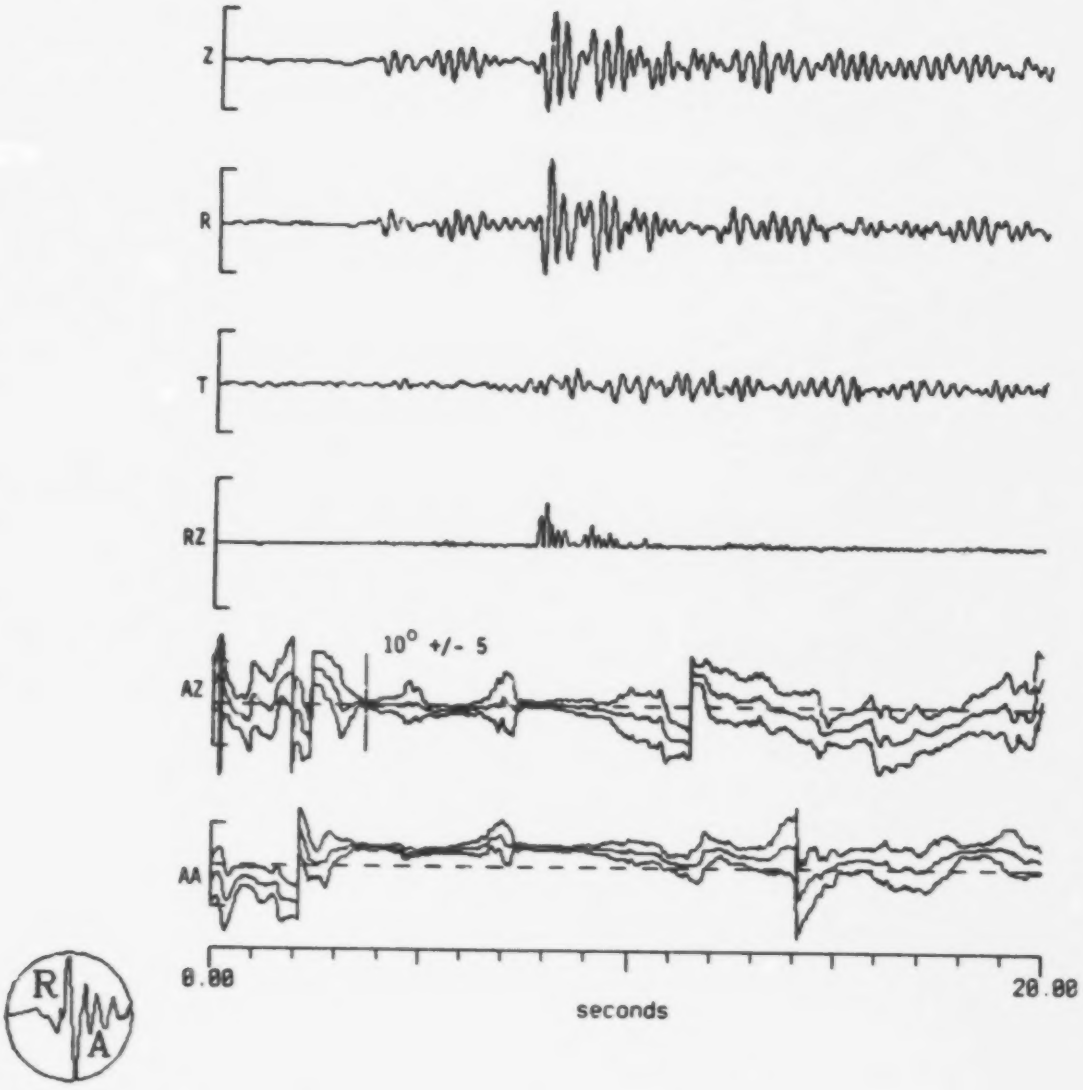

Figure 12. Adaptive polarization analysis of band pass filtered SRNY recording (1-4 Hz) of the Adirondack earthquake on 10/23/84. Labeled traces are: Z=vertical, R=adaptive radial, T=adaptive transverse, RZ=radial vertical product, AZ=back azimuth, receiver-to-source angle, AA=apparent angle of incidence.

BEST COPY AVAILABLE

BEST COPY AVAILABLE

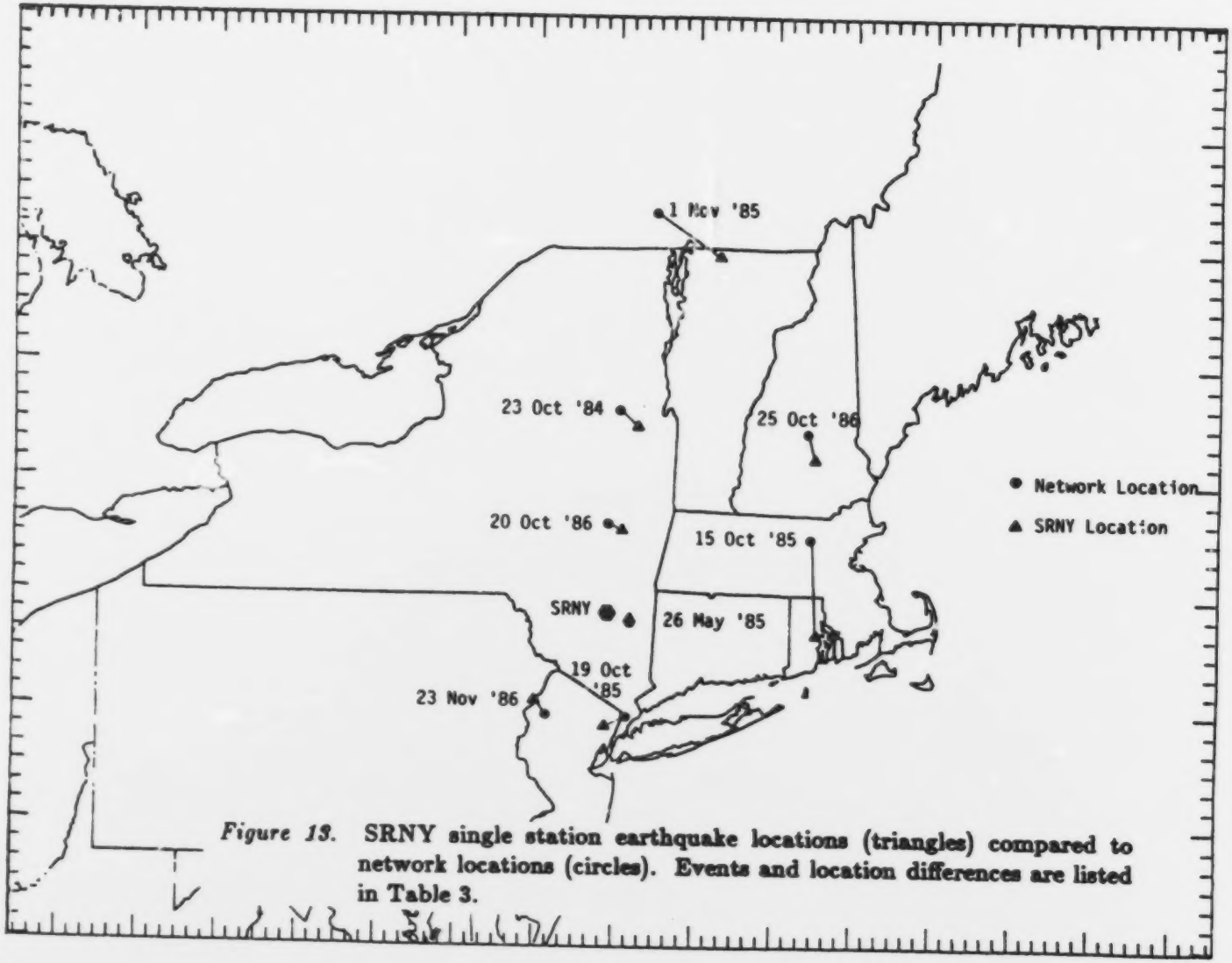

Figure 13. **SRNY single station earthquake locations (triangles) compared to network locations (circles). Events and location differences are listed in Table 3.**

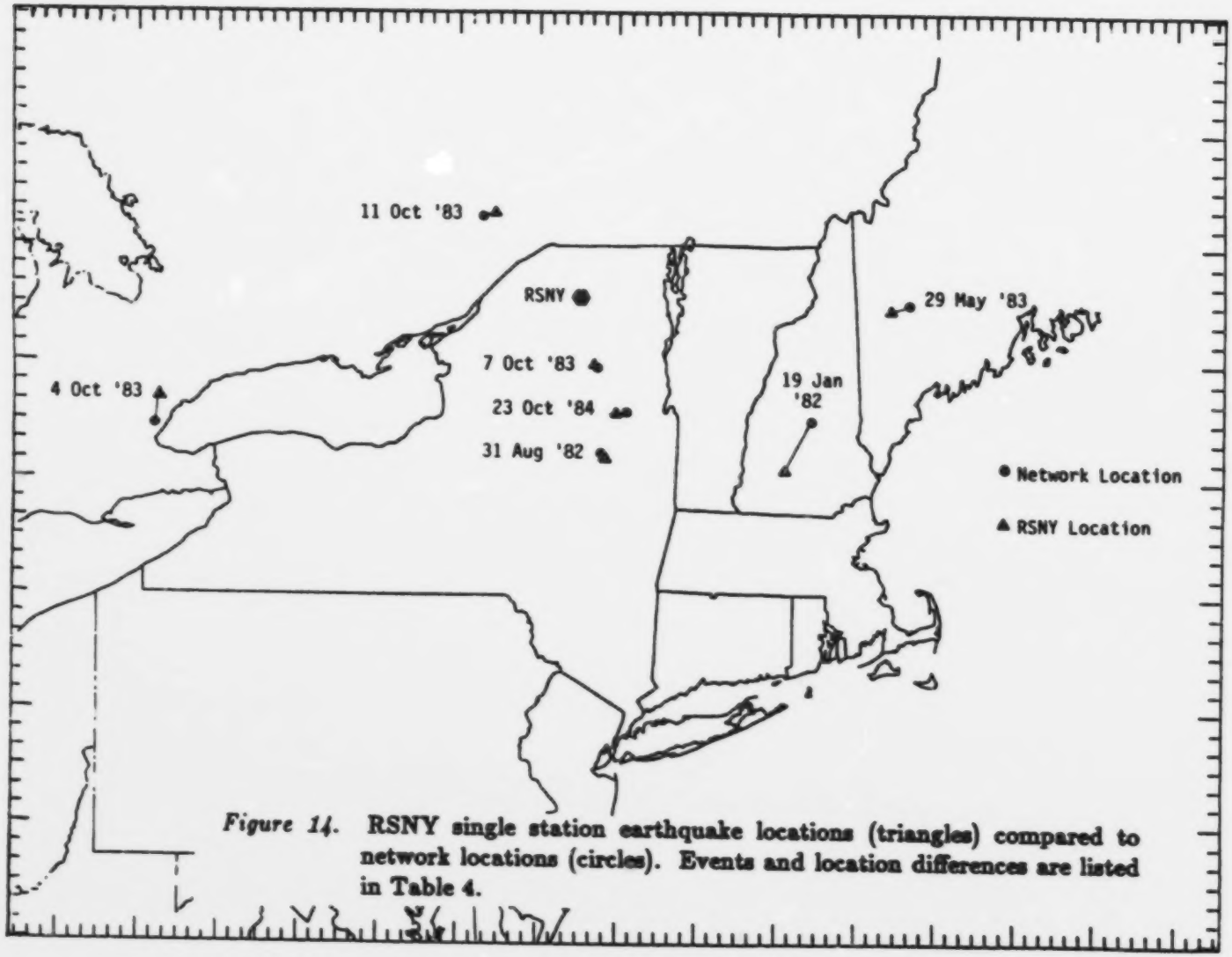

Figure 14. **RSNY single station earthquake locations (triangles) compared to network locations (circles). Events and location differences are listed in Table 4.**

BEST COPY AVAILABLE

41

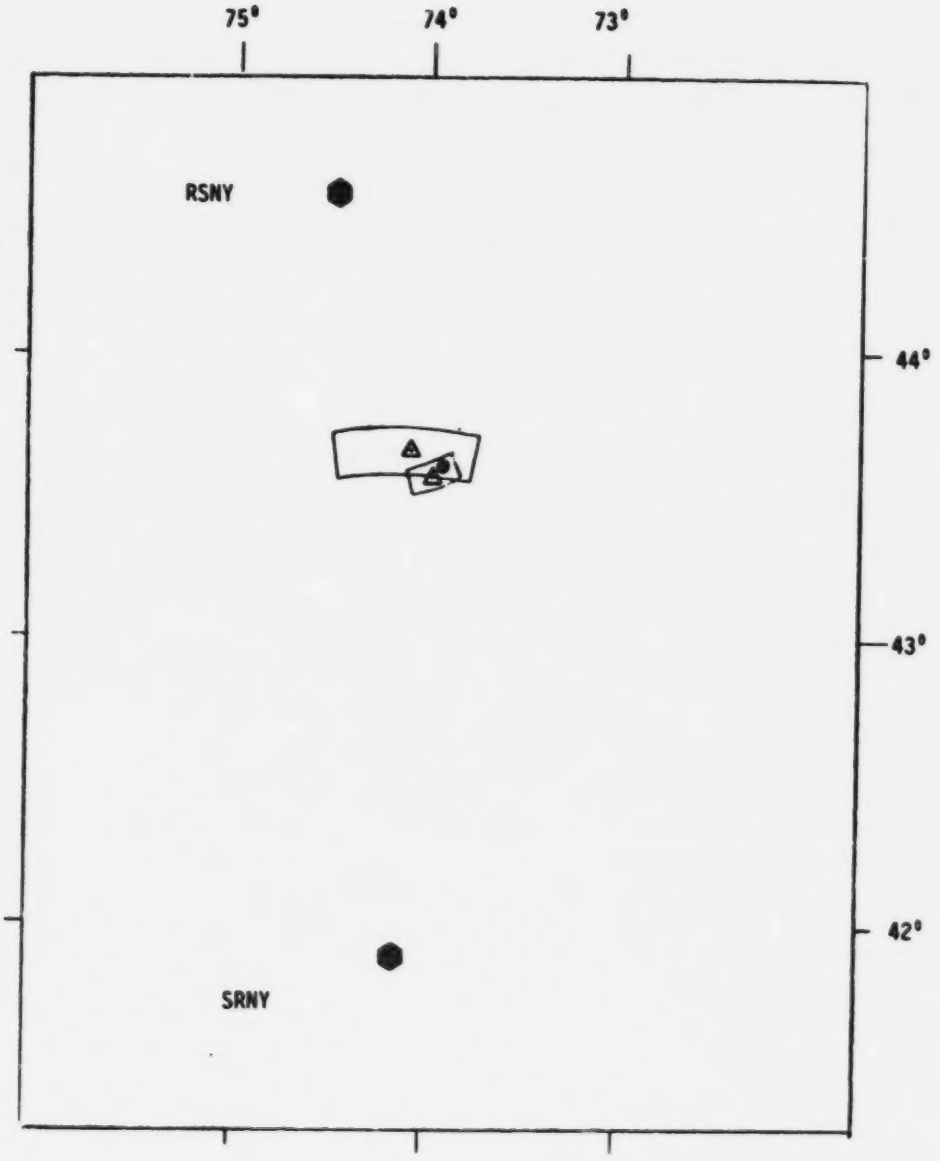

Figure 15. Locations of the 10/23/84 Adirondack earthquake. The Lamont-Doherty network location is plotted as a closed circle. Locations from RSNY and SRNY are plotted as triangles. Error boxes are ± one standard deviation in range and azimuth based on data in Tables 3 and 4.

BEST COPY AVAILABLE

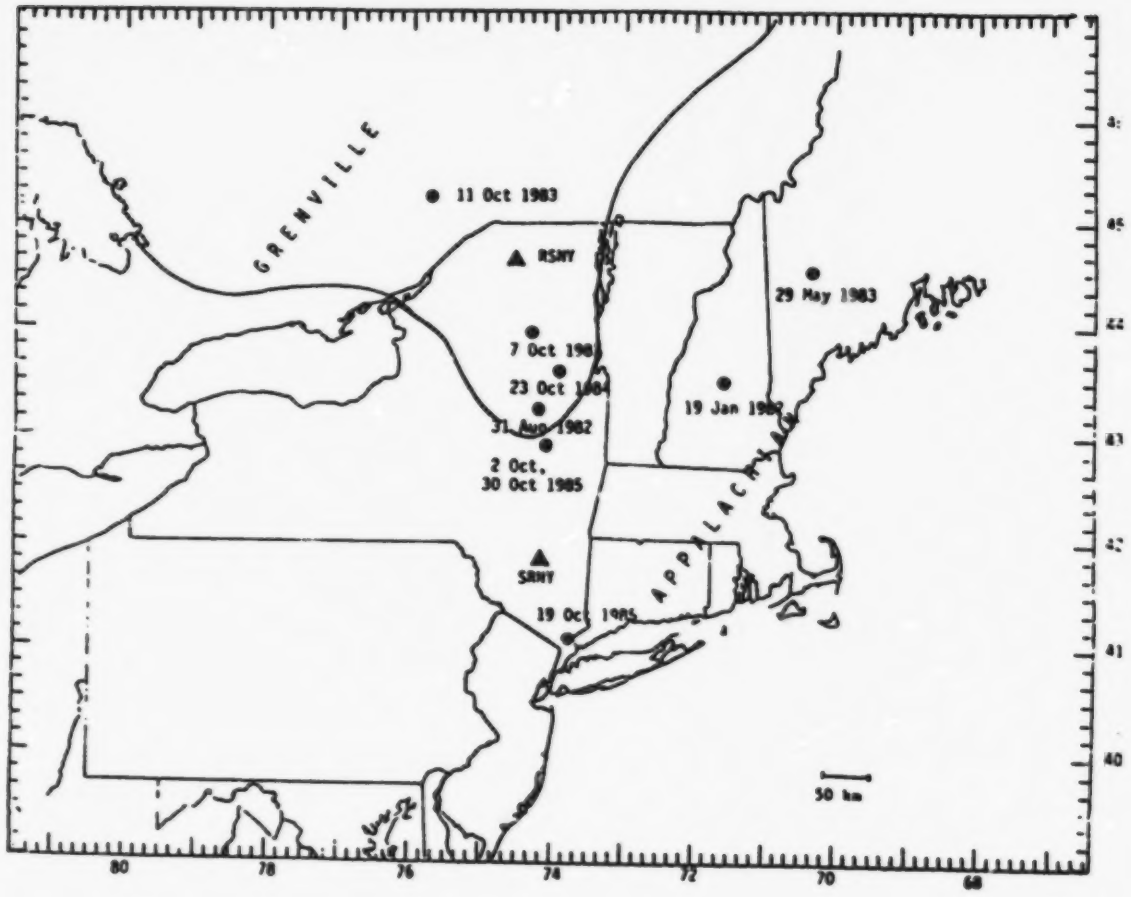

Figure 16. **Location of events and stations used in this study. Events are indicated by circles and a date. The two stations, RSNY and SRNY are indicated by triangles.**

BEST COPY AVAILABLE

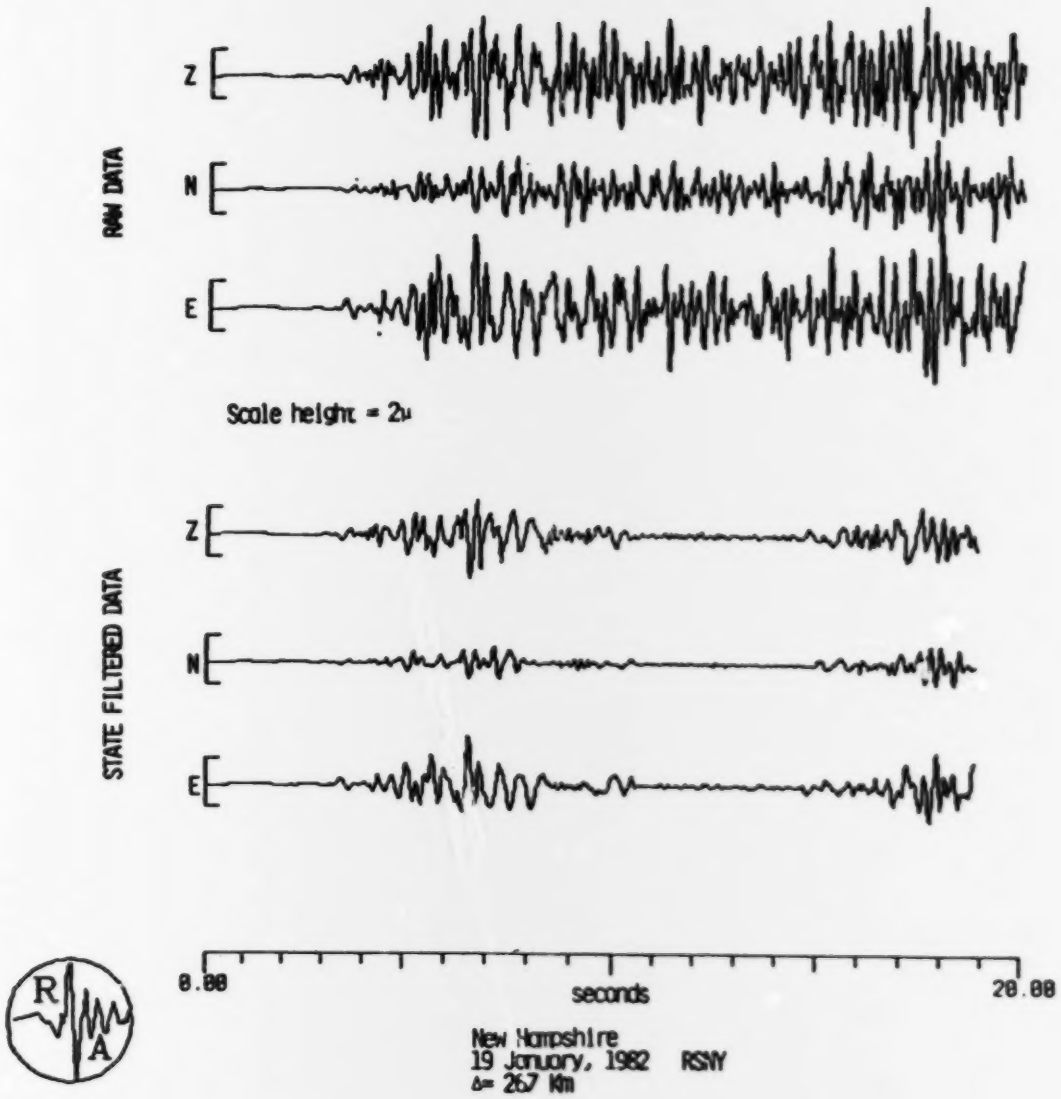

Figure 17A. **Seismograms recorded at RSNY of the January 19, 1982 New Hampshire earthquake. The top three traces are the vertical, north-south, and east-west components, unfiltered. The bottom three traces are the three components after state-filtering for rectilinear particle motion. The rest of the events shown in Figure 16 are similarly depicted in Figures 17B through 17I.**

BEST COPY AVAILABLE

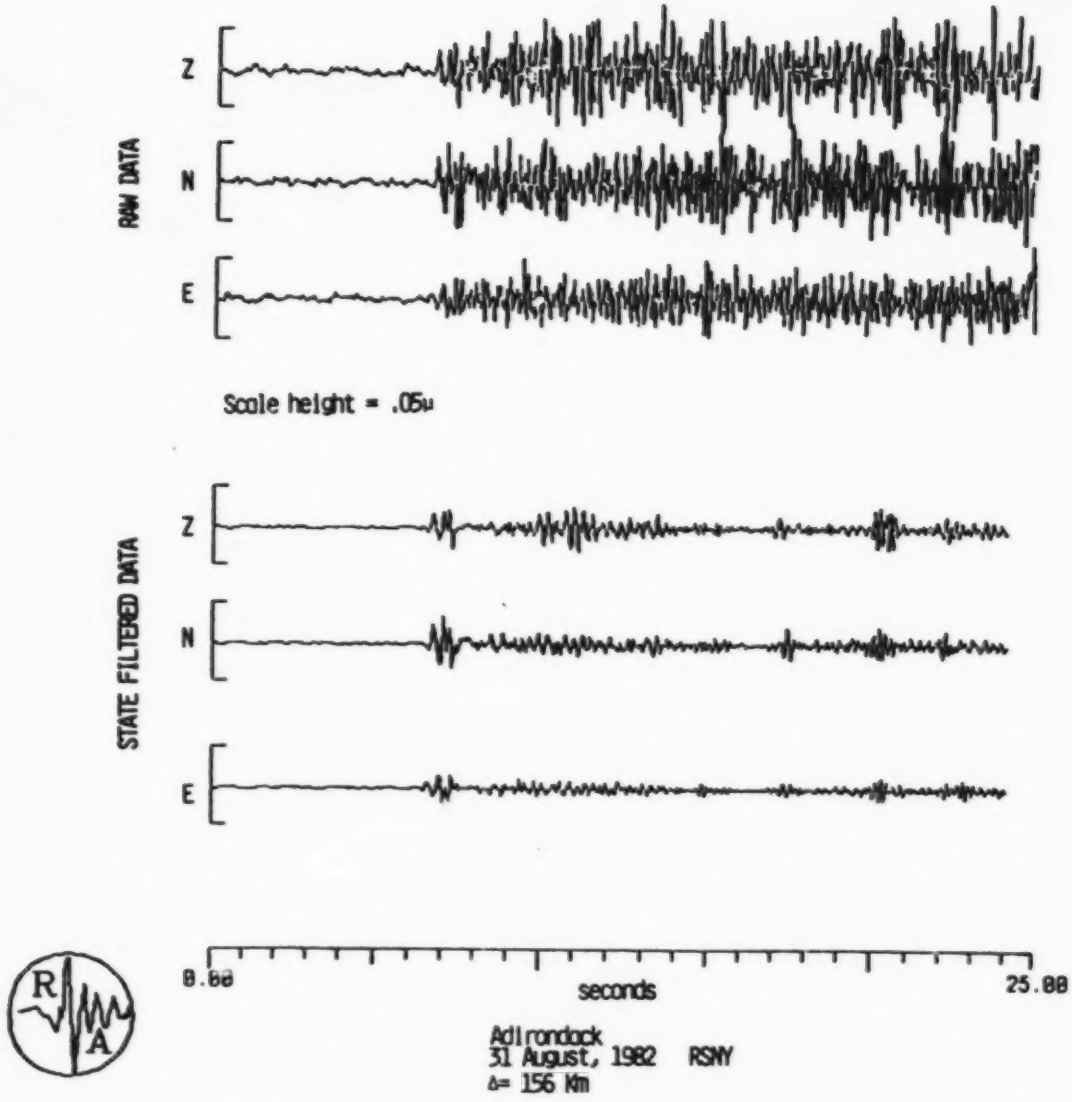

Figure 17B.

BEST COPY AVAILABLE

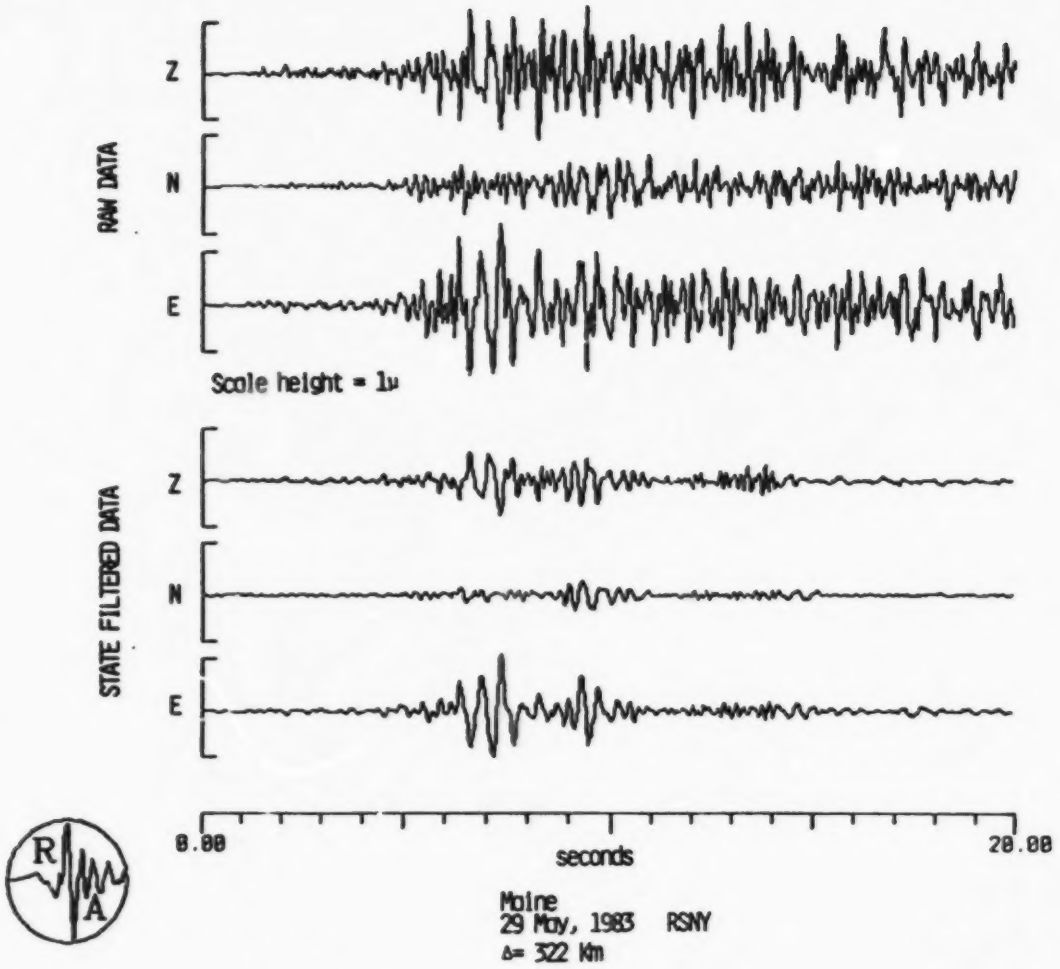

Figure 17C.

BEST COPY AVAILABLE

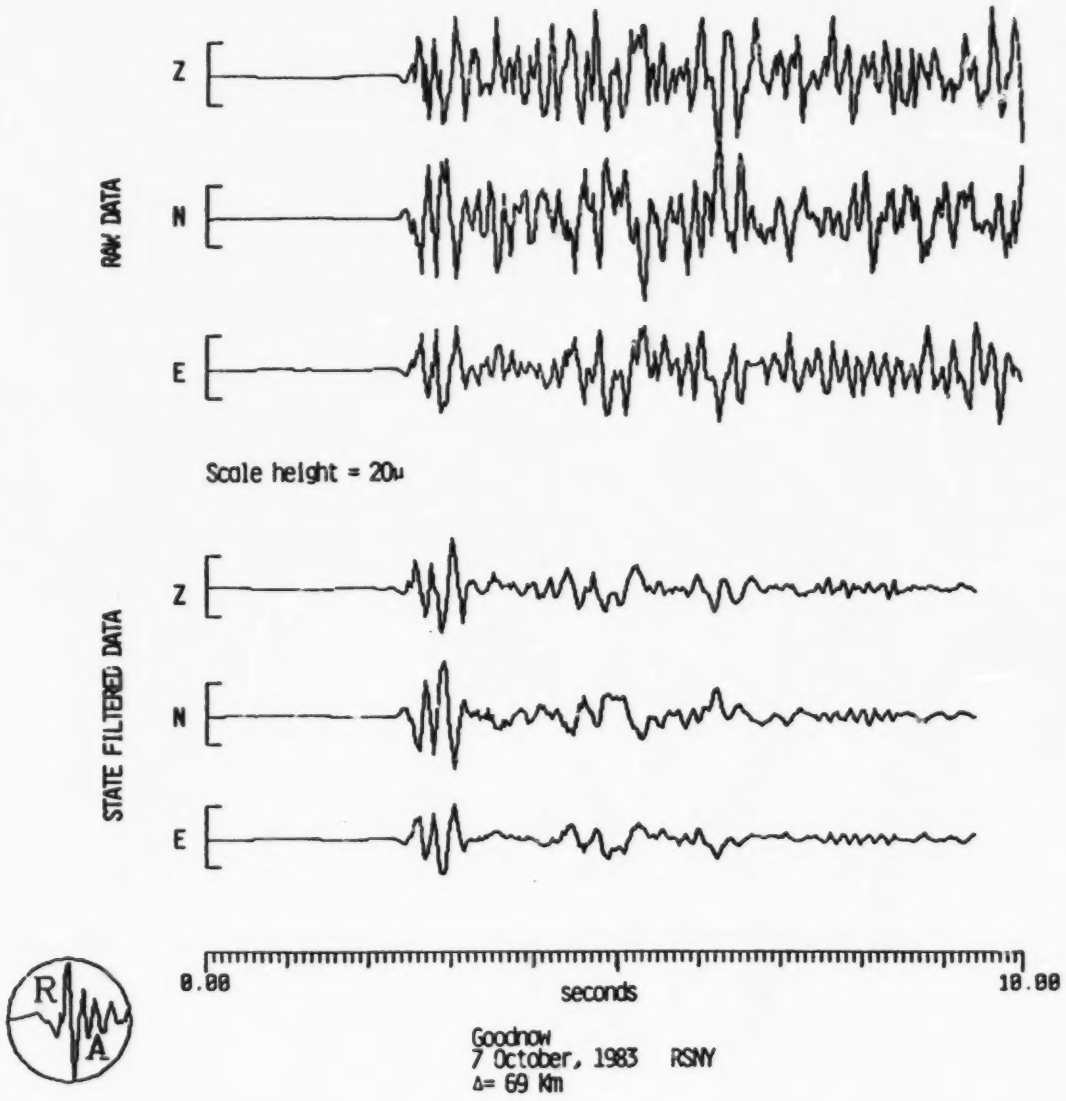

Figure 17D.

BEST COPY AVAILABLE

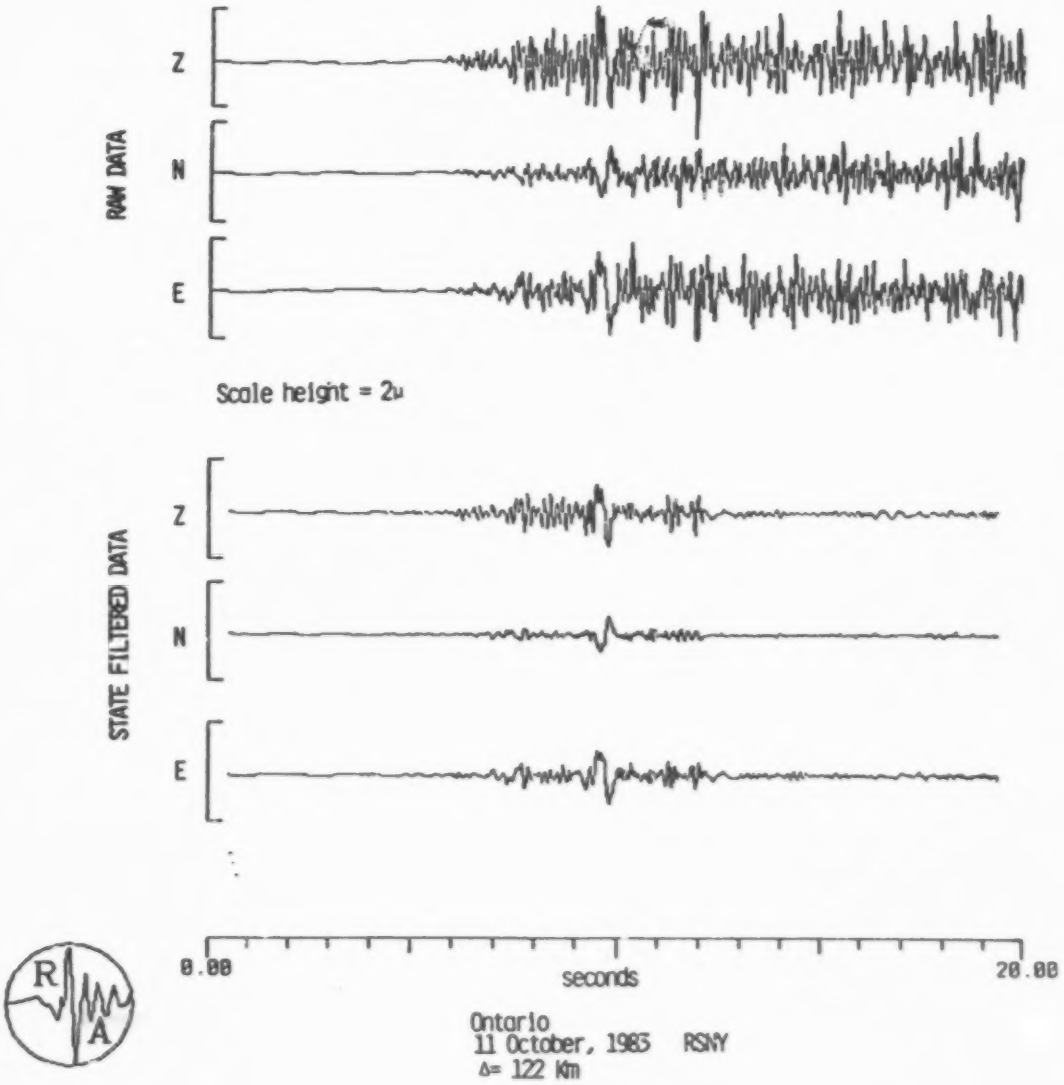

Figure 17E.

BEST COPY AVAILABLE

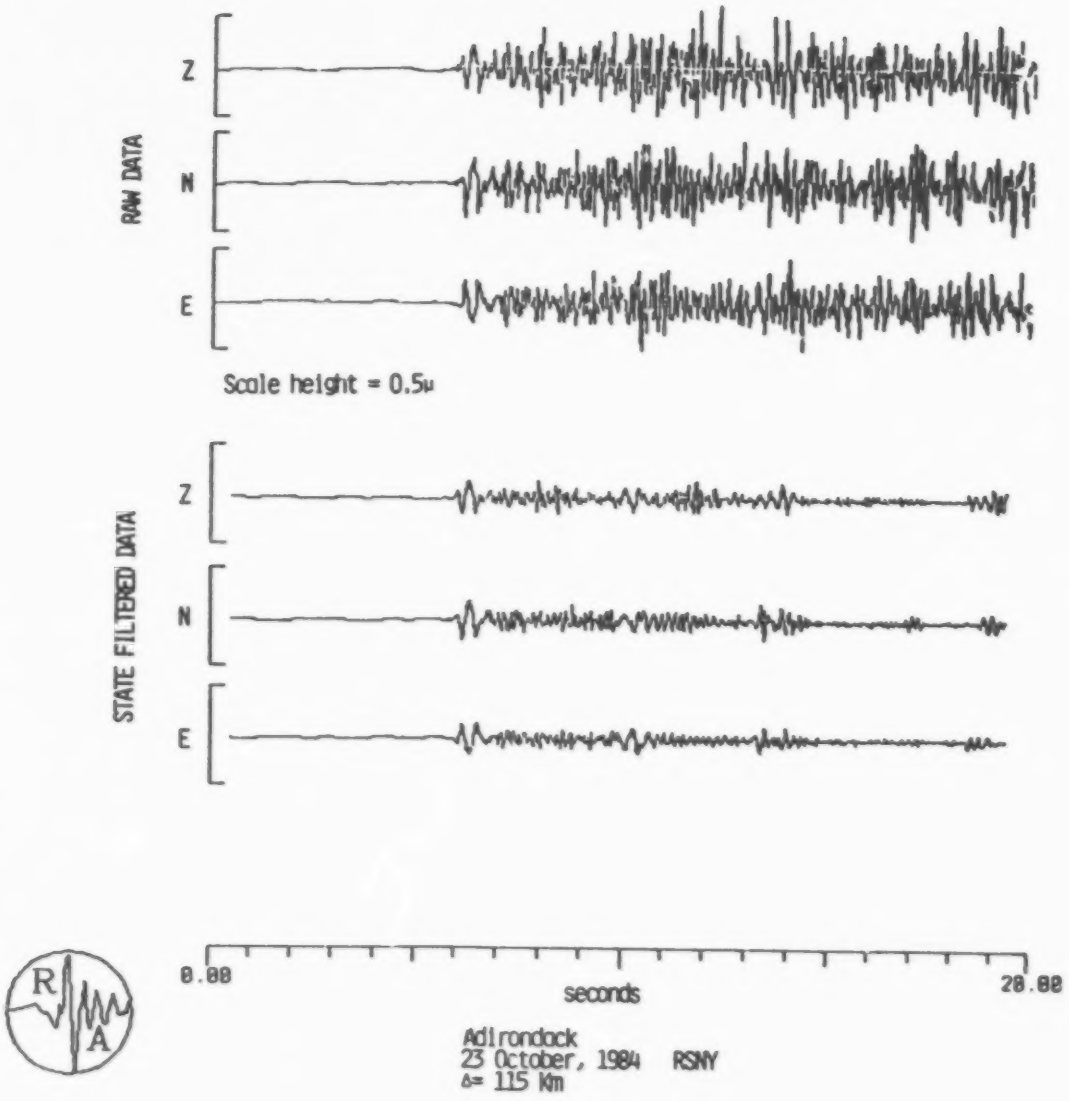

Figure 17F.

BEST COPY AVAILABLE

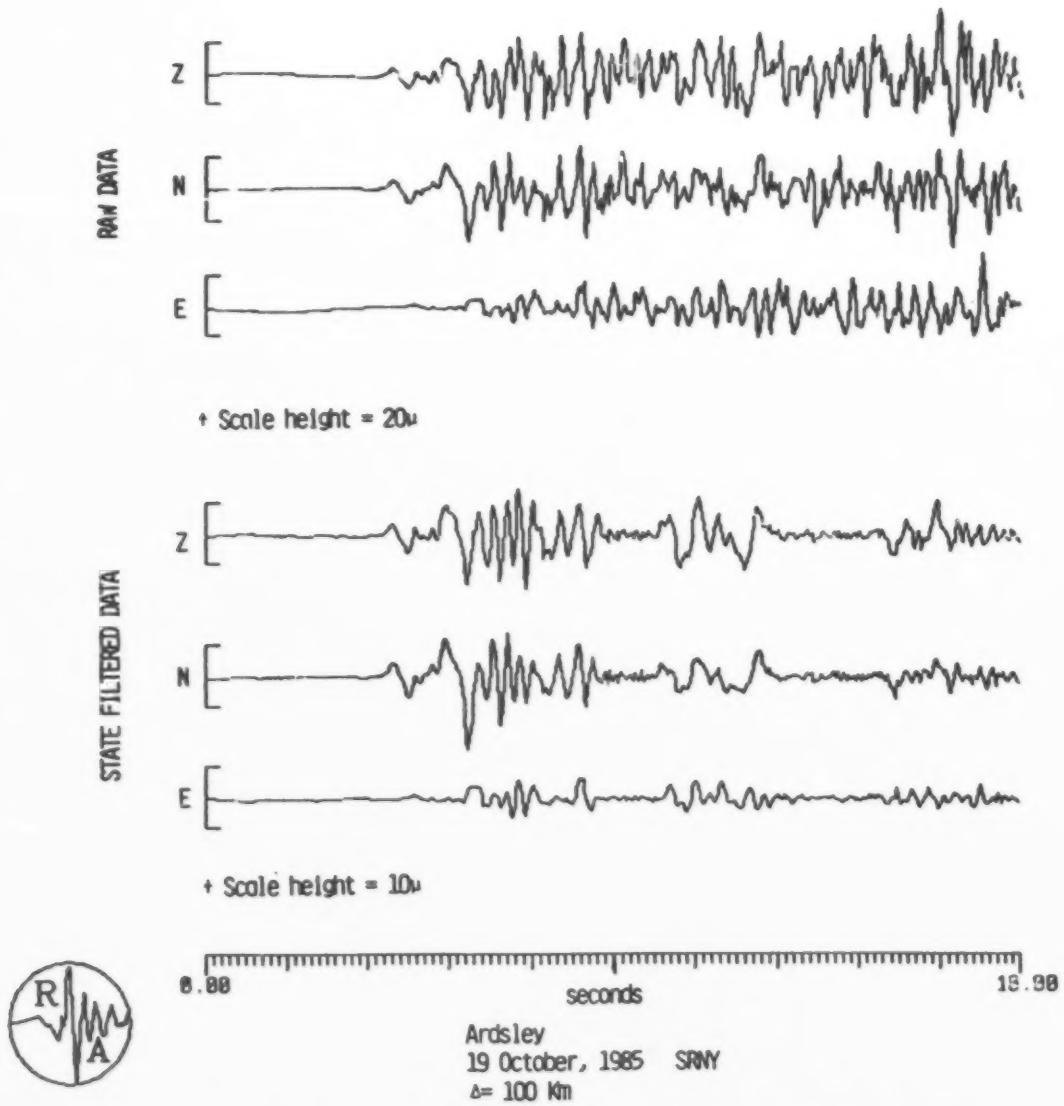

Figure 17G.

BEST COPY AVAILABLE

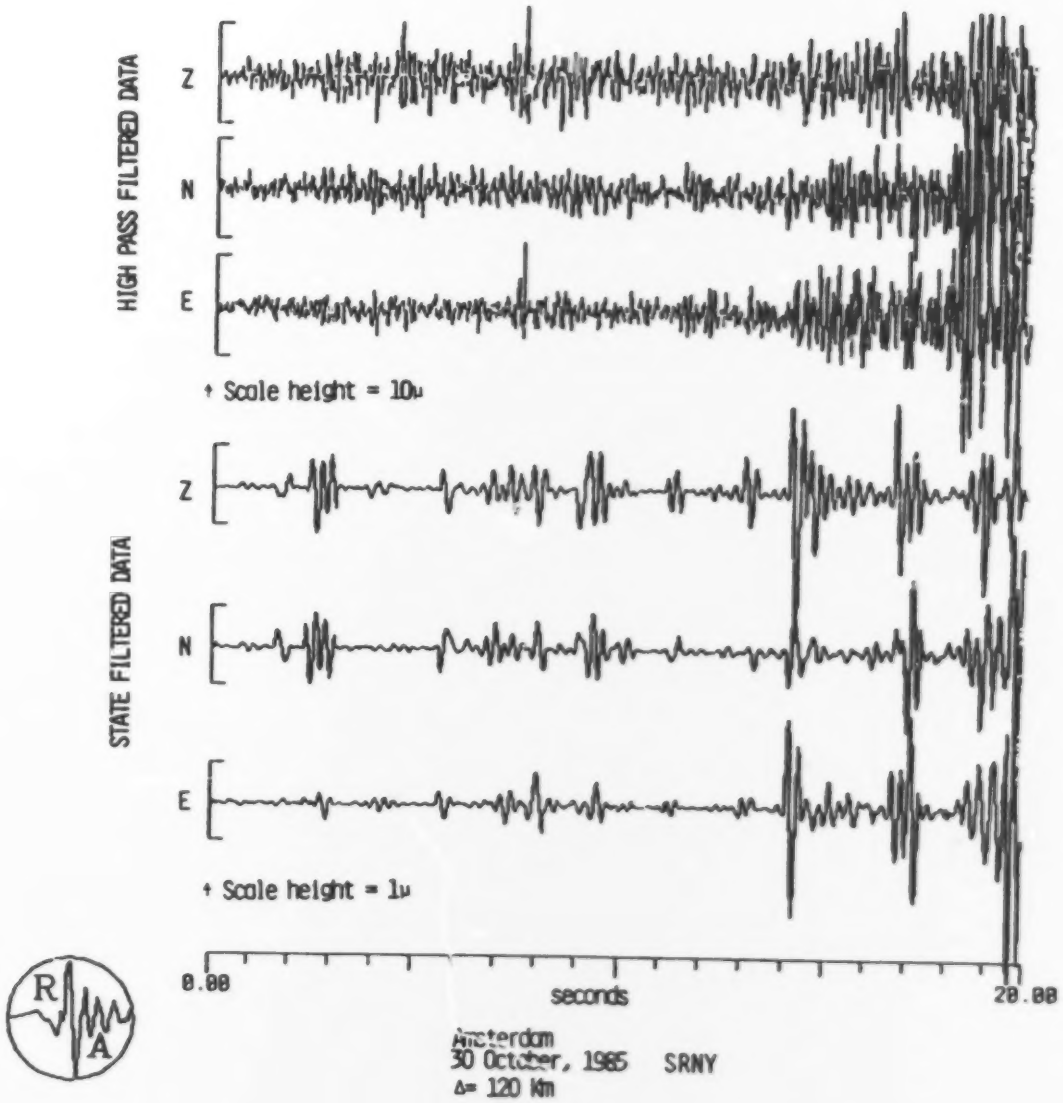

Figure 17H.

BEST COPY AVAILABLE

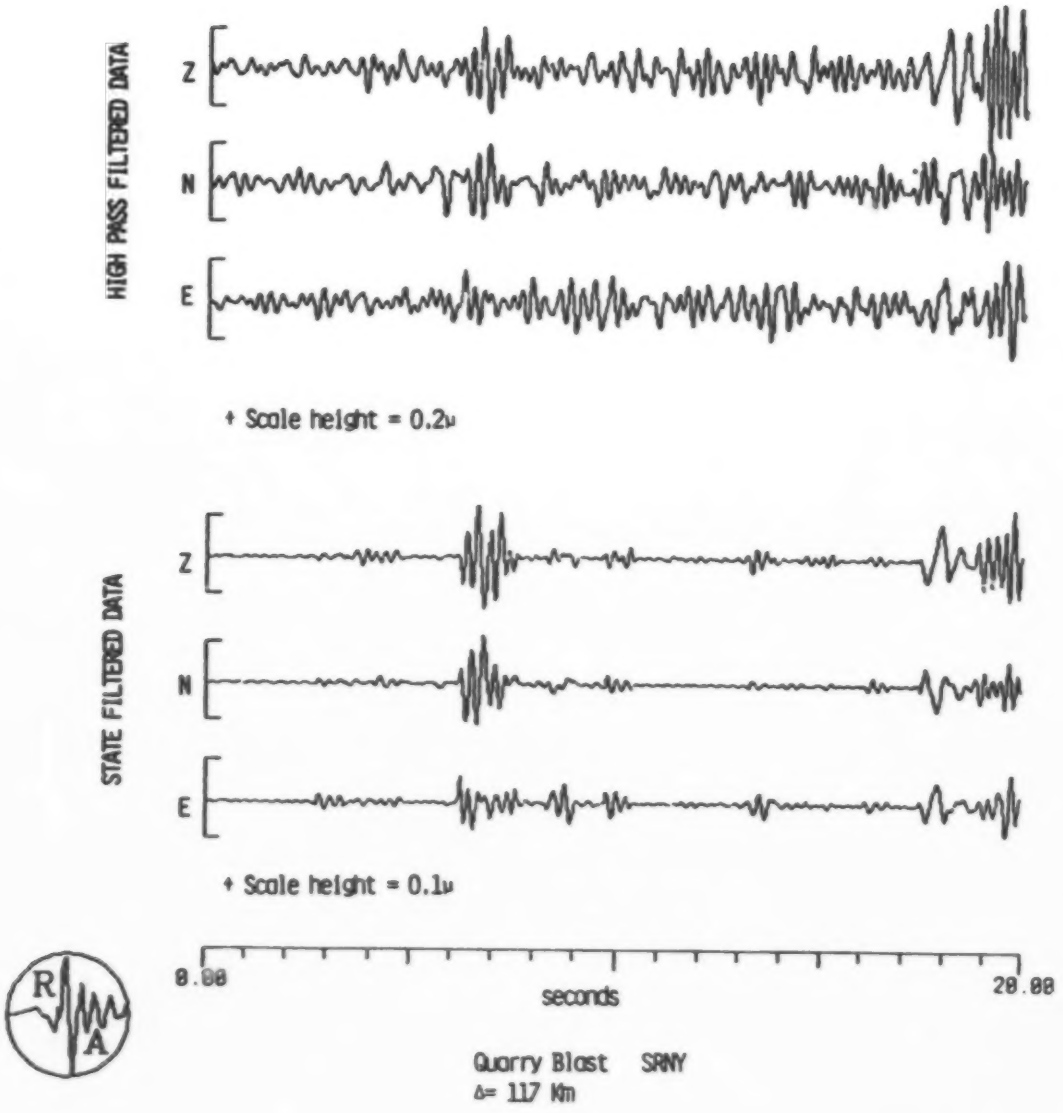

Figure 17I.

BEST COPY AVAILABLE

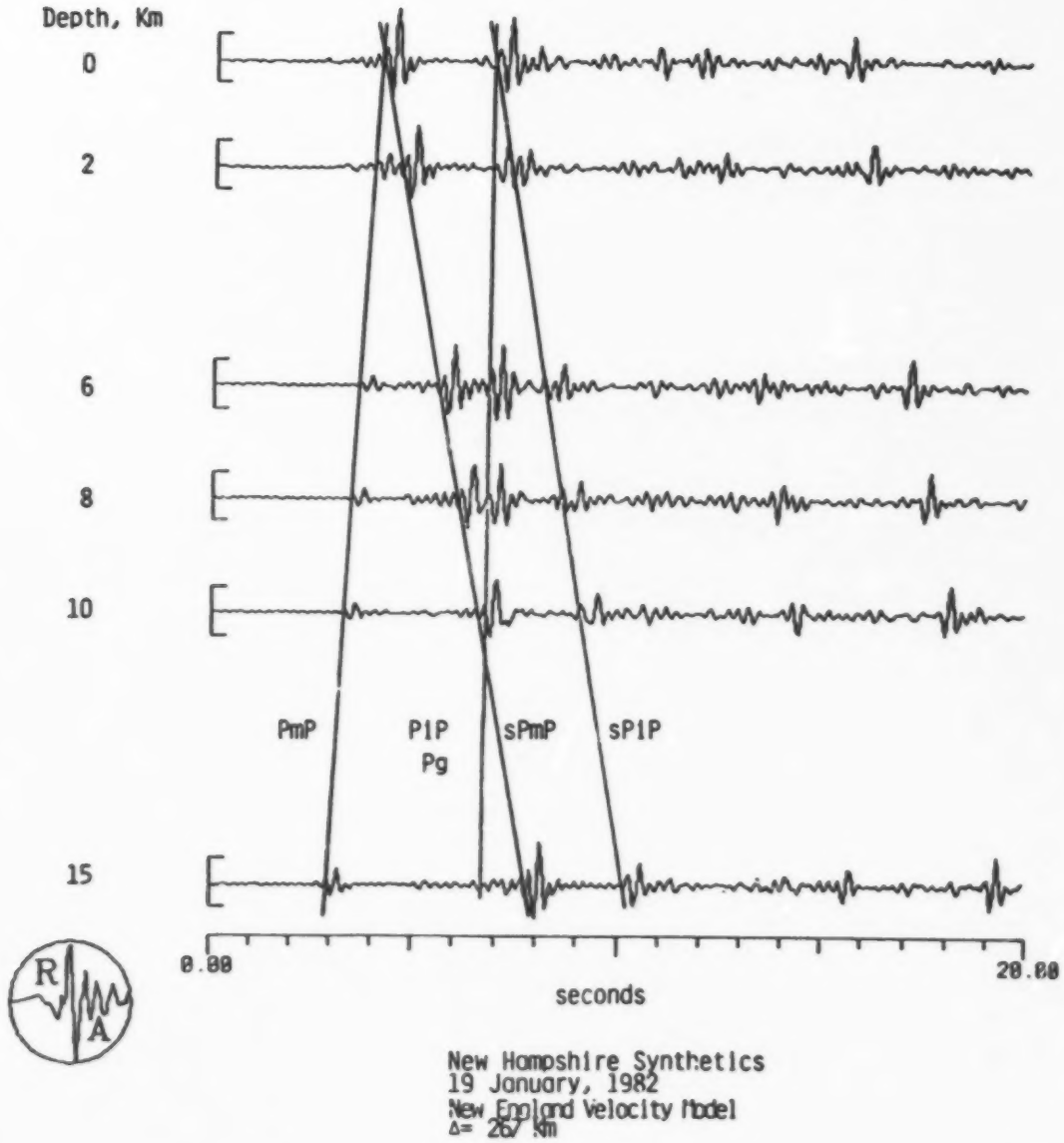

Figure 18A. Synthetic seismograms calculated for a suite of depths. Source = January 19, 1982 Earthquake. Strike = 280, Dip = 75, Rake = −11. Receiver response = RSNY short period (sp). Azimuth = 295. In Figures 18A through 18H several primary and depth phases are identified. All but Figure 18G are vertical components. *PiP* is reflected within the crust and *PmP* is reflected at the Moho.

BEST COPY AVAILABLE

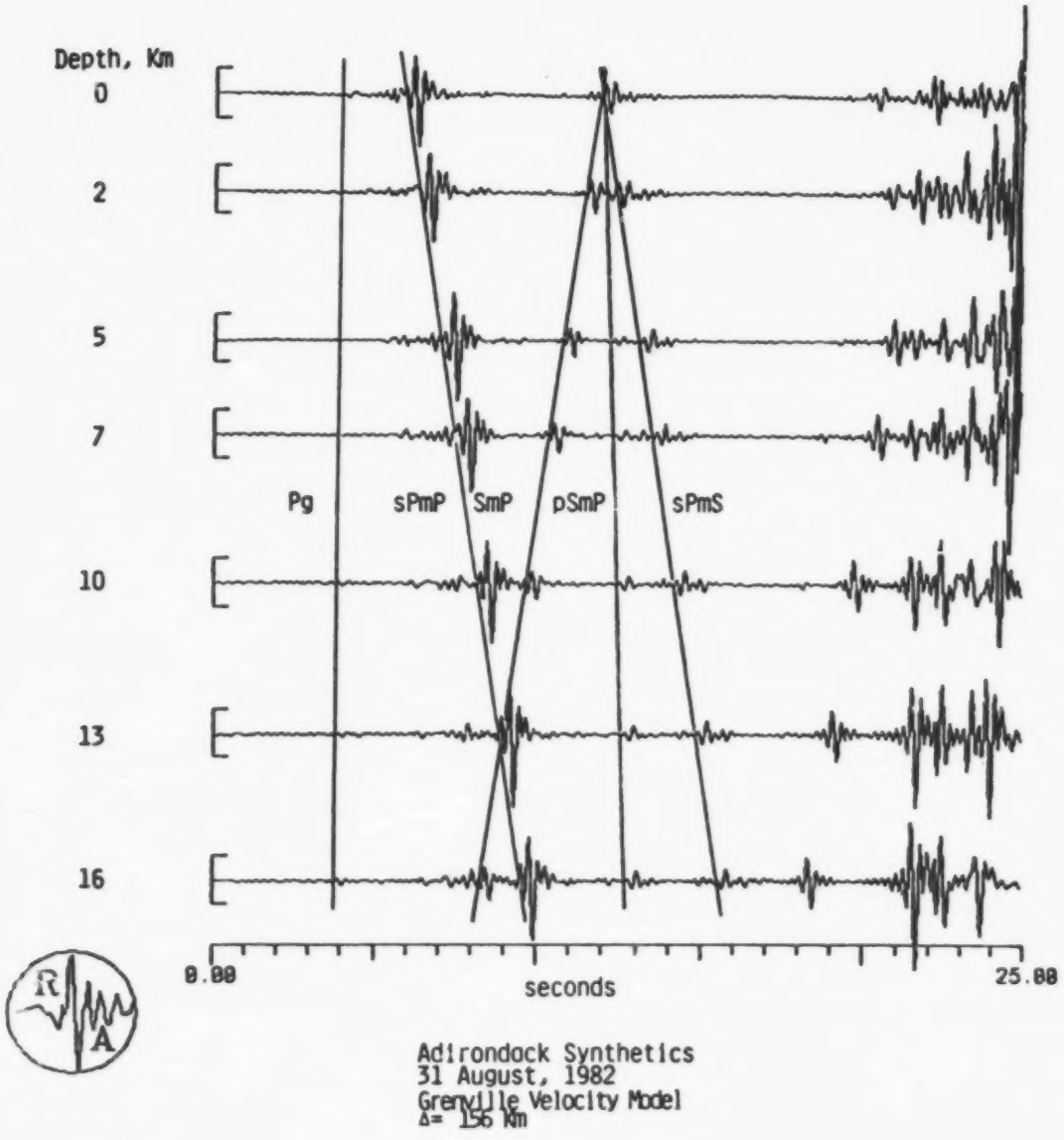

Figure 18B. Synthetic seismogram depth section. Source = 31 August, 1982 Earthquake. Strike = 173, Dip = 60, Rake = 110. Receiver response = RSNY (sp). Azimuth = 350.

BEST COPY AVAILABLE

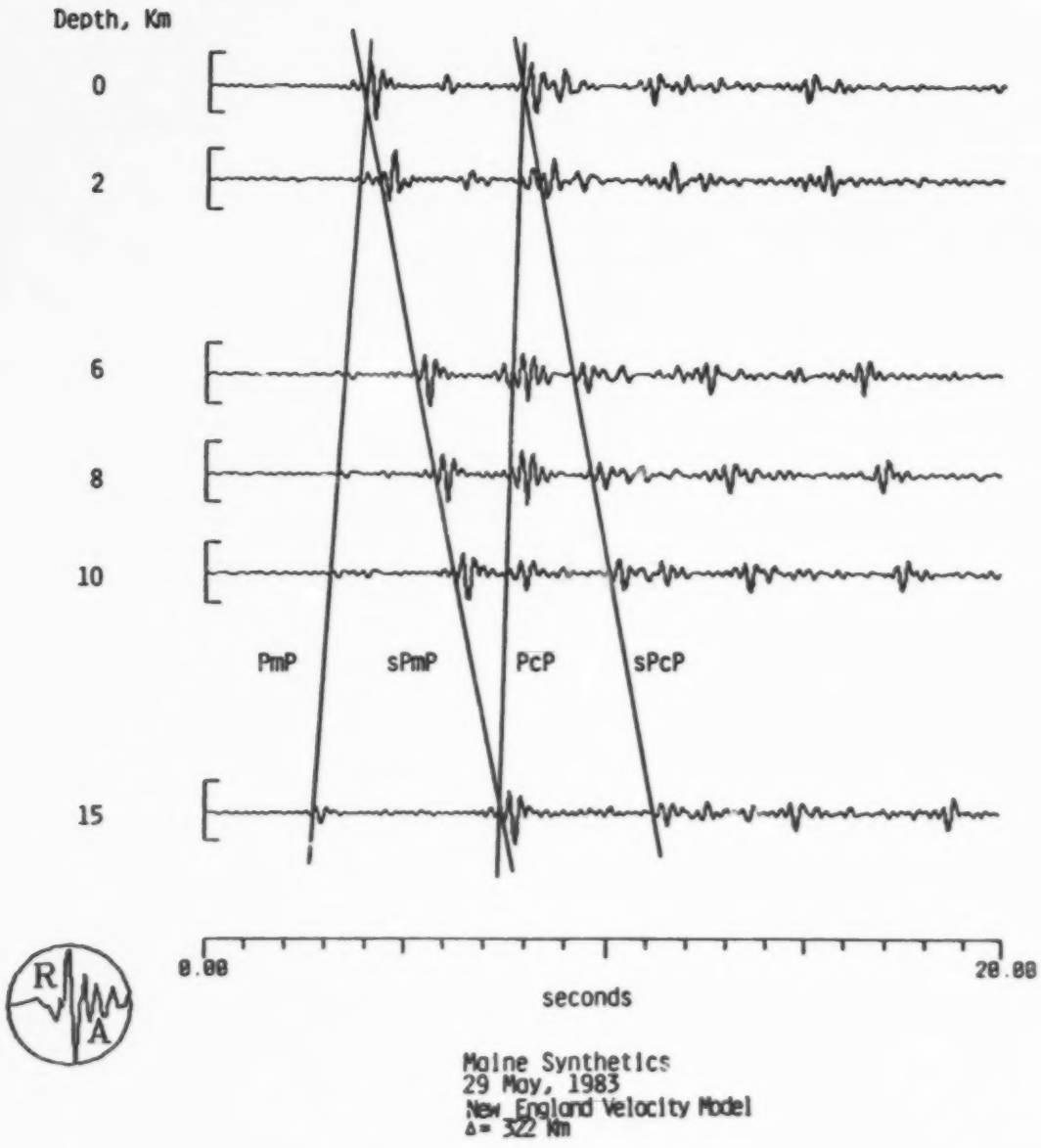

Figure 18C. Synthetic seismogram depth section. Source = 29 May, 1983 Earthquake. Strike = 355, Dip = 52, Rake = 78. Receiver response = RSNY (sp). Azimuth = 269.

BEST COPY AVAILABLE

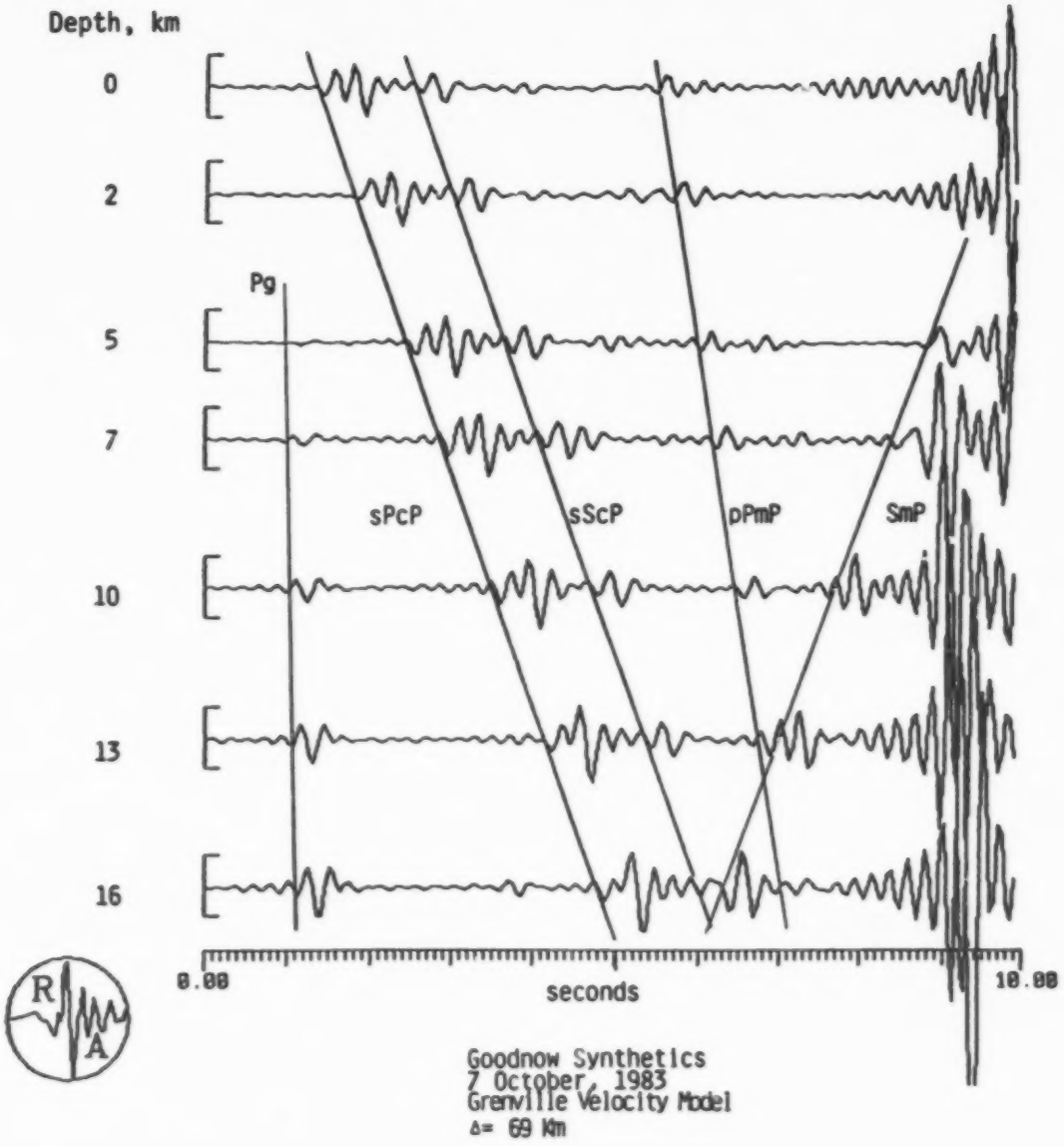

Figure 18D. Synthetic seismogram depth section. Source = 7 October, 1983 Earthquake. Strike = 173, Dip = 60, Rake = 110. Receiver response = RSNY (sp). Azimuth = 342.

BEST COPY AVAILABLE

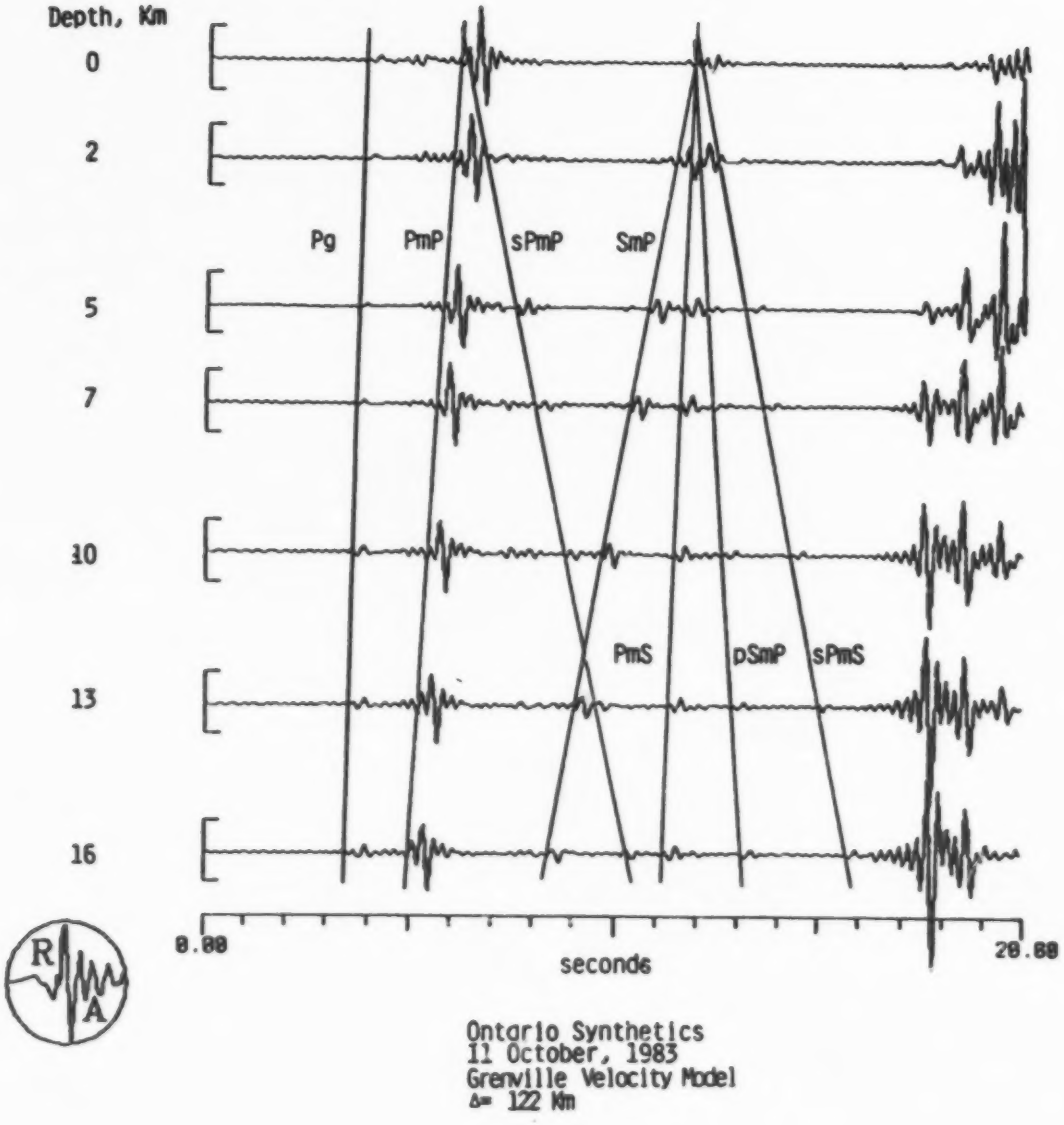

Figure 18E. Synthetic seismogram depth section. Source = 11 October 1983 Earthquake. Strike = 71, Dip = 75, Rake = 98. Receiver response = RSNY (sp). Azimuth = 127.

BEST COPY AVAILABLE

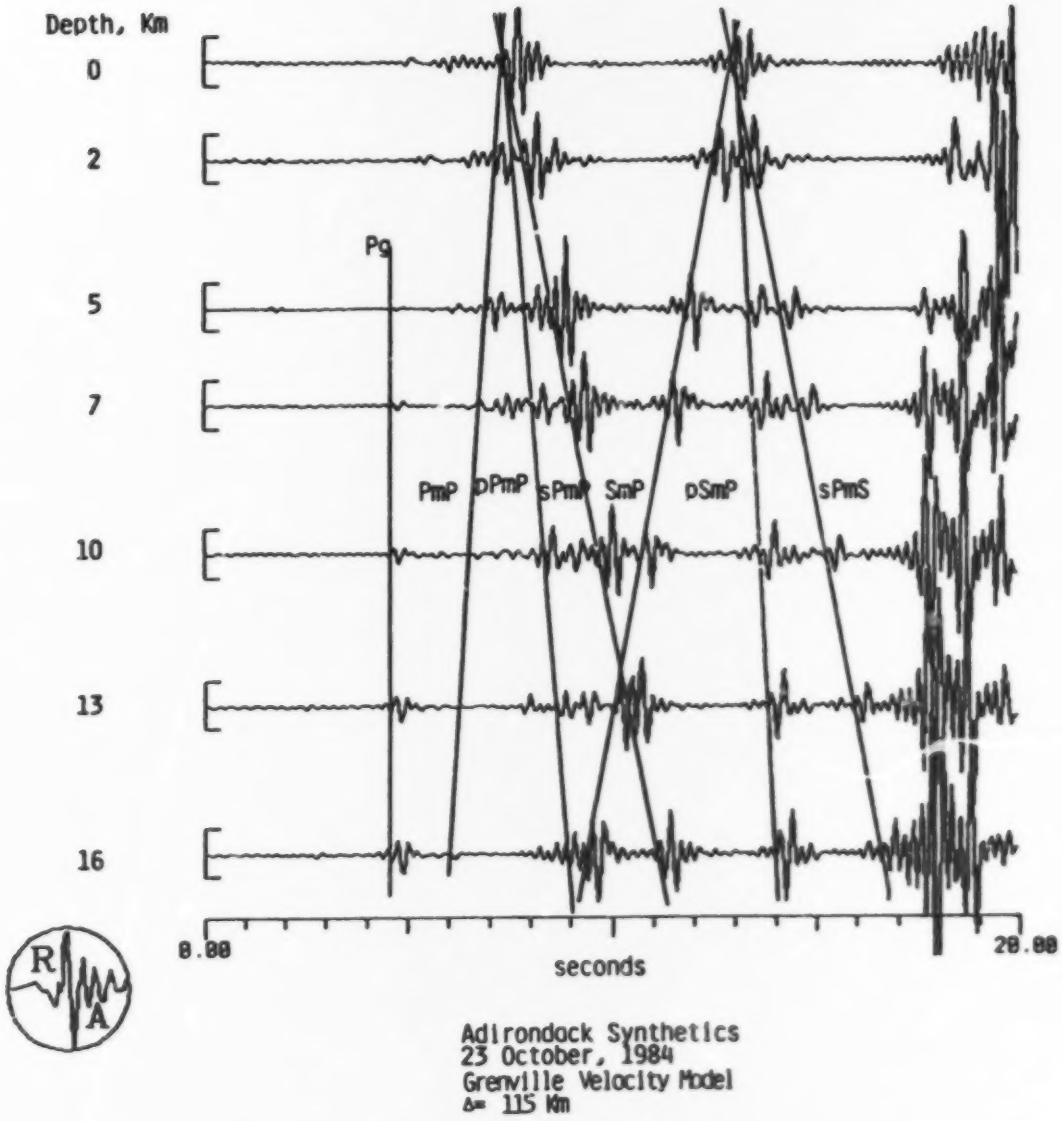

Figure 18F. Synthetic seismogram depth section. Source = 23 October, 1984 Earthquake. Strike = 173, Dip = 60, Rake = 110. Receiver response = RSNY (sp). Azimuth = 335.

BEST COPY AVAILABLE

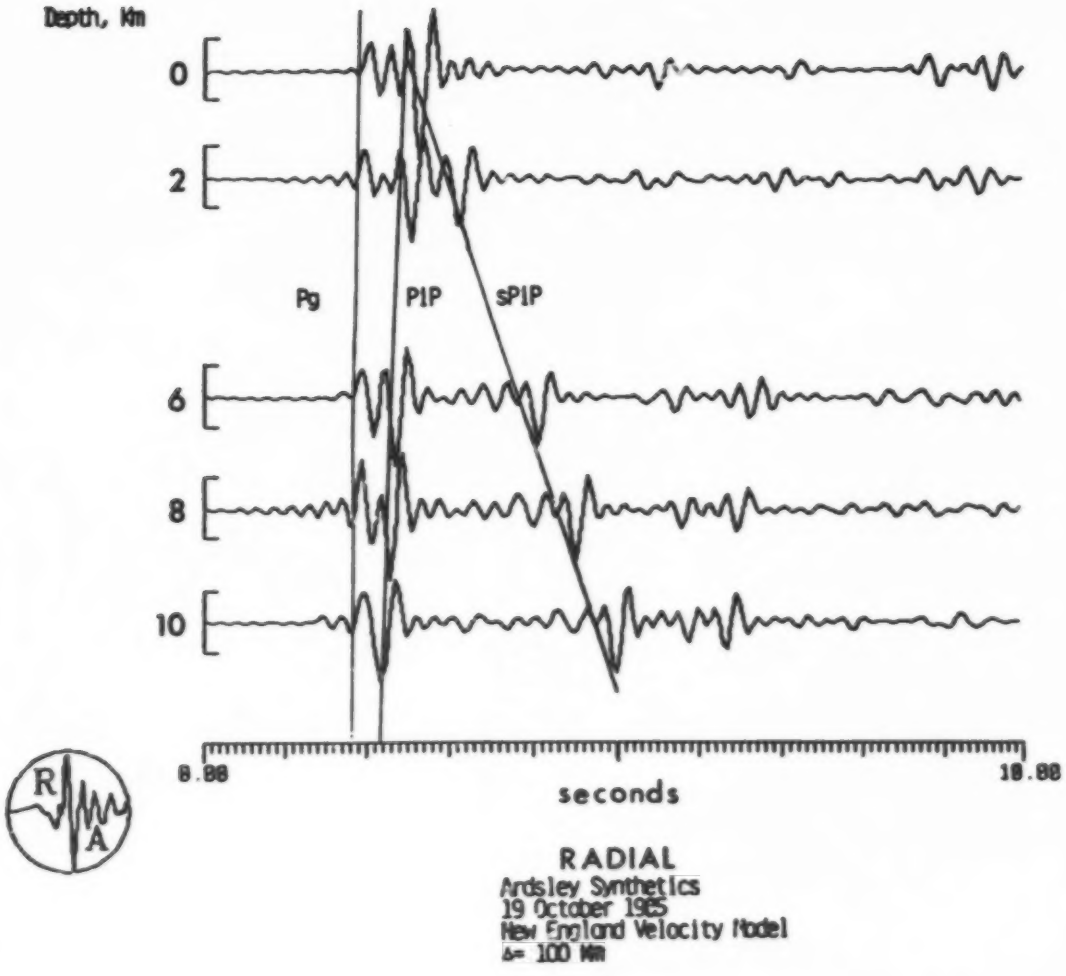

Figure 18C. Synthetic seismogram depth section. Source = 19 October 1965 Earthquake. Strike = 022, Dip = 90, Rake = 180. Receiver response = SRNY. Azimuth = 344. Radial components shown.

BEST COPY AVAILABLE

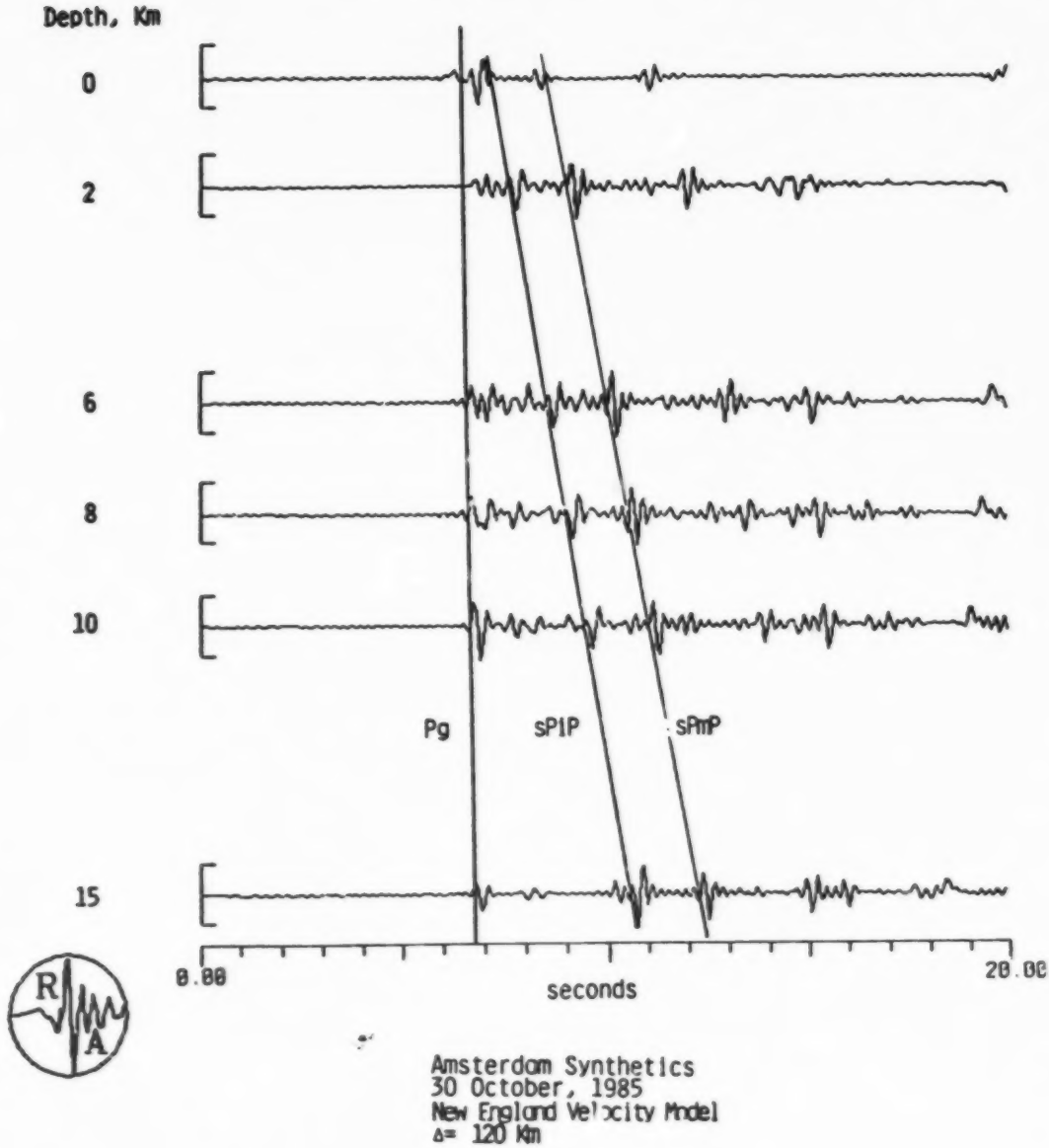

Figure 18H. Synthetic seismogram depth section. Source at zero depth = 2 October 1985 Explosion. Source at other depths = 30 October 1985 Earthquake. Strike = 18, Dip = 60, Rake = 156. Receiver response = SRNY. Azimuth = 180 from explosion and 181 from Earthquake. The blast and earthquake epicenters are only 3 km apart.

BEST COPY AVAILABLE

APPENDIX A

In this Appendix we document the software that is run on the Columbia PC of station SRNY. Two programs are described here *rai* and *scs*. *Rai* performs the data collection and recording function and is active the vast majority of the time. When the recording has stopped for any reason, *scs* can be used to diagnose problems, manipulate the tapes, and display or plot data. Most often, *scs* is used to locate the tape block at which recording stopped so that *rai* can be restarted without overwriting previously recorded data or wasting unused tape. The recording format for the 1/4" magnetic tape follows the program documentation.

BEST COPY AVAILABLE

NAME

rai

SYNOPSIS

rai [*-l drive #*] [*-o drive #*] [*-s drive #*] [*-e end*]

DESCRIPTION

rai is an interrupt driven data collection program which is used to collect data from the Ref-Tek system and the Kinemetrics satellite clock and record it on two SCS data recorders. With no options, *rai* will check the status of both drives, load the bad block table into drive 0, load the file comment.rai into block 0, and start logging data to tape. When 65,400 blocks (approximately 38 hours) have been recorded, *rai* will switch to drive 1, load the bad block table and comment and record for another 65,400 blocks, then stop. Tapes are rewound when recording has stopped. Options are available to modify this routine.

-l Loop option. If loop is specified, the recording will start with the drive specified and shuttle back and forth as long as a tape is available. After a tape has been rewound, it can be replaced with a new one. The bad block table and comment will be loaded before use. DEFAULT = stop after recording both drives.

-o One drive. If one drive is specified, recording will start with the drive specified and will stop when end is reached on that drive. DEFAULT = use both drives.

-s Starting block number. To begin at other than the first tape block. Applies only to the first drive. DEFAULT = 1.

-e Ending block number. Upon reaching ending block number, recording will stop on that drive. Depending on other options, recording may continue on the other drive. Applies to both drives. DEFAULT = 65,400.

FILES

screen1.rai screen1a.rai screen2.rai screen3.rai screen4.rai comment.rai

BEST COPY AVAILABLE

NAME

scs

SYNOPSIS

scs

DESCRIPTION

Scs is a utility program used to access the Secondary Computer Storage tape drives over the parallel interface. It is prompt line driven and therefore has no options. A description of commands follows. Most commands apply to the selected drive (see z command).

b — Read manufacturers block. The information in absolute block zero is displayed.

c — Certify. You are prompted for 'beginning' and 'ending' block and then the tape blocks between these limits are certified. The results are stored in the SCS controller memory.

d — Display. You are prompted for 'where' (which block) to begin. Information previously recorded on tape is formated and displayed. The display will continue until either the end of tape has been reached or until two quick spaces are entered. One space will force a jump to the next block.

f — Fill (diagnostic write). The range of blocks from 'begin' to 'end' are filled with a pattern consisting of integers from 127 down to 0 and 384 zeros.

i — Initialize. The controllers initialize line is strobed thus reseting the drives to their power up state. This command applies to both controllers.

k — Comment. The comment in block 1 is read in and displayed. Press any key to continue.

l — Load bad blocks. The bad block information in absolute block 8 is read in and then loaded into the controller's skip table. From then on the drive will skip over any block listed in the table.

m — Memory. To access controller memory. For reading enter 'r' and hex location (ie. r237F). For writing enter 'w', location and value (ie. w237f a0).

p — Plot. To plot data on screen enter 'where' (block number), 'scale' (plot val = val/scale), and channel number (0 - 2). A single character while plotting will stop the plot for viewing and a second character will return to menu. Plotting will continue from where until end of tape.

BEST COPY AVAILABLE

q	Quit. Return to MS-DOS.
r	Read. The drive will move to the block selected with 'where' and dump 512 unsigned integers to the screen.
s	Status. Used to report status and or clear a fault.
u	Unwind. Rewinds the selected drive.
w	Write. Enter 'where' (block number) and 'how many'. Two byte integers from 0 to 512 will be written to each block selected.
z	Select drive. Select either controller 0 or 1. Selection will remain in effect until changed. DEFAULT 0

BEST COPY AVAILABLE

1/4 Magnetic Tape Cartridge Format

A 1/4" tape cartridge can hold up to 67 megabytes of data which is written in 1024 byte blocks. Blocks 8 and 9 are used to store duplicate tables of bad block information and are read into the controllers ram. A header block of 1024 characters from the file "comment.rai" is written to block 0 at the beginning of the recording process and contains information manually entered about the status and/or configuration of the station. Also included at the end of this block is a 0 or 1 to indicate which tape drive was used to record the data.

Data is written to the tape in two byte words. The first word of a data block is the block number and the second is the buffer number. The next three words contain the time at the beginning of the block (Figure 1A). The clock words are followed by three dummy words after which comes the data. Four words are used for a single sample from each channel. The first three words give the channel number and mantissa and the fourth word contains the gain bits (Figure 1A). There are 126 data samples per block per channel.

BEST COPY AVAILABLE

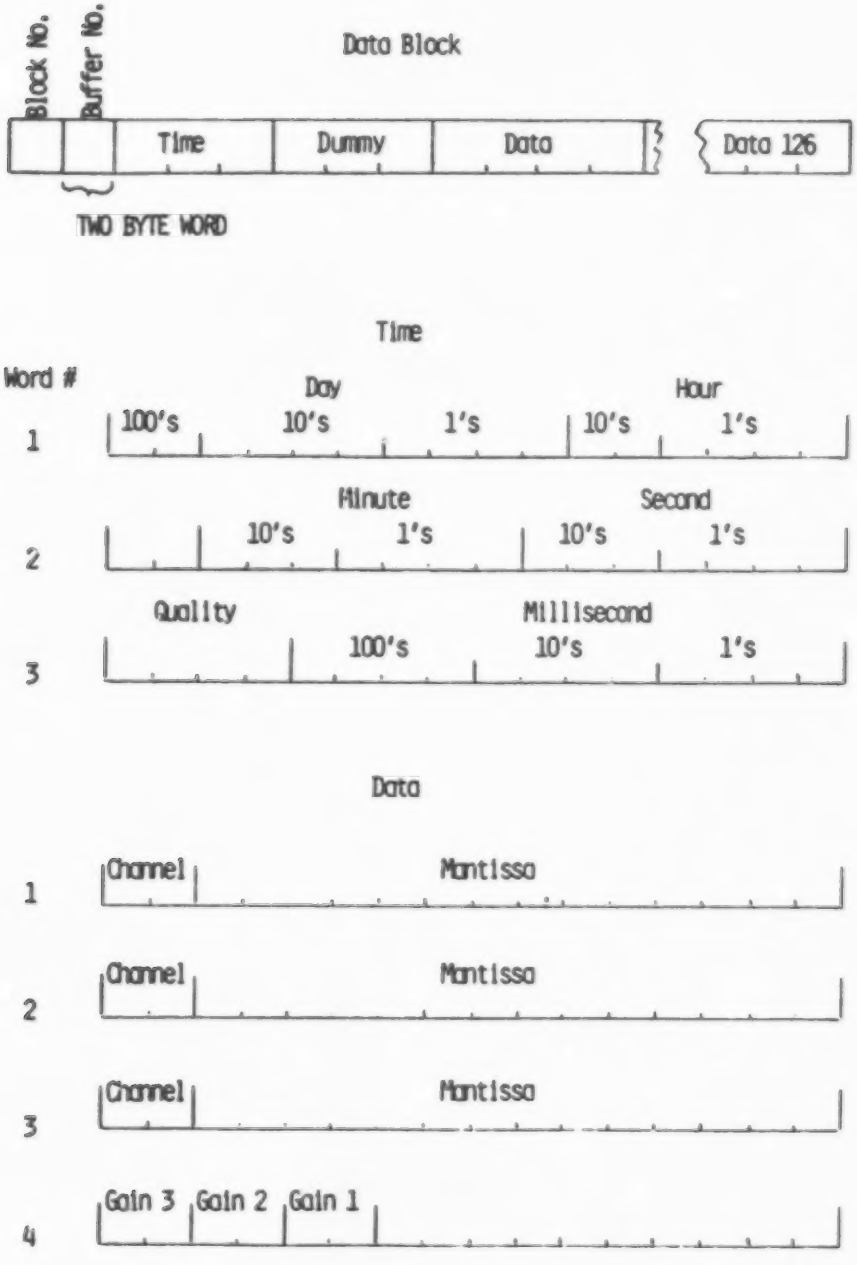

Figure A1. Data block format for 1/4" magnetic cartridge tapes.

BEST COPY AVAILABLE

APPENDIX B

Software written for tape certification, data playback, and analysis of data from station SRNY is documented in this appendix. Programs that do not utilize the interactive graphics capabilities of the SUN workstation; *bad, read, filter, apa* and *tranform* can be run on other computers. The other programs require the use of a SUN workstation or must be rewritten to use the graphics capabilities of another machine. The last section of this appendix gives the ascii file formats for the wfdisc, wfmk and wfplot files.

Certification of 1/4"

Certification of tapes is a simple process of writing a known bit pattern throughout the entire tape and then reading that pattern to verify that the pattern has been recorded properly. Tape blocks which do not pass this test are labeled as being bad and the locations of these bad blocks are stored in a table. When all blocks have been certified, the bad block table is written to blocks 8 and 9 at the beginning of the tape. Later, when the tape is used for recording or playback, the bad block information is read from blocks 8 or 9 and stored in the tape drive's memory. The tape drive will automatically skip the bad blocks whose addresses are stored in its memory. The maximum number of bad blocks that any single tape is allowed to have is 128; more than that and the tape should not be used.

Procedure

1. Load a blank tape into the tape transport not being used to record data. Tape loading will take a few minutes, be patient.

2. When the tape has loaded, the certification program may be invoked by typing "bad".

3. At the completion of the program (about an hour) one of two messages will appear; the bad block table or a message that more than 128 bad blocks were found and that the tape should not be used. The tape should rewind itself at the end of the program.

4. Apply a label to the tape and its box and initial the "certified" bland on the labels.

5. If for some reason the tape stops without unloading, it may be unloaded by typing "bad u". If this does not work, a) ask for help and b) go have a beer.

BEST COPY AVAILABLE

NAME

bad

SYNOPSIS

bad [*length*] [*u*] [*debug*]

DESCRIPTION

Bad is used to create a bad block table and write it to absolute tape blocks 8 and 9. Using the serial interface, a tape is certified (both data and keys) and a bad block table is created in the controller ram. This table is then written to the cartridge. With no options, bad will certify the entire tape.

length The ending block number if less than the entire tape is to be certified (four character capitol hex (i.e. 1C7F)).

u A flag indicating bad is to just rewind the tape.

debug Bad is normally called with one argument. If a second argument is added, the output will be more verbose.

BEST COPY AVAILABLE

Data Playback

Data retrieval from the 1/4" archive tapes consists of reading the data from the tapes, demultiplexing it, converting it to a standard format and writing it to some other medium. The starting time, the number of seconds to retrieve and the destination file are all given in the command line. Digitization rate, because it is not constant, is calculated by dividing the total number of samples retrieved by the actual time they were recorded in.

Procedure

1. Load a tape into the tape drive and wait for the tape to stop moving. This will take a minute or so, be patient.
3. Load the bad block information into ram by typing "read-l".
4. Type "read ddd hh mm ss nnnn wfp". The header block will be displayed along with the start time of the tape. As each tape block is read in, the start time of that block is displayed on the screen. At the completion of the program, the tape is not rewound so that different sections of data may be read from the tape without reloading after every run. Four files will have been created in the current directory; (wfp).bz.w, (wfp).bn.w, (wfp).be.w, and (wfp).wfdisc. The .w files are the plus vertical, north south horizontal, and east west horizontal components, respectively.
5. Unload the tape by typing "read -u".

BEST COPY AVAILABLE

NAME

read

SYNOPSIS

read [*-l*] [*-u*] [*ddd hh mm ss nnn wfp*]

Read is a data retrieval and formating program that is used to read data from a SCS 1/4" tape transport and format it into the structures used by the Center for Seismic Studies. Bad block information is read into the controller ram from tape blocks 8 and 9 and the header block and tape start time are displayed. If the requested time (ddd=julian day, hh=hour, mm=minute, ss-second) is on the tape, read advances the tape to the requested time and reads in nnn seconds of data. The output files are placed in the current directory with waveform prefix wfp. Three data files wfp.1.w, wfp.2.w, wfp.3.w and a parameter file wfp.wfdisc constitute the output. The tape is not rewound when all of the data has been retrieved.

-l Load option. Load the bad block information into ram from tape blocks 8 and 9.

-u Rewind and unload the tape.

The .w files consist of binary four byte integers with no headers. The timing and identification information is found in the ascii file (wfp).wfdisc. Each record of the .wfdisc file corresponds to one of the .w files.

BEST COPY AVAILABLE

Data Processing Software

The software developed by Rondout Associates Incorporated for the SUN computer has been designed as an integrated processing package for seismic waveform analysis. Included are programs for the display and manipulation of waveforms, filtering, spectral analysis, and polarization analysis of three component data. All of the programs make use of the CSS formats but do not require an intimate knowledge of them to use the programs. The versatile SUN interactive graphics make using the programs almost self-explanatory.

Below we list the SUN programs developed by Roundout Associates Incorporated with brief descriptions of their capabilities and functions followed by detailed descriptions of their implementation in a manual format.

display — A general purpose display program for the display and marking of data. Its two most important functions are to give quick, versatile presentations of waveform data and to give the analyst a visual method of marking the data for further processing. The time window, number of traces, amplitude scaling, trace position, marker placement, and much more are under the interactive control of the user.

filter — Data between "start" and "end" markers (set using display) are filtered according to input parameters found in an input file. The filter may be zero or minimum phase, have any number of pass or cut bands, have any length, and be windowed with a Hamming, Hanning, Blackman, Barttlet, or rectangular window. Before filtering, the amplitude and phase response of the filter may be displayed and printed for future reference.

transform — Data between "start" and "end" markers are transformed to the frequency domain and written to a binary .t file. The .t file may then be displayed using nspec or pspec.

nspec — Up to four .t files are displayed as amplitude spectra. The user interactively controls the frequency range, dB range, frequency scale type (log or linear), number of adjacent spectral estimates to average, spectrum type (Fourier, power, or signal to noise ratio), and a cursor for measurement.

specgram — Data between "start" and "end" markers on waveform data are displayed as plots of amplitude (gray scale) in dB vs frequency (vertical axis) vs time (horizontal scale). Spectragrams are useful for understanding the time variable frequency content of

BEST COPY AVAILABLE

seismograms and can be used to intelligently design filters. Again, several parameters are interactively controlled by the analyst.

apa — Adaptive Polarization Analysis uses three component polarization techniques to determine the azimuth and apparent angle of incidence of the propagating energy and from the azimuth, the time variable radial and transverse traces. Apa is a valuable tool for single station event location and is also useful for phase identification.

apdisp — A format similar to displays with the same interactive control is used to display the results of apa. Relative error bars are displayed on the azimuth and apparent angle of incidence traces.

A number of utility programs are also available for deglitching data with bad bits, simple rotation of three component data, performing Hilbert transforms, differentiating data, etc.

Software currently in the development stages will remove or add instrument responses from seismic waveform data based on the most recent calibration data in the form of either poles and zeroes or amplitudes and phases.

BEST COPY AVAILABLE

NAME

apa – adaptive polarization analysis

SYNOPSIS

apa [*wfdisc*] [*station*] [*vertical channel*] [*output prefix*]

DESCRIPTION

apa (adaptive polarization analysis) analyzes orthogonal three component data given an assumed back azimuth to the event from the recording station. The direction of predominant motion is determined by finding the zero value of the zero lag cross correlation over a small window of orthogonal, three component data. If that direction is within the quadrants bisected by the assumed back azimuth, the motion is assumed to be p, sv or Rayleigh; otherwise it is assumed to be sh or Love. The size of the cross correlation window is read in from an input parameter file "apain" (one is created by the program if it does not already exist). The length of the input data to be analyzed is set by "start" and "end" markers in the .wfmk file. If no markers are present, the entire trace is analyzed.

Output traces include the vertical, adapted radial, and adapted transverse components of motion; the square root of the absolute value of the product of the adapted radial and vertical traces times the sign of the product; the azimuth and its error; and the apparent angle of incidence and its error. The results can be displayed using "apdisp" on a SUN microcomputer.

FILES

apain

SEE ALSO

apdisp

BEST COPY AVAILABLE

NAME

apdisp – display the results of apa on a SUN

SYNOPSIS

apdisp [*w/disc*]

DESCRIPTION

apdisp displays data output from *apa*(1a) with the same format and options used in *display*(1a). The major difference between *display*(1a) and *apdisp* is that *apdisp* assumes that the sixth .w file is the error trace for the fifth .w file and that the eighth .w file contains the errors of the seventh .w file.

SEE ALSO

display(1a), apa(1a)

BEST COPY AVAILABLE

NAME

display – display data in Center for Seismic Studies format on a SUN

SYNOPSIS

display [*wfdisc*] [*station*] [*channel*]

DESCRIPTION

display is an interactive tool with which the operator can display time series data stored in the Center for Seismic Studies digital seismic database format (Berger et al., 1983). The user is given control over the placement of the data traces on the screen, their amplitudes, the amount of data to display, and the placement of markers. Most of the operations can be performed on either the entire group of waveforms or on individual traces. ***display***'s main purposes are to allow the user to obtain hard copy of data in flexible format and to make available a method of marking data for further processing.

display can be initiated in a number of ways depending on the data that one wishes to present. Generally, an event group will contain many different waveform files from several stations with up to nine components each. If ***display*** is called with just the wfdisc prefix, then the first nine waveforms listed in the wfdisc file will be displayed. The remaining traces can be accessed through the up/down option to be discussed later. The screen format is saved in the .wfplot file so subsequent calls to ***display*** will pick up where the previous session left off. ***display*** may also be called with the wfdisc prefix and station or the wfdisc prefix and component to present either all components from a particular station for that event or a single component from all stations for that event. If only a single trace is desired, ***display*** may be called with wfdisc prefix, station, and component.

Upon initialization, the program will display 60 seconds of the requested traces (or the format of the previous session) including any markers that may be inside the time interval, identification for each trace, a time line, a button descriptor line, and a horizontal menu. The traces are identified on their immediate left by station and channel, an amplitude measure for the trace, and in small characters the date and time of the beginning of the trace. The button descriptor line at the top of the screen is:

group operations: accept menu item alternate menu return

Below the button descriptor line is printed the horizontal menu with the first item, **plot**, in reverse video. A menu option is selected by moving the mouse horizontally over the mouse pad until the desired operation appears in reverse video. Pressing the left hand mouse button, **accept menu item**,

BEST COPY AVAILABLE

causes the desired action to be stored until the next replot. If the middle, **alternate menu**, button is pushed, then the individual operations menu appears. The individual operations work on single traces only, in contrast to the group operations which perform their tasks on all of the traces. Pressing the right or **return** button exits the program.

Group operations:

plot redraws the entire screen. Several operations may be performed before redrawing.

shifts moves the time window through which the data is displayed. The user is queried as to how many seconds to shift the window. A positive value will move the traces to the left and a negative one will move them to the right.

expand sets the amount of data to be displayed. The user must type in the number of seconds to be displayed.

amps multiplies the scale factor of the traces by the given amount. The user is queried for the amount.

up/down moves the entire screen of traces up or down a specified number of inches. If a positive number is specified, the traces will all move up; negative moves them down. Any trace which is moved out of the range of the screen window through this operation will not be displayed on the next **replot**. Conversely, any trace which moves into the screen window will be plotted.

zeros draws or erases a dashed zero line on each trace.

markers is an on/off switch for turning the markers on and off. The first call to markers turn them off, the next on and so forth.

dates prints or erases the date line in the trace headers.

times prints or erases the time line in the trace headers.

reset resets the plot parameters to their original values as if display were being called for the first time.

save creates a file "raster" in the current directory and places a raster screen dump in it.

Individual Operations:

plot redraws the entire screen. Several operations may be performed before replotting.

yank/put moves a waveform from one position to another on the screen. A vertical bar with a small crosshair appears on one of the

BEST COPY AVAILABLE

traces and the mouse line changes to

choose option: accept accept no move

At the bottom of the page on the status line will be displayed the relative time from the beginning of the window to the position of the vertical bar, the absolute time at the vertical bar position, and the amplitude at the position of the small horizontal crosshair. By moving the mouse vertically on its pad, the vertical bar will shift from trace to trace as it enters the amplitude windows of the individual traces. Moving the mouse horizontally moves the bar along the trace. When either the left or middle button are pushed, the waveform on which the vertical bar is drawn is chosen as the one to be moved. A horizontal bar will then appear which can be moved vertically with the mouse. When the desired position is reached, pushing either the left or middle button will determine where that trace will be plotted on the next call to replot. If at any time, the right (**no move**) button is pushed, control will return the group menu options.

make mark

allows the user to mark individual waveforms. The vertical bar appears and when the proper waveform and time has been chosen the program queries the user for the marker name. The marker is immediately displayed on the trace.

amp works the same way that **amps** does in the group options except that after typing in the scale factor, the vertical bar appears so that a particular trace may be picked.

shift works the same way that **shifts** does in the group options except that after typing in the number of seconds to shift, a vertical bar appears so that a particular trace may be picked for shifting.

zero draws or erases a dashed zero line on the trace chosen using the vertical bar.

align lines up all of the traces with "align" markers on the trace chosen using the vertical bar.

erase removes a waveform from the screen. The trace to be erased is chosen using the vertical bar.

unerase allows the user to decide which of the traces currently erased should be unerased. Each of the waveforms not displayed is printed on the mouse line in succession

BEST COPY AVAILABLE

station channel: accept reject no more.

If the **accept** button is pushed then that trace will be plotted on the next call to replot. **Reject** means that the trace will remain "erased" and **no more** returns control to the group menu.

save creates a file named "raster" in the current directory and places a raster screen dump in it.

A .wfplot plot file is generated on the first call to display. It contains information on the placement and size of the traces, how much time to display, which traces to display and what time to start the display. Markers are placed in a .wfmk marker file. The marker file contains station, channel, epochal marker time, and marker name.

BUGS

Opens and closes files too often. After the file table fills, the program bombs.

COPY AVAILABLE

NAME

filter – filters time series data in Center for Seismic Studies format

SYNOPSIS

filter [*-n*] [*wfdisc*] [*station*] [*channel*]

DESCRIPTION

The corners of an "ideal" filter in the frequency domain are read in from the input parameter file "filterin" along with the filter length and window type. The ideal filter is transformed into the time domain, windowed, retransformed to the frequency domain, and plotted for inspection. If acceptable, the data between "start" and "end" markers in the .wfmk file (or by default the entire trace) is filtered in the time domain. The -n option omits the plotting of the filter response. If the file "filterin" does not exist, one is created in the current directory. The available windows include Bartlett, Hanning, Hamming, Blackman, and rectangular. An ideal filter is specified by giving the frequency and amplitude of the corners. For instance, to build a 101 pt, zero phase, 10 Hz high pass filter with a Hanning window, one might put the following lines in the the "filterin" file.

```
101     length of filter
0       minimum phase (1) or zero phase (0) filter?
hn      window (re rect, ba bartlett, hn hanning, hm hamming, bl blackman)
10.0 0.0        frequency, amplitude
10.0 1.0        frequency, amplitude
```

The zero and nyquist frequencies need not be specified. They are assumed to be the same amplitude as the lowest and highest frequencies given, respectively. Frequency must increase with successive lines in the input file.

A processing identifier, f, is added to the wfdisc prefix and a wfdisc record for the new trace is appended to the wfdisc file. If no wfdisc file is found for the process, one is created in the current directory.

FILES

filterin

BEST COPY AVAILABLE

NAME

nspec – plot the spectra from transform files

SYNOPSIS

nspec [*transform file 1 (tf1)*] [*tf2*] [*tf3*] [*tf4*]

DESCRIPTION

nspec is an interactive program for a SUN microcomputer that plots up to four spectra on the same graph using transform files generated by *transform*(1a). After invoking the program, an input parameter file "nspecin" is read (or created in the current directory if one does not exist) and a button definition line appears at the top of the screen in reverse video. The user is given the option of plotting the spectra, editing the input parameters, or quitting the program. Invoking the editing option produces a horizontal mouse menu whose choices are selected by moving the mouse across the mouse pad horizontally and pressing the **accept menu item** button on the mouse (left hand button). The menu choices are given below.

replot plot the spectra.

cursor a mouse controlled cursor appears on the graph in the lower left hand corner. The frequency and amplitude values of the cursor position are displayed at the bottom of the screen. Pushing any mouse button returns to the edit menu.

frequency limits
user is prompted to input the lower and upper frequency limits.

dB limits user is prompted to enter the lower and upper dB limits.

average smoother spectra are produced by averaging adjacent spectral estimates. The number prompted for should be a power of 2.

spectrum type
three types of spectra are available, Fourier spectrum for use with transients, power spectrum for use with noise, or signal-to-noise ratio. The Fourier spectrum is defined as

$$\text{Fourier}(f) = 20 * \log10\ (\text{abs}\ (X(f))$$

and the power spectrum is defined as

$$\text{power}(f) = 20 * \log10\ (\text{abs}\ (X(f))/\text{sqrt}\ (N * dt))$$

where

$$X(f) = dt * \text{sum}\ (x(t) * \exp\ (-i * 2 * pi * k * t/N))\ \ k = 1...N$$

BEST COPY AVAILABLE

If the signal-to-noise ratio type is chosen, the first transform file is considered the signal and the second transform file the noise of the first trace and so on.

log scale the frequency scale may be plotted either linear (input 0) or logrithmic (input 1).

When the spectra have been plotted, the user is given the choice via the button descriptor line of saving the raster, editing the inputs or quitting the program. Pushing the left or **save raster** button creates a file named "raster" in the current directory and writes a versatec raster image of the screen to it. At the end of the program, the input parameter file "nspecin" is updated to reflect the changes made during the course of the program.

FILES

nspecin

SEE ALSO

transform (1a)

BEST COPY AVAILABLE

NAME

track

SYNOPSIS

track [wfdisc prefix] [station] [vertical channel] [output prefix]

DESCRIPTION

Track is an adaptive polarization technique that has been taylored to track the largest component of motion in three component data. The direction of predominant motion is determined by finding the zero value of the zero lag cross correlation over a small window of orthogonal, three component data. The size of the cross correlation window is read in from an input parameter file "apain" (one is created by the program if it does not already exist). The length of the input data to be analyzed is set by "start" and "end" markers in the prefix.wfmk file. If no markers are present, the entire trace is analyzed.

Output traces include the vertical, adapted radial, and adapted transverse components of motion; the square root of the absolute value of the product of the adapted radial and vertical traces times the sign of the product; the azimuth and its error; and the angle of incidence and its error. The results can be displayed using "apdisp" on a SUN microcomputer.

FILES

apain

SEE ALSO

apdisp

BEST COPY AVAILABLE

NAME

transform – transform a time series to the frequency domain

SYNOPSIS

transform [*wfdisc*] [*station*] [*channel*]

DESCRIPTION

A real time series, or a specified portion of a real time series, is transformed into the frequency domain. The program checks for "start" and "end" markers in the .wfmk file. If they exist that portion of the data is transformed; if not, the lesser of the entire file or 10 seconds is transformed. Output is placed in the file prefix.#.t, where # corresponds to the .w file from which the data was taken. The number of samples in the output file is the power of 2 greater than the number of input samples. Frequency ranges from zero to nyquist with a real and imaginary sample at each frequency.

x(0) = sample rate
x(1) = number of data bytes
x(2) = zero frequency real part
x(3) = zero frequency imaginary part
:

The transform is defined by

$$X(f) = dt * \text{sum}\,(x(t) * \exp(-i * 2 * pi * k * t/N)); \quad k = 1...N$$

where t is time, f is frequency, dt is the sample interval and N is the total number of samples being transformed.

BEST COPY AVAILABLE

NAME

specgram – draw a spectrogram on a SUN workstation

SYNOPSIS

specgram [*wfdisc*] [*station*] [*channel*]

DESCRIPTION

specgram is an interactive program for a SUN microcomputer that plots power in dB as a gray scale with horizontal and vertical axies of time and frequency, respectively. The time series being analyzed is plotted just above the spectrogram. Input parameters are read from file "specgin" which is created if it does not already in the current directory exist. The user may choose to plot the spectrogram, edit the input parameters, or quit the program after invoking it by pressing the left, middle, or right button of the mouse respectively. If the edit option is chosen a horizontal menu line appears whose choices are selected by moving the mouse horizontally over the mouse pad. An option is chosen by pushing the left mouse button when the desired option appears in reverse video. The options are described below.

replot plot the spectrogram.

number of samples
the number of points in a single transform is prompted for. This number must be a power of 2.

frequency limits
user is prompted to give lower and upper frequency limits.

average a smoother spectrum is produced by averaging adjacent spectral estimates. The number prompted for should be a power of 2. Resolution along the frequency axis will be decreased.

dB limits user is prompted to give the lower dB limit and the dB step size. There are nine grey shades so the step size should be appropriate for the total dB range that is being plotted. (The two extremes of dB are given after plotting the spectrogram.)

title a 30 character title may be entered that will appear across the top of the plot.

When the spectrogram has been plotted, the user is given the choice of saving the raster, editing the inputs, or quitting. If the left or **save raster** button is pushed, a file named "raster" is created in the current directory and a versatec raster image of the screen written to it. The portion of the waveform file to be analyzed is marked with "start" and "end" markers in the .wfmk file. If no markers exist, then the first 10 seconds of data are used as the default.

BEST COPY AVAILABLE

FILES

specgin

BEST COPY AVAILABLE

File Formats:

wfdisc			
NAME	*FORMAT*	*CHARACTER POSITION*	*DESCRIPTION*
date	i8	1-8	julian date
time	f15.3	10-24	epoch time
sta	a6	26-31	station code
chan	a2	33-34	channel code
nsamp	i8	36-43	number of points
smprat	f11.7	45-55	sample rate (in samples/sec)
calib	f9.6	57-65	nominal calibration
calper	f7.4	67-73	calibration period
instyp	a6	78-80	instrument code
segtyp	a1	82-82	indexing method
dattyp	a2	84-85	numeric storage
clip	a1	87-87	clipping flag
chid	i8	89-96	instrument id
wfid	i8	98-105	waveform id
dir	a30	107-136	waveform directory
file	a20	138-157	waveform data file
foff	i10	159-168	byte offset
adate	i8	170-177	date last accessed
remark	a30	179-208	comment

wfmk			
NAME	*FORMAT*	*CHARACTER POSITION*	*DESCRIPTION*
sta	a6	1-6	station
chan	a2	8-9	channel
mktime	f15.3	11-25	epochal marker time
mark	a30	27-56	marker name

BEST COPY AVAILABLE

wfplot			
NAME	*FORMAT*	*CHARACTER POSITION*	*DESCRIPTION*
sta	a6	1-6	station
chan	a2	8-9	channel
y-pos	f8.5	11-18	vertical screen position
y-siz	f8.5	20-27	vertical window size
start-time	f15.3	29-43	display start time
end-time	f15.3	45-59	display end time
amp-scale	f8.4	61-68	amplitude scale
amp-units	a8	70-77	amplitude units
remark	a30	79-108	comment/remark

BEST COPY AVAILABLE

NRC FORM 335 (2-84) NRCM 1102, 3201, 3202

U.S. NUCLEAR REGULATORY COMMISSION

BIBLIOGRAPHIC DATA SHEET

SEE INSTRUCTIONS ON THE REVERSE

1 REPORT NUMBER (Assigned by TIDC, add Vol. No., if any)

NUREG/CR-4822

2 TITLE AND SUBTITLE

Broad Band Seismic Data Analysis
September 1984 - September 1986

3 LEAVE BLANK

4 DATE REPORT COMPLETED

MONTH	YEAR
December	1986

5 AUTHOR(S)

J.A. Carter, N. Barstow, G.H. Sutton, P.W. Pomeroy

6 DATE REPORT ISSUED

MONTH	YEAR
April	1987

7 PERFORMING ORGANIZATION NAME AND MAILING ADDRESS (Include Zip Code)

Rondout Associates, Incorporated
P.O. Box 224
Stone Rodge, NY 12484

8 PROJECT/TASK/WORK UNIT NUMBER

9 FIN OR GRANT NUMBER

FIN D1196

10 SPONSORING ORGANIZATION NAME AND MAILING ADDRESS (Include Zip Code)

Division of Engineering Safety
Office of Nuclear Regulatory Research
U.S. Nuclear Regulatory Commission
Washington, DC 20555

11a TYPE OF REPORT

Final Technical

b PERIOD COVERED (Inclusive dates)

September 1984-September 1986

12 SUPPLEMENTARY NOTES

13 ABSTRACT (200 words or less)

This report contains a detailed description of the SRNY station including its response function, description of the techniques and software used to analyze the data, and evaluations of both the station and processing methods. The station was evaluated through noise studies under both quiet and noisy conditions; its detection and location thresholds; and the frequency, duration, and causes of data loss. The report has been divided into three main sections. The first section gives a description of the broad band digital seismic station SRNY installed near the Rondout Associates, Incorporated (RAI) offices in Stone Ridge, NY. Included in the discussion are the system response functions and an analysis of the causes of data loss. The second section gives details of the data analysis methods used in studying broad band and array data. Although several methods have been studied, much of this section is devoted to the adaptive polarization methods which has shown promise as a single station location tool. The final section examines the noise characteristics at SRNY during both quiet and noisy conditions and compares these levels to the Regional Seismic Test Network station RSNY in the Adirondack Mountain region of northern New York. The detection and location capabilities of SRNY are also described and single-station locations at SRNY, as well as RSNY, are compared to network locations.

14 DOCUMENT ANALYSIS - a KEYWORDS/DESCRIPTORS

SRNY
noise detection
seismic station
polarization
depth determination
event location

b IDENTIFIERS/OPEN-ENDED TERMS

15 AVAILABILITY STATEMENT

Unlimited

16 SECURITY CLASSIFICATION

(This page)
Unclassified
(This report)
Unclassified

17 NUMBER OF PAGES

18 PRICE

*U.S. GOVERNMENT PRINTING OFFICE: 1987- 181-682:60139

88

BEST COPY AVAILABLE